

NEUTRON SLOWING DOWN WITH
INELASTIC SCATTERING

Thesis by
Michael Jay Lineberry

In Partial Fulfillment of the Requirements
for the Degree of
Doctor of Philosophy

California Institute of Technology
Pasadena, California

1972

(Submitted April 3, 1972)

ACKNOWLEDGMENTS

In the course of nine years of collegiate work I have incurred many debts I shall never be able to repay.

One of the foremost of these is owed my thesis advisor, Professor Noel Corngold. His keen insight and demanding encouragement provided a great deal of inspiration, and it has been my good fortune to have studied under him.

Three years of my graduate education were financed by an Atomic Energy Commission special fellowship, followed by a one year National Science Foundation traineeship. Throughout my doctoral work I received Ford Foundation loan funds. I gratefully acknowledge the generous support of these and other sponsors.

Finally, I owe so very much to my patient and diligent wife. The seemingly endless years of sacrifice were met by her with unfailing encouragement, and this was a constant source of strength.

ABSTRACT

The emphasis in reactor physics research has shifted toward investigations of fast reactors. The effects of high energy neutron processes have thus become fundamental to our understanding, and one of the most important of these processes is nuclear inelastic scattering. In this research we include inelastic scattering as a primary energy transfer mechanism, and study the resultant neutron energy spectrum in an infinite medium. We assume that the moderator material has a high mass number, so that in a laboratory coordinate system the energy loss of an inelastically scattered neutron may be taken as discrete. It is then consistent to treat elastic scattering with an age theory expansion. Mathematically these assumptions lead to balance equations of the differential-difference type.

The steady state problem is explored first by way of Laplace transformation of the energy variable. We then develop another steady state technique, valid for multiple inelastic level excitations, which depends on the level structure satisfying a physically reasonable constraint. In all cases the solutions we generate are compared with results obtained by modeling inelastic scattering with a separable, evaporative kernel.

The time dependent problem presents some new difficulties. By modeling the elastic scattering cross section in a particular way, we generate solutions to this more interesting problem. We conjecture the method of characteristics may be useful in analyzing time dependent problems with general cross sections. These ideas are briefly explored.

TABLE OF CONTENTS

<u>Chapter</u>	<u>Title</u>	<u>Page</u>
	ACKNOWLEDGMENTS	ii
	ABSTRACT	iii
I	INTRODUCTION	1
	A. Introduction to Slowing Down Theory	1
	B. Review of Slowing Down Research	3
	C. Motivation for this Research	12
II	STEADY STATE SLOWING DOWN WITH INELASTIC SCATTERING	14
	A. General Steady State Formalism	14
	B. Linear Inelastic Cross Section - Single Level	17
	C. Linear Inelastic Cross Sections - Multiple Level	31
	D. Constant Inelastic Cross Section - Single Level	42
	E. Arbitrary Inelastic Cross Section - Single Level	52
III	STEADY STATE MULTIPLE LEVEL ANALYSIS	64
VI	TIME DEPENDENT SLOWING DOWN WITH INELASTIC SCATTERING	73
	A. Elastic Scattering Excluded Above Threshold	73
	B. Elastic Scattering Included in a Simple Form	80
	I. A Simple Inelastic Cross Section	83
	II. Generalization to Any Inelastic Cross Section	94
	C. Prospects of Extension to More General Elastic Cross Sections	102
	REFERENCES	105
	Appendix I - The Mechanics of Inelastic Scattering	109
	Appendix II - Steady State Recovery	113

I. INTRODUCTION

A. Introduction to Slowing Down Theory

Within the energy range reactor physicists deal with, a neutron passing close to a nucleus can interact in two ways. One of these processes is potential elastic scattering, with the neutron changing direction and laboratory speed due to the physical presence of the nucleus. The other interaction can be viewed as a formation of a compound nucleus. If the compound nucleus is created, completion of the reaction can proceed in several ways. Some of these decay schemes are neutron re-emission at the incident center-of-mass energy (compound elastic scattering), neutron re-emission at a lower center-of-mass energy (compound inelastic scattering), or gamma ray emission (neutron absorption).

In the study of neutron slowing down, the effect of elastic scattering is well documented^(1, 2, 3). When a neutron scatters elastically from a nucleus, the center-of-mass energy is unchanged. When viewed in the laboratory, however, the neutron loses up to a certain fraction of its energy. Given A , the atomic mass number, that fraction is

$$1 - \alpha = \frac{4A}{(A + 1)^2}.$$

For hydrogen ($\alpha = 0$) the incident neutron can lose all its energy. For heavy nuclei α is very nearly unity, and only a small portion of the energy can be lost in a single collision. Provided that the angular

distribution of the emergent neutrons is isotropic in center-of-mass coordinates, the probability distribution of final laboratory energies is constant within the interval $(\alpha E_{inc}, E_{inc})$, where E_{inc} is the incident laboratory energy of the neutron.

The mechanics of nuclear inelastic scattering is only slightly more complicated, the difference being due to the Q-value of the reaction. Inelastic interactions are characterized by a threshold energy, below which no inelastic interactions occur. Such thresholds vary from several million electron volts for light nuclei, to tens of kilovolts for heavy nuclei. Briefly (see Appendix I), in the center-of-mass system the neutron incident energy is reduced by the Q-value of the reaction. As viewed in the laboratory, the neutron emerges with a distribution of final energies. The minimum and maximum laboratory final energies are⁽⁴⁾:

$$E_{max} = E_{inc} \left[\frac{1}{2}(1 + \alpha) + \frac{1}{2}(1 - \alpha) \sqrt{1 - \frac{E_{th}}{E_{inc}}} \right] - \beta^2 E_{th}$$

$$E_{min} = E_{inc} \left[\frac{1}{2}(1 + \alpha) - \frac{1}{2}(1 - \alpha) \sqrt{1 - \frac{E_{th}}{E_{inc}}} \right] - \beta^2 E_{th}$$
(1.1)

where E_{inc} = the incident laboratory energy
 $\beta = A/(A + 1)$
 $E_{th} = Q/\beta$, the threshold energy.

Again provided that the emerging neutron is emitted isotropically in the center-of-mass system, the probability distribution of final energies is constant in the range (E_{min}, E_{max}) ⁽⁴⁾. For heavy nuclei ($\alpha \rightarrow 1$) the

final laboratory energy distribution becomes very narrow. The laboratory energy that the neutron loses then approaches the threshold energy E_{th} .

B. A Brief History of Pertinent Slowing Down Research

Consider the neutron balance equation describing the neutron flux in an infinite, non-multiplying medium:

$$\frac{1}{v} \frac{\partial \varphi(E, t)}{\partial t} = S(E, t) - \Sigma_t(E) \varphi(E, t) + \int_E^{E/\alpha} K_s(E' \rightarrow E) \Sigma_s(E') \varphi(E', t) dE' + \int_E^{\infty} K_{in}(E' \rightarrow E) \Sigma_{in}(E') \varphi(E', t) dE', \quad (1.2)$$

where

$S(E, t)$ = the neutron source distribution

$\Sigma_s(E)$ = the elastic scattering cross section (cm.^{-1})

$\Sigma_t(E)$ = the total cross section

$\Sigma_{in}(E)$ = the inelastic scattering cross section

$K_s(E' \rightarrow E)$ = the probability density that neutrons scattered elastically at energy E' will emerge with energy E $\left[\int_0^{\infty} K_s(E' \rightarrow E) dE = 1 \right]$

$K_{in}(E' \rightarrow E)$ = the probability density that neutrons scattered inelastically at energy E' will emerge with energy E $\left[\int_0^{\infty} K_{in}(E' \rightarrow E) dE = 1 \right]$.

Equations similar to Eqn. 1.2, neglecting inelastic scattering, formed the basic theory reviewed by Marshak⁽⁵⁾ in a classic 1947 paper. This

theory provided the framework supporting the next twenty years of research.

Slowing down in hydrogenous media was first investigated. The fact that a neutron scattering elastically from hydrogen can lose all its energy led to mathematical benefits, and to closed form solutions in many problems. When heavier isotopes were considered, a complication arose. Because only a fraction of the neutron energy can be carried away by the struck nucleus, mathematical difficulties appeared. The balance equation can be cast as a differential difference equation in the lethargy variable ($u = \ln \frac{E_0}{E}$). Solutions are then harder to obtain, and it was Placzek⁽⁶⁾ and Adler⁽⁷⁾ who first solved the slowing down equation without time dependence or absorption.

As more complicated cases involving neutron capture, time dependence, or spatial variation were considered, it was necessary to treat elastic scattering in an approximate manner. For heavy isotopes, the narrow range of final energies ($\alpha \approx 1$) allowed replacement of the elastic scattering term by a continuous slowing down model. Mathematically the process simply involved expanding $\Sigma_s(E')\varphi(E', t)$ in the elastic integral, and keeping terms through the first derivative. Such a treatment became known as Fermi age theory.⁽³⁾ Consider the elastic scattering term in Eqn. 1.2, where we assume isotropic scattering in the center-of-mass system. The elastic integral ($\equiv S_s(E, t)$) is then

$$S_s(E, t) = \int_E^{E/\alpha} \frac{\Sigma_s(E')\varphi(E', t)}{E'(1-\alpha)} \cdot$$

By expanding

$$\Sigma_s(E') \varphi(E', t) = \Sigma_s(E) \varphi(E, t) + (E' - E) \left. \frac{\partial [\varphi(E', t) \Sigma_s(E')]}{\partial E'} \right|_{E'=E} + \dots,$$

we have

$$S_s(E, t) = \xi \frac{\partial}{\partial E} \left(\Sigma_s(E) E \varphi(E, t) \right) + \Sigma_s(E) \varphi(E, t) + O(\alpha - 1)^2,$$

where $\xi = 1 + \frac{\alpha \ln \alpha}{1 - \alpha}$. The new balance equation with a modeled elastic scattering term is

$$\begin{aligned} \frac{1}{v} \frac{\partial \varphi(E, t)}{\partial t} = & S(E, t) + \xi \frac{\partial}{\partial E} \left(\Sigma_s(E) E \varphi(E, t) \right) - \Sigma_{ne}(E) \varphi(E, t) \\ & + \int_E^\infty K_{in}(E' \rightarrow E) \Sigma_{in}(E') \varphi(E', t) dE, \end{aligned} \quad (1.3)$$

where $\Sigma_{ne}(E) = \Sigma_t(E) - \Sigma_s(E)$, the nonelastic cross section.

Fermi age theory is thus particularly suited to cases where very heavy nuclei are present. In 1960 Goertzel and Greuling⁽⁸⁾ devised an improvement to age theory, especially tailored for slowing down in the presence of nuclei with intermediate A. One treats an approximate elastic scattering kernel, rather than the one shown above. This kernel contains one other parameter besides ξ .

Consideration of inelastic scattering as an important energy transfer process became mandatory when interest in fast reactors began to grow. In typical fast assemblies much of the neutron population is at energies above the first inelastic threshold. In 1954

Volkin⁽⁹⁾ first incorporated inelastic scattering into slowing down theory. He considered slowing down in a mixture of heavy moderator ($A \gg 1$) and hydrogen, and neglected elastic scattering in the heavy material. Referring to Eqn. 1.1 and the remarks that follow it, consideration of a heavy inelastic scatterer allows the inelastic kernel to be cast in a simple approximate form. For $A \gg 1$ we approximate the kernel by

$$K_{in}(E' \rightarrow E) \cong \sum_{k=1}^n \delta(E' - E - E_k), \quad (1.4)$$

where E_k denotes the k^{th} threshold energy. The inelastic term in the neutron balance equation then becomes

$$\sum_{k=1}^n \Sigma_{in}^k(E + E_k) \varphi(E + E_k, t)$$

where Σ_{in}^k refers to the inelastic scattering cross section for the k^{th} inelastic level.* Volkin solved the resultant differential difference equation numerically, marching downward in energy from the source energy. This highly computational approach is greatly complicated by

*There are two energy "scales" of interest. Inelastic scattering occurs on a scale measured by E_1 , the lowest threshold. Elastic scattering has a scale $E(1-\alpha)$, or the range over which elastic scattering can occur for given E . If elastic scattering were treated exactly, the famous Placzek oscillations⁽⁶⁾ would occur. It is consistent to demand oscillations induced by the inelastic difference terms not have a comparable wavelength. This translates, for large A , to $4E/A \ll E_1$. This imposes a condition on energies, mass numbers, and thresholds that we should allow. We observe this condition in all examples considered.

the inelastic level structure. Because of the complexity involved in solving differential difference equations, Volkin's kernel did not gain much acceptance. Rather it became popular to approximate the inelastic contribution in other, less precise, ways.

If a neutron has incident energy high enough to excite many inelastic levels, the liquid drop model of the nucleus may be used to predict the distribution of scattered neutrons. The neutrons boil off the compound nucleus with a characteristic evaporation spectrum⁽¹⁰⁾

$$K_{in}(E' \rightarrow E) \sim E e^{-E/T(E')}.$$

Thus the kernel in Eqn. 1.3 is replaced by a smooth function. Instead of a differential difference equation, we have a more tractable integro-differential equation. The equation is convertible to a pure differential equation if the kernel $K_{in}(E' \rightarrow E)$ is separable. The application of this idea to fast neutron spectra was first suggested by Okrent, et. al.⁽¹¹⁾. Okrent's inelastic kernel was

$$K_{in}(E' \rightarrow E) = C(E') E f(E) e^{-E/T}$$

with

$$f(E) = \begin{cases} 1 & E \geq E_0 \\ \sqrt{\frac{E_0}{E}} & E \leq E_0, \end{cases}$$

where

E_0 = some reference energy

T = a nuclear temperature (assumed constant).

This model found considerable favor among reactor physicists, and many investigators^(12, 13) over the next several years based their treatment of inelastic scattering on an evaporative kernel.

In 1966 Mihalcz⁽¹⁴⁾ found that changes in the nuclear temperature could induce relatively large changes in certain parameters. A 30% change in nuclear temperature induced only about a 1% change in the multiplication factor of a hypothetical uranium metal assembly. The mean generation time, however, varied by 10%, and the average energy of core neutrons varied by 14%. Large variations in the same parameters were also noted when the inelastic model was changed to a level excitation model (Volkin kernel) below 2 meV, but again the multiplication factor varied only slightly.

A well known result of classical slowing down theory is that for energies below all sources, the neutron flux becomes inversely proportional to energy. This is strictly true for zero absorption, and approximately correct for small absorption. This result was of key importance in application of the theory. The characterization of spectra in fast assemblies has no such simple form, though many attempts have been made to suggest that one exists. Murley and Kaplan^(14, 15) considered the neutron spectrum in a fast multiplying assembly as a linear combination of a fission spectrum plus a softer, "moderated" spectrum. The softer spectrum was then found by a variational technique. Driscoll and Kaplan⁽¹⁶⁾ found a fast reactor flux shape function containing two adjustable parameters. One of these parameters depended primarily on the moderating ratio at low energy, while the

other depended primarily on the magnitude of the inelastic scattering.

Cadhilac and Pujol^(17, 18) incorporated inelastic scattering by grouping elastic scattering and inelastic scattering contributions together in one separable kernel. The kernel was chosen from two requirements:

- (1) neutron conservation
- (2) the new, separable kernel must have the same effect on a "reference" spectrum as the original kernel.

Given that the above two constraints on the approximate kernel are satisfied, solutions can be generated and compared with numerical results. Rather impressive agreement was observed.

Another method of treating inelastic scattering which has been recently developed is to incorporate the effect of inelastic scattering by modifying the elastic moderation parameters in the Goertzel-Greuling model discussed earlier^(15, 19, 20, 21, 22). The two parameters are taken as functions of energy, and are adjusted according to the magnitude of the inelastic contribution. The problem is then reduced to an elastic scattering analysis with a new kernel to describe the energy transfer.

Wälti and Grossman⁽²³⁾ generated a synthetic kernel for fast slowing down. This generalized kernel included both the evaporation model and the G-G model.

Burns and Becker^(24, 25) have recently shown that the method of adjusting the G-G moderation parameters is entirely equivalent to the

Cadhilac-Pujol method of treating the scattering process with a single separable kernel. They provide the equations necessary to transform from one notation to the other.

On rather different fronts inelastic scattering was given a more fundamental role. Syros⁽²⁶⁾ used an approximate inelastic scattering kernel which approached the exact kernel at energies well above the inelastic threshold. Segev⁽²⁷⁾ developed an analysis, particularly well suited for mixtures containing light and intermediate nuclei, in which the inelastic scattering is treated exactly. An approximate solution to the slowing down equation is then generated by series expansion, and truncation of high order terms.

Study of time dependent slowing down in fast systems was first stimulated by investigations using the lead slowing down spectrometer⁽²⁸⁾. As general interest in fast systems grew, experimental data became more available. Beghian and co-workers was among the first to do pulsed neutron experiments in fast non-multiplying assemblies^(29, 30). Later elegant experiments on fast multiplying systems were performed by several investigators, among them Gozani⁽³¹⁾ using depleted uranium spheres, and Hiraoka⁽³²⁾, et. al. using lead and natural uranium assemblies.

Theoretical investigations in time dependent slowing down have lagged considerably behind the experiments, probably because of the complexity of some high energy processes. Asymptotic analysis, valid for times long enough that high energy processes become unimportant due to a diminished high energy neutron population, can be carried out

by classical methods. (5, 28)

In the analysis of initial value problems in thermal systems, it is valuable to know the nature of the time eigenvalues. In particular it was found that asymptotic reactor theory could be applied to predict the disappearance of a fundamental time eigenvalue for small enough systems⁽³³⁾. Many subsequent investigations of thermal systems dealt with predicting the disappearance of the fundamental time mode, and with the description of the resultant decay.

The mathematical techniques developed for thermal systems have recently been applied to the analysis of fast systems^(34, 35). Adalioglu⁽³⁶⁾ included inelastic scattering via an evaporation kernel, and predicted the existence and disappearance of the fundamental time mode. All of the above analyses depend heavily on the assumption that spatial dependence in fast systems can be approximated by diffusion theory or asymptotic reactor theory. This assumption, which is well verified in thermal systems, is subject to considerable debate for fast systems.

Albrecht and Williamson⁽³⁷⁾ have done numerical multi-group analysis using an ingenious method to include accurately the effect of inelastic scattering while retaining elastic scattering. Graphical displays of the time dependent neutron spectrum demonstrate the effect of pulse dispersion at early times due to inelastic scattering. Evidence of the elastic scattering mechanism taking over to focus the distribution toward sharper energy values as time evolves is clearly presented.

Beynon, Coleman, and Mondal⁽³⁸⁾ have recently analyzed the time dependent slowing down of a pulse injected at a source energy slightly above the inelastic threshold. Using a multi-group technique, they demonstrate the profound effect inelastic scattering has on the slowing down time and the energy distribution at early times.

C. Motivation for This Research

Very often the bulk of neutron slowing down takes place in an energy range where only a few nuclear states are subject to excitation. Also, one is often interested in the solution near inelastic thresholds. In either of these situations evaporation modeling or G-G modeling for inelastic scattering become questionable techniques.

The moderation of neutrons in fast assemblies typically involves slowing down in very heavy moderating materials. It is realistic to return to the Volkin kernel (discrete energy losses following inelastic collisions) to model inelastic scattering. It is also consistent to treat elastic scattering using Fermi age theory. Such was the approach used by Corngold and Yan⁽³⁹⁾ when studying slowing down with inelastic scattering, and it is the approach used in this research. Rather than treating the inelastic scattering process as a stepchild, we will study the phenomenon of neutron slowing down with inelastic scattering playing a key role in the determination of the neutron energy spectrum.

In Chapter II the work of Corngold and Yan for excitation of a single inelastic level, with a linear inelastic cross section above threshold, is reviewed and extended. Then the solution is compared with that obtained by modeling inelastic scattering with an evaporation

kernel. Excitation of two levels with ramp cross sections is considered and the solution compared with the evaporative model solution. The generalization to many levels is discussed. The case of constant inelastic cross section is then considered for a single level. Again the solution is compared with that gained using the evaporative model. We then analyze the neutron spectrum when a single inelastic level is present with arbitrary cross section variation. The asymptotic spectrum (source far above threshold, no absorption) is examined, and an approximate analytical form (similar to $1/E$ for the elastic scattering case) is presented.

Chapter III contains a discussion of the many-level problem, with arbitrary cross sections, assuming certain reasonable conditions on the level structure are fulfilled. An example is presented and the solution again compared with the evaporative model solution.

Chapter IV deals with approaches to the time dependent problem with a single level of inelastic scattering. After first examining the solution when elastic scattering is neglected, we consider a simple elastic scattering cross section, and include elastic transfer by Fermi age theory. Suggestions of generalizations to arbitrary elastic cross sections are then reviewed.

II. STEADY STATE SLOWING DOWN WITH INELASTIC SCATTERING

A. General Steady State Formalism

We begin our study of slowing down theory with inelastic scattering by considering the general steady state problem. Assume the host nuclei are massive ($1/A \rightarrow 0$), and that the elastic scattering cross section is a fairly smooth function of energy. Fermi age theory is then acceptable for treating the elastic scattering term. Also, assume that the Volkin model is a good approximation to the inelastic integral. The equation for the neutron flux becomes (combining Eqns. 1.2 and 1.3)

$$\xi \frac{d}{dE} (\Sigma_s(E) E \varphi(E)) - \Sigma_{ne}(E) \varphi(E) + S(E) + \sum_{k=1}^N \Sigma_{in}^k(E + E_k) \varphi(E + E_k) = 0, \quad (2.1)$$

where all terms have been previously defined.

Equation 2.1 is a first order ordinary differential difference equation of the retarded type. The theory of these equations has been investigated extensively, especially in the case of constant coefficients⁽⁴⁰⁾. The general technique used in this research is to treat the difference term by Laplace transformation.

We can make Eqn. 2.1 dimensionless by introducing the dimensionless variable $\epsilon = E/E_1$. Define

$$\varphi(E) dE = \varphi(\epsilon) d\epsilon$$

$$S(E) dE = S(\epsilon) d\epsilon$$

$$\Sigma_j(E) = \Sigma_j(\epsilon) \quad (j \text{ refers to all reactions considered}).$$

Substitution into Eqn. 2.1 yields

$$\xi \frac{d}{d\epsilon} (\Sigma_s(\epsilon) \epsilon \varphi(\epsilon)) - \Sigma_{ne}(\epsilon) \varphi(\epsilon) + S(\epsilon) + \sum_{k=1}^N \Sigma_{in}^k(\epsilon + \epsilon_k) \varphi(\epsilon + \epsilon_k) = 0, \quad (2.2)$$

where
$$\epsilon_k = \frac{E_k}{E_1} \quad k = 1, 2, \dots, N.$$

If we assume that the only high energy reaction of interest is the inelastic scattering reaction (so that we neglect $(n, 2n)$, etc.), the non-elastic cross section can be written

$$\Sigma_{ne}(\epsilon) = \Sigma_{in}(\epsilon) + \Sigma_a(\epsilon),$$

where $\Sigma_a(\epsilon)$ is the absorption cross section. For the present we shall assume that the elastic scattering cross section is constant for all energies. This approximation, crude as it is, can be substantiated somewhat by noting that many isotopes have elastic cross sections that change quite slowly with energy. Two examples are ${}_{73}\text{Ta}$ and ${}_{78}\text{Pt}$.⁽⁴¹⁾ We will relax this assumption later when the time dependent problem is considered.

If we consider the absorptionless version of Eqn. 2.2 when a single inelastic level is excited, we have

$$\xi \Sigma_s \frac{d}{d\epsilon} (\epsilon \varphi(\epsilon)) - \Sigma_{in}(\epsilon) \varphi(\epsilon) + \Sigma_{in}(\epsilon+1) \varphi(\epsilon+1) + S(\epsilon) = 0.$$

We shall assume the neutrons are injected at a single energy $E = E_s$, and define $s = E_s / E_1$. If we also define a new dependent variable

$$\psi(\epsilon) = \epsilon \varphi(\epsilon), \quad (2.3)$$

then

$$\xi \Sigma_s \frac{d\psi(\epsilon)}{d\epsilon} - \frac{\Sigma_{in}(\epsilon)}{\epsilon} \psi(\epsilon) + \frac{\Sigma_{in}(\epsilon+1)}{\epsilon+1} \psi(\epsilon+1) = -\xi \Sigma_s \delta(\epsilon - s), \quad (2.4)$$

where the source amplitude has been chosen to be $\xi \Sigma_s$. The function $\psi(\epsilon)$ is defined to be zero for $\epsilon > s$. We can integrate Eqn. 2.4 over a small region about $\epsilon = s$ to discover that $\psi(s^-) = 1$. Thus $\psi(\epsilon)$ is discontinuous at $\epsilon = s$. Further examination of Eqn. 2.4 tells us that the first derivative of $\psi(\epsilon)$ is thus discontinuous at $\epsilon = s - 1$. Differentiation of the homogeneous version of Eqn. 2.4 shows that the second derivative is discontinuous at $\epsilon = s - 2$. Discontinuities in higher derivatives appear at successively lower values of energy.

We should remark about the general behavior of the solution to Eqn. 2.4 as the inelastic scattering becomes more dominant. As $\Sigma_{in}(\epsilon) / \Sigma_s \rightarrow \infty$, Eqn. 2.4 becomes an algebraic difference equation. Without getting involved in theory, it is reasonable to say the solution should tend to a series of pulses at $\epsilon = s, s - 1, s - 2, \dots$. These pulses will have amplitudes determined by $\Sigma_{in}(\epsilon)$. We can see such a solution satisfies Eqn. 2.4 within the above limit. We shall later observe an increasing "spikiness" in solutions as Σ_{in} / Σ_s grows.

The function $\Sigma_{in}(\epsilon)$ is a threshold cross section. In laboratory coordinates the threshold energy is very nearly the Q value of the

reaction (see Appendix I). In dimensionless energies, $\Sigma_{in}(\epsilon)$ vanishes for $\epsilon \leq 1$. This fact essentially makes Eqn. 2.4 a two-region problem, and we solve it by generating a solution for $\epsilon > 1$, and then using this solution as a source for the subthreshold region $\epsilon < 1$.

If multiple levels are considered, the result is somewhat more complicated. The multiple level version of Eqn. 2.4 is

$$\xi \Sigma_s \frac{d\psi(\epsilon)}{d\epsilon} - \frac{\Sigma_{in}(\epsilon)}{\epsilon} \psi(\epsilon) + \sum_{k=1}^N \frac{\Sigma_{in}^k(\epsilon + \epsilon_k)}{\epsilon + \epsilon_k} \psi(\epsilon + \epsilon_k) = -\xi \Sigma_s \delta(\epsilon - s), \quad (2.5)$$

where

$$\Sigma_{in}(\epsilon) = \sum_{k=1}^N \Sigma_{in}^k(\epsilon).$$

In Eqn. 2.5 each of the inelastic cross sections for the individual levels is of the threshold type. Thus Eqn. 2.5 is essentially an $(N+1)$ region problem, where N is the number of inelastic levels considered. This analysis will be expanded later, and some specific examples cited.

Returning now to the case of single level inelastic scattering, described by Eqn. 2.4, we review the solution for a particular inelastic cross section first investigated by Corngold and Yan⁽³⁹⁾.

B. Linear Inelastic Cross Section - Single Level

The easiest way to include a single level of inelastic scattering is to demand that $\Sigma_{in}(\epsilon)$ be the linear function:

$$\Sigma_{in}(\epsilon) = \begin{cases} \alpha \epsilon & \epsilon \geq 1 \\ 0 & \epsilon < 1. \end{cases} \quad (2.6)$$

This cross section does not continuously approach zero at the inelastic threshold ($\epsilon = 1$), and so is somewhat unphysical. There are, however, many isotopes whose inelastic cross sections rise very rapidly after threshold, and modeling the cross section as in Eqn. 2.6 is not as unreasonable as it might appear. The first inelastic level of U^{238} , at 44kev, is an example. ⁽³⁾ In any case the mathematical benefits are substantial.

Given the inelastic cross section above, we can pose the problem for the neutron distribution in the following way:

$$\psi(\epsilon) = 0 \quad \epsilon > s \quad (2.7a)$$

$$\frac{d\psi(\epsilon)}{d\epsilon} + \frac{\mu}{\xi} [\psi(\epsilon+1) - \psi(\epsilon)] = 0 \quad ; \quad \psi(s) = 1 \quad 1 \leq \epsilon \leq s \quad (2.7b)$$

$$\frac{d\psi_b(\epsilon)}{d\epsilon} + \frac{\mu}{\xi} \psi(\epsilon+1) = 0 \quad ; \quad \psi_b(1^-) = \psi(1^+) \quad 0 \leq \epsilon \leq 1, \quad (2.7c)$$

where $\mu = \alpha/\Sigma_s$, a ratio of the inelastic to elastic strength.

In Eqns. 2.7 the regional nature of the problem is demonstrated. The first equation states the collision density above the source energy is zero. The second equation is a balance equation above the inelastic threshold, and the delta function source has been replaced by an initial condition. The third equation is for the below-threshold distribution. The source term for this equation comes from the inelastic interactions above threshold which carry neutrons below.

Since the solution to Eqn. 2.7c is seen to depend on the distribution in the region $1 \leq \epsilon \leq s$, we shall first deal with Eqn. 2.7b. The

solution to this equation will be generated using the Laplace transform. Formally we extend the range of ϵ in Eqn. 2.7b to $-\infty < \epsilon \leq s$, and define the following transform:

$$\tilde{\Psi}(\lambda) = \int_{-\infty}^s e^{\lambda \epsilon} \psi(\epsilon) d\epsilon. \quad (2.8)$$

Application of the transform operator to Eqn. 2.7b yields

$$\tilde{\Psi}(\lambda) = \frac{e^{\lambda s}}{\lambda + \frac{\mu}{\xi} [1 - e^{-\lambda}]} \quad (2.9)$$

Inverting the transformation to recover $\psi(\epsilon)$ is straightforward:

$$\psi(\epsilon) = \frac{1}{2\pi i} \int_{\text{Br}} \frac{e^{\lambda(s-\epsilon)} d\lambda}{\lambda + \frac{\mu}{\xi} [1 - e^{-\lambda}]}, \quad (2.10)$$

where the Bromwich contour is in the ordinary sense, with the path of integration chosen to the right of all singularities of the integrand.

We evaluate $\psi(\epsilon)$ by using the theory of residues. The integrand in Eqn. 2.10 has simple poles in the λ -plane corresponding to the zeroes of the denominator:

$$\lambda + \frac{\mu}{\xi} [1 - e^{-\lambda}] = 0. \quad (2.11)$$

There are thus an infinite number of simple poles which occur in conjugate pairs. Further, $\lambda = 0$ is always a root of Eqn. 2.11.

We can learn a great deal about the nature of the poles by breaking up Eqn. 2.11 into separate equations for real and imaginary parts. Letting $\lambda = \sigma + i\tau$, we have

$$\sigma + \frac{\mu}{\xi} [1 - e^{-\sigma} \cos \tau] = 0 \quad (2.12)$$

$$\tau + \frac{\mu}{\xi} e^{-\sigma} \sin \tau = 0. \quad (2.13)$$

Since roots occur in conjugate pairs, we need consider only positive imaginary parts. From Eqn. 2.13, roots certainly cannot occur if τ and $\sin \tau$ are simultaneously positive. Thus "forbidden" zones are present. In fact roots can only occur in the following bands of positive τ :

$$(2n+1)\pi < \tau < (2n+2)\pi \quad n=0, 1, \dots$$

An analogous expression holds for negative values of τ . Representative forbidden regions are shown in Figure 2.1.

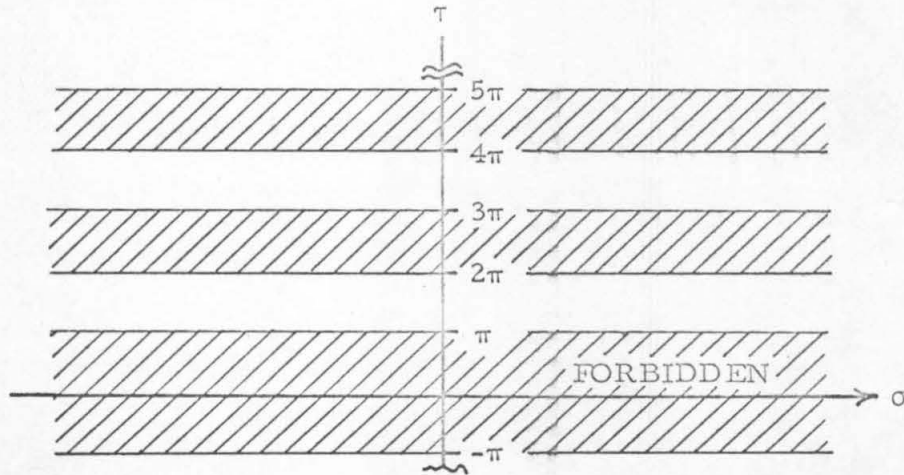


Figure 2.1 Forbidden Bands

One can show by further examination of Eqns. 2.12 and 2.13 that at least one, and at most three, roots occur in each allowed band.

Further, for $\mu/\xi < 0.28$, one and only one root occurs in each band. If $\mu/\xi > 0.28$, then as many as three roots are possible in the lower allowed bands, but only one is possible in higher bands. Practically speaking, however, only one is observed to occur. Also one can easily show from Eqn. 2.12 that in allowed bands roots must have $\text{Re}(\lambda) \leq 0$ ($\sigma \leq 0$).

As a final note concerning the nature of the roots of Eqn. 2.11, we can predict the location of the root in the n^{th} zone as n becomes large. By applying simple geometrical arguments to solutions of Eqns. 2.12 and 2.13, we find

$$\begin{aligned} \lim_{n \rightarrow \infty} \tau_n &= \left(2n + \frac{3}{2}\right)\pi \\ \lim_{n \rightarrow \infty} \sigma_n &= -\ln \left[\frac{(2n + \frac{3}{2})\pi}{\frac{\mu}{\xi}} \right]. \end{aligned} \tag{2.14}$$

The distribution of the first several roots for various μ/ξ is shown in Figure 2.2. One can verify the asymptotic predictions given by Eqn. 2.14 are quite good after the first few roots.

The residue of the k^{th} pole can be extracted from Eqn. 2.10:

$$R_k = \lim_{\lambda \rightarrow \lambda_k} \frac{\lambda - \lambda_k}{\lambda + \frac{\mu}{\xi} [1 - e^{-\lambda}]},$$

or

$$R_k = \frac{1}{1 + \frac{\mu}{\xi} e^{-\lambda_k}}.$$

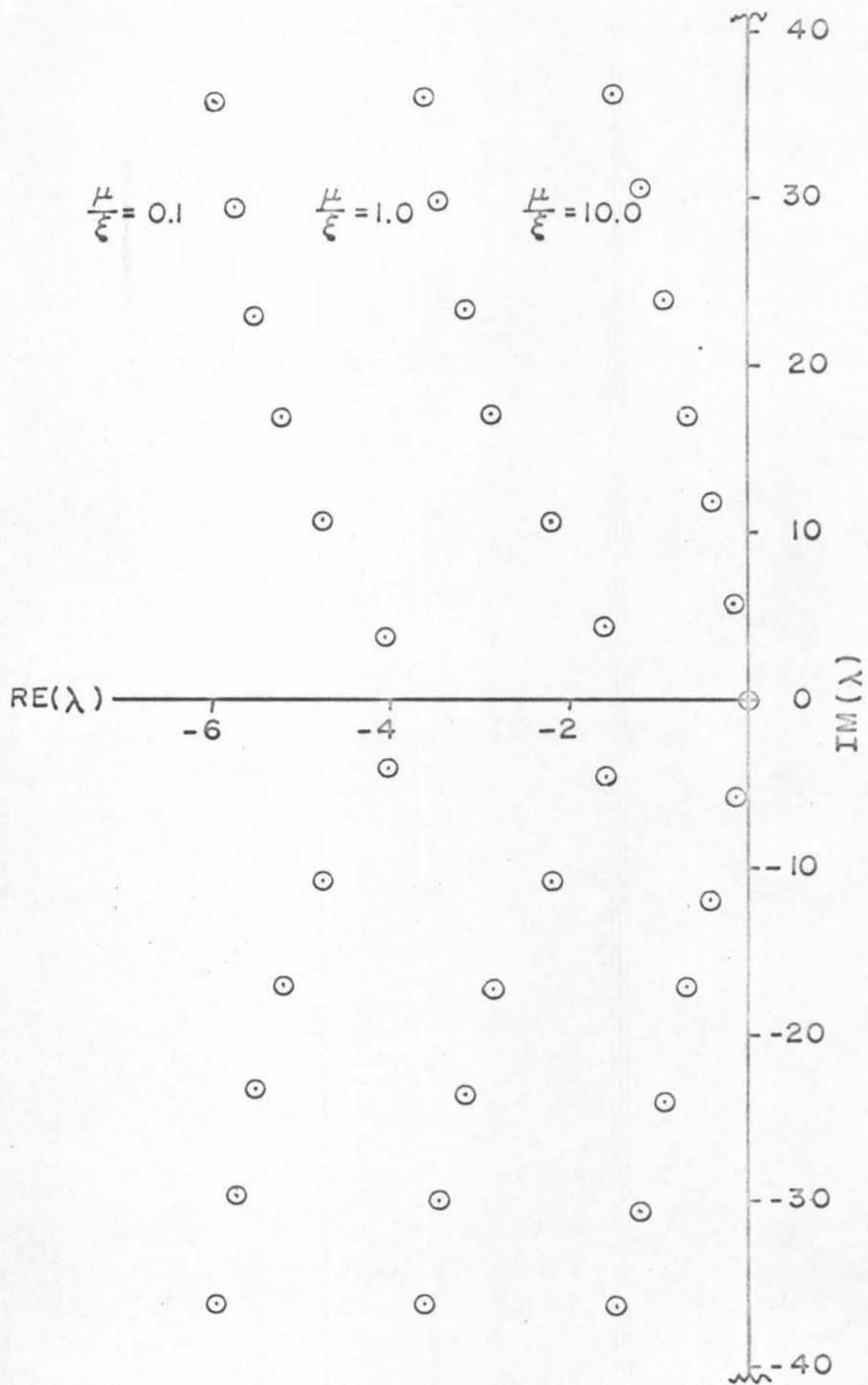


FIGURE 2.2 SAMPLE POLE LOCATIONS

By factoring out the contribution from the pole at the origin, and summing over conjugate pairs, we obtain the solution for $\psi(\epsilon)$:

$$\psi(\epsilon) = \frac{1}{1 + \frac{\mu}{\xi}} + 2 \sum_{k=1}^{\infty} e^{-\alpha_k(s-\epsilon)} \quad (2.15)$$

$$\frac{(1 + \frac{\mu}{\xi} e^{-\alpha_k} \cos \tau_k) \cos \tau_k(s-\epsilon) - (\frac{\mu}{\xi} e^{-\alpha_k} \sin \tau_k) \sin \tau_k(s-\epsilon)}{(1 + \frac{\mu}{\xi} e^{-\alpha_k} \cos \tau_k)^2 + (\frac{\mu}{\xi} e^{-\alpha_k} \sin \tau_k)^2}$$

The uniform convergence of this infinite series has been established by Bellman and Cooke⁽⁴⁰⁾. The convergence proof holds only for this constant coefficient case. We note the asymptotic solution, valid when $1 \leq \epsilon \ll s$, can be identified as the constant leading term

$$\psi(\epsilon) \sim \frac{1}{1 + \frac{\mu}{\xi}} \quad (2.16)$$

With the solution thus specified in the region above threshold, we can turn our attention to the subthreshold region distribution, described by Eqn. 2.7c. The solution to the equation can be written down:

$$\psi_b(\epsilon) = \psi(1) + \frac{\mu}{\xi} \int_{\epsilon+1}^2 \psi(\epsilon') d\epsilon', \quad (2.17)$$

where $\psi(\epsilon)$ comes from Eqn. 2.15.

The complete solution is demonstrated in Figure 2.3 for various values of the inelastic to elastic ratio μ/ξ (and a source energy chosen arbitrarily at $s=10$). We see that as μ/ξ increases the solution becomes

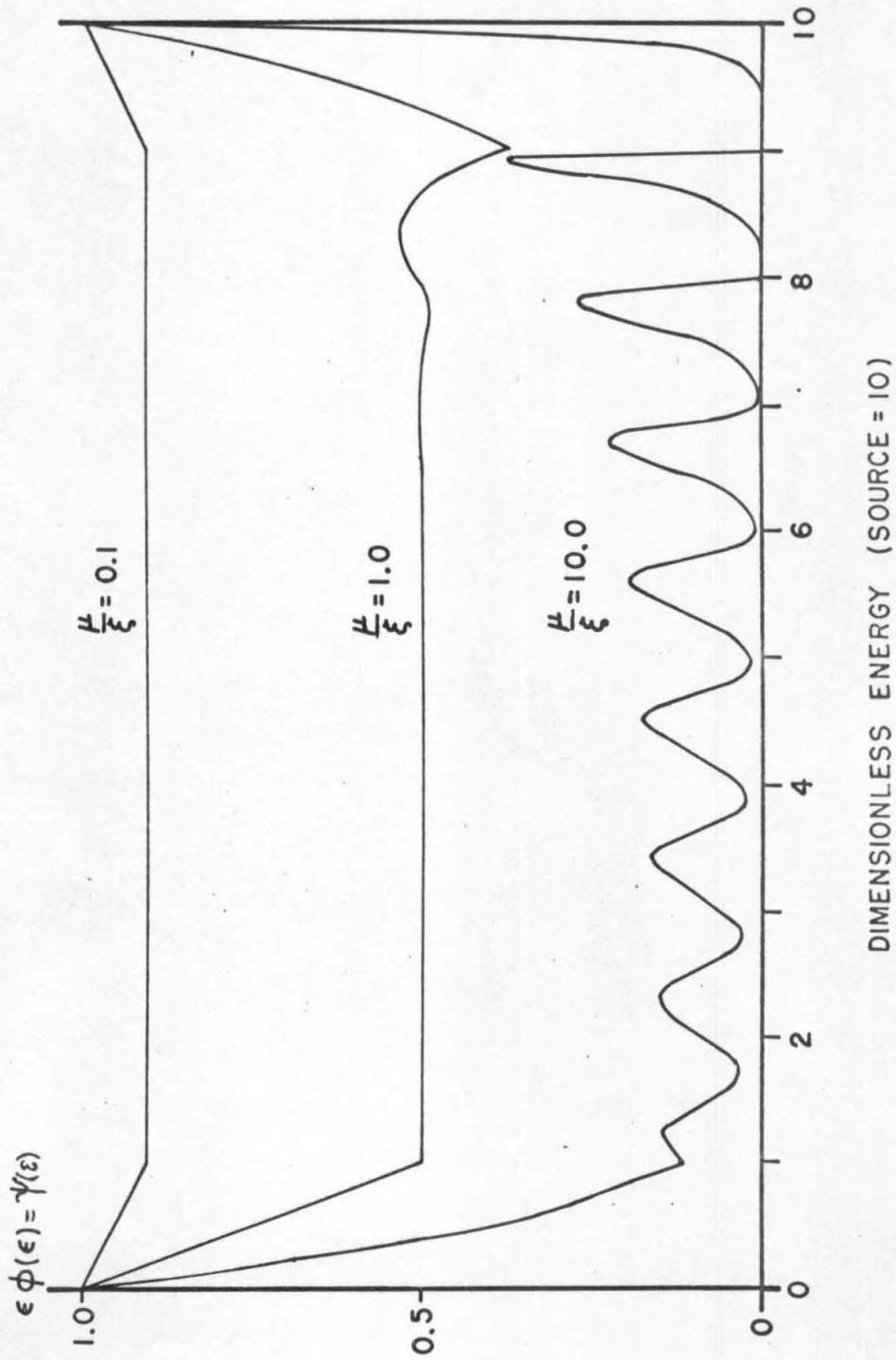


FIGURE 2.3 ONE LEVEL SOLUTIONS

more oscillatory in nature. This reflects the trend mentioned before, that in the limit as μ/ξ becomes very large, the only areas of non-zero solution lie very close to s , $s-1$, $s-2$,

If inelastic scattering were not present, the solution for $\psi(\epsilon)$ would be unity. This is a consequence of modeling elastic scattering with Fermi age theory. Thus inclusion of inelastic scattering distorts the distribution considerably. However, the solution for $\epsilon\varphi(\epsilon)$ does recover to unity as $\epsilon \rightarrow 0$ for all values of μ/ξ shown. This is indeed no accident, for it is demanded by neutron conservation in this absorptionless case. In Appendix II we prove that the recovery is to be expected under broad assumptions about the inelastic and elastic mechanisms.

In Chapter I it was pointed out that a popular method for treating inelastic scattering was to approximate the inelastic kernel by an evaporation kernel. Having calculated the distribution directly for a single discrete inelastic level, we can now do a comparison calculation using the synthetic kernel. This comparison may be unfair because the validity of the evaporation kernel hinged on the excitation of a large number of inelastic levels. Certainly no claim is made that good results can be obtained with a single level. On the other hand we see these techniques of approximate analysis applied, as an expediency, to many cases where the inelastic process is dominated by very few levels.

We shall employ a separable inelastic kernel similar to the form suggested by Okrent⁽¹¹⁾, and mentioned in Chapter I:

$$K_{in}(E' \rightarrow E) = h(E')g(E), \quad (2.18)$$

where

$$g(E) = \frac{E}{T^2} e^{-E/T}. \quad (2.19)$$

The function $h(E')$ is related to $g(E)$ via a requirement of neutron conservation. Since we require that the inelastically scattered neutron appear with unit probability at some lower energy than it originally had, we have

$$h(E') \int_0^{E'} g(E) dE = 1.$$

Thus

$$h(E') = \left[1 - e^{-\frac{E'}{T}} \left(1 + \frac{E'}{T} \right) \right]^{-1}. \quad (2.20)$$

If we call the inelastic threshold energy E_1 , then the steady state balance equation for energies above the threshold becomes

$$\xi \frac{d}{dE} (\Sigma_s(E) \cdot E\varphi(E)) - \Sigma_{ne}(E)\varphi(E) + S(E) + g(E) \int_E^{E_s} h(E') \Sigma_{in}(E')\varphi(E') dE' = 0 \quad E_1 \leq E < E_s. \quad (2.21)$$

Here, E_s is the energy above which no source neutrons appear. The balance equation below threshold, $0 \leq E \leq E_1$, is similar, except that the lower limit of integration in the inelastic integral is fixed at $E = E_1$. The resultant equation is much easier to solve.

To make Eqn. 2.21 dimensionless we perform the same transformation as that which led to Eqn. 2.2, defining in addition

$$g(E) = \bar{g}(\epsilon) \quad (2.22)$$

$$h(E') = \bar{h}(\epsilon').$$

We thus obtain, for $1 \leq \epsilon \leq s$:

$$\xi \frac{d}{d\epsilon} \left(\sum_s(\epsilon) \psi(\epsilon) \right) - \frac{\sum_{ne}(\epsilon)}{\epsilon} \psi(\epsilon) + S(\epsilon) + \bar{g}(\epsilon) E_1 \int_{\epsilon}^s \bar{h}(\epsilon') \frac{\sum_{in}(\epsilon')}{\epsilon'} \psi(\epsilon') d\epsilon' = 0, \quad (2.23)$$

where $\psi(\epsilon) = \epsilon \varphi(\epsilon)$.

If we now make the same assumptions about the cross sections and source as we made in the discrete level analysis (constant elastic cross section, linear inelastic cross section, no absorption, mono-energetic source), we have the following set of equations:

$$\psi(\epsilon) = 0 \quad \epsilon > s \quad (2.24a)$$

$$\frac{d\psi(\epsilon)}{d\epsilon} + \frac{\mu}{\xi} [E_1 \bar{g}(\epsilon)] \int_{\epsilon}^s \bar{h}(\epsilon') \psi(\epsilon') d\epsilon' - \frac{\mu}{\xi} \psi(\epsilon) = 0 \quad ; \quad \psi(s) = 1 \quad 1 \leq \epsilon \leq s \quad (2.24b)$$

$$\frac{d\psi_b(\epsilon)}{d\epsilon} + \frac{\mu}{\xi} [E_1 \bar{g}(\epsilon)] \int_1^s \bar{h}(\epsilon') \psi(\epsilon') d\epsilon' = 0 \quad ; \quad \psi_b(1) = \psi(1) \quad 0 \leq \epsilon \leq 1. \quad (2.24c)$$

Given the inelastic kernel specified in Eqns. 2.19 and 2.20, we evaluate the components of the dimensionless kernel:

$$[E_1 \bar{g}(\epsilon)] = \gamma^2 \epsilon e^{-\gamma \epsilon} \quad (2.25)$$

$$\bar{h}(\epsilon') = [1 - e^{-\gamma \epsilon'} (\gamma \epsilon' + 1)]^{-1},$$

where $\gamma = E_1/T$, the ratio of the threshold energy to the nuclear temperature selected. How is this parameter to be assigned? From Eqn. 2.25

we find that the peak in the probability of final energies occurs at $\epsilon = 1/\gamma$. Quite crudely, we should thus choose γ somewhere in the range $1/s < \gamma < \infty$. This hardly serves as a guide, but rather suggests limits we must observe.

The solution to Eqn. 2.24c is generated once the solution to Eqn. 2.24b is known. Because we've chosen the kernel to be separable, we can differentiate the latter equation to obtain a second order ordinary differential equation:

$$\frac{d}{d\epsilon} \left[\frac{1}{E_1 \bar{g}(\epsilon)} \frac{d\psi(\epsilon)}{d\epsilon} \right] - \frac{\mu}{\xi} \frac{d}{d\epsilon} \left[\frac{1}{E_1 \bar{g}(\epsilon)} \psi(\epsilon) \right] - \frac{\mu}{\xi} \bar{h}(\epsilon) \psi(\epsilon) = 0; \quad (2.24b')$$

$$\psi(s) = 1, \quad \left. \frac{d\psi(\epsilon)}{d\epsilon} \right|_{\epsilon=s} = \frac{\mu}{\xi}, \quad 1 \leq \epsilon \leq s.$$

Rather than deal with Eqn. 2.24b', we can find a numerical solution to Eqn. 2.24 for a given value of nuclear temperature.

We now calculate the solution for two of the values of μ/ξ studied in the discrete level analysis. Nuclear temperatures are varied in both cases between physically reasonable values of $.1 < \gamma < 1$. The results are shown in Figure 2.4.

We note a rather large discrepancy between the discrete level solution and any of the evaporative kernel distributions. While these results were to some extent anticipated, the variations due to changes in nuclear temperature (even for small values of μ/ξ) are surprising. This theme will recur throughout the several examples presented in this study. Sweeping conclusions should not be made on the basis of

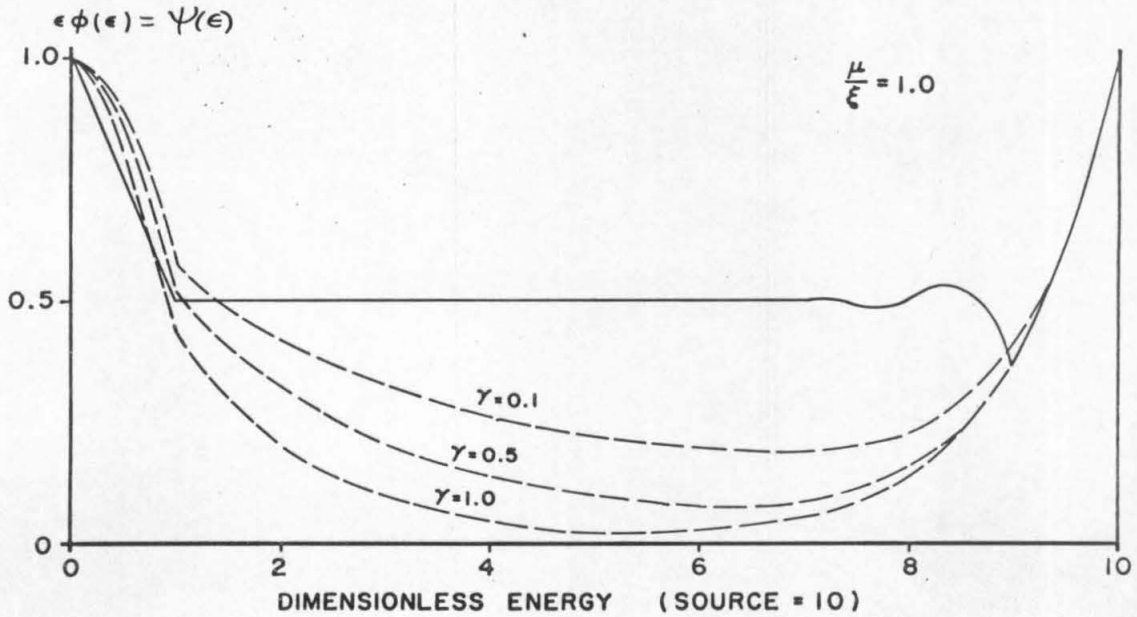
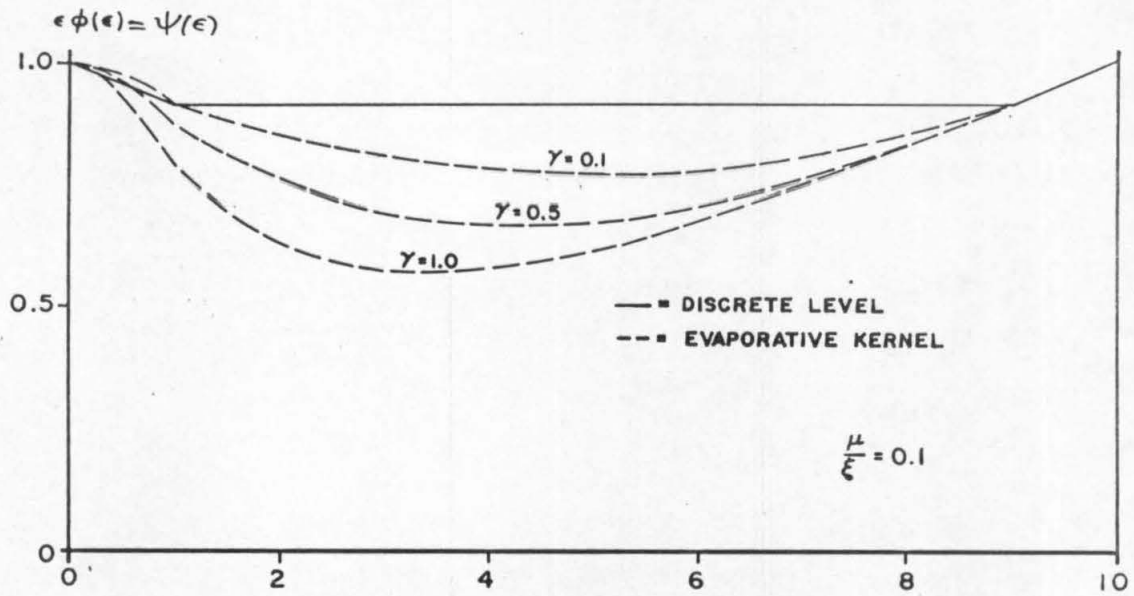


FIGURE 2.4 SINGLE LEVEL COMPARISON

this comparison with a single inelastic level. Rather, we should keep the result in mind as we consider multiple level problems in a later section.

Finally, we can use the solution found in this section as a one-sided Green's function to specify the solution for an arbitrary source distribution. With the cross sections we've taken, the solution above threshold can be written down:

$$\psi(\epsilon) = \int_{\epsilon}^s G(x - \epsilon; \frac{\mu}{\xi}) S(x) dx \quad 1 \leq \epsilon \leq s \quad (2.26)$$

where $G(z; \frac{\mu}{\xi})$ is the solution to Eqn. 2.7b with the coordinates transformed to $z = s - \epsilon$:

$$\frac{dG(z; \frac{\mu}{\xi})}{dz} - \frac{\mu}{\xi} G(z-1; \frac{\mu}{\xi}) + \frac{\mu}{\xi} G(z; \frac{\mu}{\xi}) = 0 \quad (z > 0), \quad (2.27)$$

with

$$G(0^+, \frac{\mu}{\xi}) = 1 \quad , \quad G(z, \frac{\mu}{\xi}) = 0 \quad (z < 0).$$

The functions $G(z; \frac{\mu}{\xi})$ are shown in Figure 2.3 for three values of μ/ξ . We view this figure in z language by remembering $\epsilon = s$ corresponds to $z = 0$. We see that the asymptotic form in z coordinate is:

$$\lim_{z \rightarrow \infty} G(z; \frac{\mu}{\xi}) = \frac{1}{1 + \frac{\mu}{\xi}}. \quad (2.28)$$

Below threshold we use an equation analogous to Eqn. 2.7c, where the source of neutrons is computed from Eqn. 2.26.

C. Linear Inelastic Cross Sections – Multiple Levels

Consider now the inclusion of additional inelastic levels. Retaining zero absorption and constant elastic scattering cross section, we assume that the inelastic cross sections of the individual levels are all linear:

$$\frac{\Sigma_{in}^j(\epsilon)}{\Sigma_s} = \begin{cases} \mu_j \epsilon & \epsilon \geq \epsilon_j \\ 0 & \epsilon < \epsilon_j \end{cases} \quad (2.29)$$

The regional nature of the multiple level problem was mentioned before. We can, however, write a compact balance equation for this multiple level case:

$$\frac{d\psi(\epsilon)}{d\epsilon} + \sum_{j=1}^N \frac{\mu_j}{\xi} \psi(\epsilon + \epsilon_j) - \left[\sum_{j=1}^N \frac{\mu_j}{\xi} H(\epsilon - \epsilon_j) \right] \psi(\epsilon) = 0, \quad (2.30)$$

with

$$\psi(s) = 1$$

$$\psi(\epsilon) = 0 \quad \epsilon > s$$

$H(\epsilon - \epsilon_j)$ = the Heaviside function

N = the number of inelastic levels considered

ϵ_j = dimensionless thresholds ($\epsilon_1 = 1, \epsilon_2 = \frac{E_2}{E_1}; \dots$).

If we agree that a region is defined by the inelastic thresholds, then Eqns. 2.7 are actually $N + 1$ equations describing the distribution in each region. An example of the result of explicitly writing out Eqn. 2.30 for each region is shown by Eqns. 2.7 for a single inelastic level.

The solution to Eqn. 2.30 is greatly complicated by the level structure. In order to demonstrate the analytical difficulties involved in making the transition to multiple levels, consider the case of only two excited states. We will return to a discussion of the general problem somewhat later.

Equation 2.30 is then three equations describing the interesting regions:

$$\psi(\epsilon) = 0 \quad \epsilon > s \quad (2.31a)$$

$$\frac{d\psi(\epsilon)}{d\epsilon} + \frac{\mu_1}{\xi} \psi(\epsilon+1) + \frac{\mu_2}{\xi} \psi(\epsilon+\epsilon_2) - \left(\frac{\mu_1 + \mu_2}{\xi}\right) \psi(\epsilon) = 0 \quad ; \quad \psi(s) = 1 \quad \epsilon_2 \leq \epsilon \leq s \quad (2.31b)$$

$$\frac{d\psi(\epsilon)}{d\epsilon} + \frac{\mu_1}{\xi} \psi(\epsilon+1) + \frac{\mu_2}{\xi} \psi(\epsilon+\epsilon_2) - \frac{\mu_1}{\xi} \psi(\epsilon) = 0 \quad ; \quad \psi(\epsilon_2^-) = \psi(\epsilon_2^+) \quad 1 \leq \epsilon \leq \epsilon_2 \quad (2.31c)$$

$$\frac{d\psi_b(\epsilon)}{d\epsilon} + \frac{\mu_1}{\xi} \psi(\epsilon+1) + \frac{\mu_2}{\xi} \psi(\epsilon+\epsilon_2) = 0 \quad ; \quad \psi_b(1^-) = \psi(1^+) \quad 0 \leq \epsilon \leq 1 \quad (2.31d)$$

The most difficult equation is Eqn. 2.31b, containing both difference terms simultaneously. Once the solution is known, we can cascade through the remaining two equations using solutions in higher regions as source terms.

Defining the Laplace transform as in Eqn. 2.8, we continue Eqn. 2.31b into the region $\epsilon < \epsilon_2$ and take the transform:

$$\tilde{\psi}(\lambda) = \frac{e^{\lambda s}}{\lambda + \left(\frac{\mu_1 + \mu_2}{\xi}\right) - \frac{\mu_1}{\xi} e^{-\lambda} - \frac{\mu_2}{\xi} e^{-\lambda \epsilon_2}} \quad (2.32)$$

Formal inversion yields

$$\psi(\epsilon) = \frac{1}{2\pi i} \int_{\text{Br}} \frac{e^{\lambda(s-\epsilon)}}{\left[\lambda + \frac{\mu_1 + \mu_2}{\xi} - \frac{\mu_1}{\xi} e^{-\lambda} - \frac{\mu_2}{\xi} e^{-\lambda \epsilon_2} \right]} d\lambda. \quad (2.33)$$

The transcendental expression for the singularities is now somewhat more complicated. There are still an infinity of simple poles, which occur in conjugate pairs, corresponding to the zeroes of the denominator:

$$\lambda + \frac{\mu_1 + \mu_2}{\xi} - \frac{\mu_1}{\xi} e^{-\lambda} - \frac{\mu_2}{\xi} e^{-\lambda \epsilon_2} = 0. \quad (2.34)$$

Again let $\lambda = \sigma + i\tau$. Substitution into Eqn. 2.34, followed by consideration of real and imaginary parts, yields

$$\sigma + \frac{\mu_1 + \mu_2}{\xi} - \frac{\mu_1}{\xi} e^{-\sigma} \cos \tau - \frac{\mu_2}{\xi} e^{-\sigma \epsilon_2} \cos \epsilon_2 \tau = 0 \quad (2.35)$$

$$\tau + \frac{\mu_1}{\xi} e^{-\sigma} \sin \tau + \frac{\mu_2}{\xi} e^{-\sigma \epsilon_2} \sin \epsilon_2 \tau = 0. \quad (2.36)$$

Statements about the general nature of the roots to Eqn. 2.34 are less informative than in the single level case considered in the last section (Eqn. 2.11). Again the origin is always a solution, giving rise once more to a constant asymptotic solution. Since roots occur in conjugate pairs, we need only examine the upper half of the complex plane. In Eqn. 2.36, clearly no solutions are possible in the upper half-plane if $\sin \tau$ and $\sin \epsilon_2 \tau$ are simultaneously positive. Thus forbidden zones again appear, but their periodicity and extent is greatly reduced.

Given a pole at $\lambda_k = \alpha_k + i\tau_k$, we can calculate the residue:

$$R(\lambda_k) = \frac{1}{1 + \frac{\mu_1}{\xi} e^{-\lambda_k} + \frac{\mu_2}{\xi} \epsilon_2 e^{-\lambda_k \epsilon_2}}. \quad (2.37)$$

By summing over conjugate pairs, the solution valid in the region $\epsilon_2 \leq \epsilon \leq s$ can be obtained:

$$\psi(\epsilon) = \frac{1}{1 + \frac{\mu_1}{\xi} + \frac{\mu_2 \epsilon_2}{\xi}} + 2 \sum_{k=1}^{\infty} \frac{e^{\alpha_k (s-\epsilon)}}{c_k^2 + f_k^2} \left[c_k \cos \tau_k (s-\epsilon) - f_k \sin \tau_k (s-\epsilon) \right] \quad (2.38)$$

where

$$c_k = \left(1 + \frac{\mu_1}{\xi} e^{-\alpha_k} \cos \tau_k + \frac{\mu_2 \epsilon_2}{\xi} e^{-\epsilon_2 \alpha_k} \cos \epsilon_2 \tau_k \right)$$

$$f_k = \left(\frac{\mu_1}{\xi} e^{-\alpha_k} \sin \tau_k + \frac{\mu_2 \epsilon_2}{\xi} e^{-\epsilon_2 \alpha_k} \sin \epsilon_2 \tau_k \right).$$

The solution specified in Eqn. 2.38 can again be viewed as a one-sided Green's function for the two-level operator in the region above the highest inelastic threshold. Thus for arbitrary source distribution, we can calculate the solution above the second threshold by:

$$\psi(\epsilon) = \int_{\epsilon}^s G(x-\epsilon; \frac{\mu_1}{\xi}; \frac{\mu_2}{\xi}) S(x) dx \quad \epsilon_2 \leq \epsilon < s. \quad (2.39)$$

The function $G(z; \frac{\mu_1}{\xi}; \frac{\mu_2}{\xi})$ is the solution to Eqn. 2.31b with the coordinate transformed to $z = s - \epsilon$, $z \geq 0$:

$$\frac{dG\left(z; \frac{\mu_1}{\xi}; \frac{\mu_2}{\xi}\right)}{dz} + \frac{\mu_1 + \mu_2}{\xi} G\left(z; \frac{\mu_1}{\xi}; \frac{\mu_2}{\xi}\right) - \frac{\mu_1}{\xi} G\left(z-1; \frac{\mu_1}{\xi}; \frac{\mu_2}{\xi}\right) - \frac{\mu_2}{\xi} G\left(z-\epsilon_2; \frac{\mu_1}{\xi}; \frac{\mu_2}{\xi}\right) = 0 \quad (z > 0) \quad (2.40)$$

with

$$G\left(0^+, \frac{\mu_1}{\xi}; \frac{\mu_2}{\xi}\right) = 1, \quad G\left(z, \frac{\mu_1}{\xi}; \frac{\mu_2}{\xi}\right) = 0 \quad (z < 0).$$

Returning to the original problem posed in Eqn. 2.31, we can use our known solution for $\epsilon_2 \leq \epsilon \leq s$ to solve Eqn. 2.31c for $\psi(\epsilon)$ in the region $1 \leq \epsilon < \epsilon_2$. Since in this energy region only a single inelastic level operates, we can use the one-sided Green's function shown in the previous section to calculate the solution. We use Eqn. 2.38 to specify the source, and we must supply the homogeneous solution to match fluxes at $\epsilon = \epsilon_2$:

$$\psi(\epsilon) = \psi(\epsilon_2) G\left(\epsilon_2 - \epsilon; \frac{\mu_1}{\xi}\right) + \int_{\epsilon}^{\epsilon_2} G\left(\epsilon' - \epsilon; \frac{\mu_1}{\xi}\right) S(\epsilon') d\epsilon' \quad 1 \leq \epsilon \leq \epsilon_2, \quad (2.41)$$

where $\psi(\epsilon_2)$ comes from Eqn. 2.38, and $G(z; \frac{\mu_1}{\xi})$ is the solution to Eqn. 2.27. The term $S(\epsilon')$ in the integrand is the source of neutrons in $1 \leq \epsilon < \epsilon_2$ due to inelastic events above $\epsilon = \epsilon_2$. We have, by computation of reaction rates,

$$S(\epsilon') = \begin{cases} \frac{\mu_2}{\xi} \psi(\epsilon' + \epsilon_2) + \frac{\mu_1}{\xi} \psi(\epsilon' + 1) & \epsilon_2 - 1 \leq \epsilon' \leq \epsilon_2 \\ \frac{\mu_2}{\xi} \psi(\epsilon' + \epsilon_2) & 1 \leq \epsilon' < \epsilon_2 - 1, \end{cases} \quad (2.42)$$

where the functions $\psi(x)$ are computed from Eqn. 2.38. Note that if $\epsilon_2 - 1 \leq 1$, then the first option above is the only component of the source. If the source energy is high enough so that $\psi(\epsilon)$ in Eqn. 2.38 takes on its asymptotic value around $\epsilon = \epsilon_2^+$, then the source term given in Eqn. 2.42 is shown in Figure 2.5.

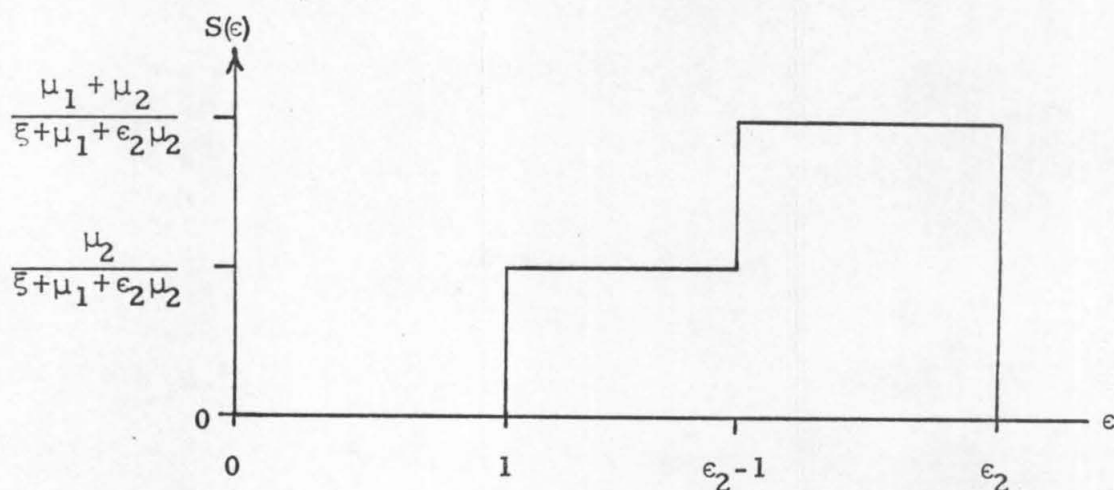


Figure 2.5 Source in Intermediate Region

Finally the solution for the distribution below all thresholds ($0 \leq \epsilon < 1$) is found by solving Eqn. 2.31d. We find

$$\psi_b(\epsilon) = \psi(1) + \frac{\mu_1}{\xi} \int_{\epsilon+1}^2 \psi(\epsilon') d\epsilon' + \frac{\mu_2}{\xi} \int_{\epsilon+\epsilon_2}^{\epsilon_2+1} \psi(\epsilon') d\epsilon', \quad (2.43)$$

where the functions ψ are determined by the value of the argument.

Considering now an example of two inelastic levels with linear cross sections, we take the following conditions:

$$\epsilon_2 = 2.0 \quad \frac{\mu_1}{\xi} = 1.0 \quad \frac{\mu_2}{\xi} = 0.2.$$

The inelastic cross sections are thus depicted in Figure 2.6.

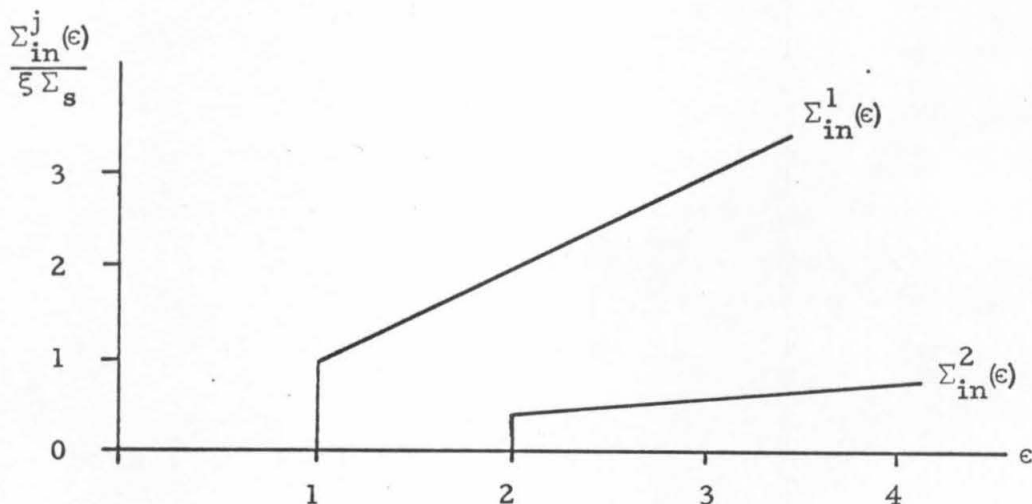


Figure 2.6 Example Inelastic Cross Sections

The first several poles corresponding to solutions to Eqn. 2.34 are shown in Figure 2.7. These poles form the solution for the two-level Green's function $G(z; 1.0; 0.2)$. With the pole locations known, application of Eqn. 2.38 yields the solution for $\epsilon_2 \leq \epsilon \leq s$. In the one level region $1 \leq \epsilon \leq \epsilon_2$, the one-sided Green's function, $G(z; 1.0)$, is known. In this example the function G is particularly simple because we choose $\epsilon_2 = 2$. Since $\epsilon_2 - \epsilon_1 (\equiv \epsilon_2 - 1)$ is not greater than unity, the Green's function for the region can be found by considering Eqn. 2.27 in the region $0 < z < 1$. We then have a simple first order equation to solve. That solution is

$$G\left(x-\epsilon; \frac{\mu_1}{\xi}\right) = e^{-\frac{\mu_1}{\xi}(x-\epsilon)} \quad 0 \leq x - \epsilon \leq 1.$$

If $\epsilon_2 > 2$, then $G(x-\epsilon; \frac{\mu_1}{\xi})$ is much more complicated (see Figure 2.3). In this case we use the infinite series representation of $G(z; \frac{\mu_1}{\xi})$ (Eqn. 2.15).

Choosing the source at $s=10$, we allow essentially complete development of the asymptotic value of $\psi(\epsilon)$ for $\epsilon > \epsilon_2$. The source for the solution in the intermediate region is like that shown in Figure 2.5 (remember that $\epsilon_2 - 1 = 1$ in this case).

As in the previous section, we now compare the results of our discrete level solution with the solution given by assuming an evaporative inelastic kernel. Using the kernel described in Eqn. 2.18, we follow the same procedure as before, and numerically solve a set of equations analogous to Eqns. 2.24, except that we add the second inelastic level. The evaporative kernel solution for various nuclear temperatures is compared with the discrete level solution in Figure 2.8. Again we see wide variations from different nuclear temperatures.

Returning now to the problem of an arbitrary number of inelastic levels characterized by linear cross sections (posed by Eqn. 2.30), we can generalize the methods used for one and two levels. To avoid confusion, we define regions bounded by inelastic thresholds

$$k^{\text{th}} \text{ region} \equiv \epsilon \in [\epsilon_k, \epsilon_{k+1}).$$

If N inelastic levels are considered, the highest energy region is the N th, with boundaries ϵ_N and $\epsilon_{N+1} \equiv s$ (the source energy). The lowest region (region 0) is bounded by zero and the first inelastic threshold

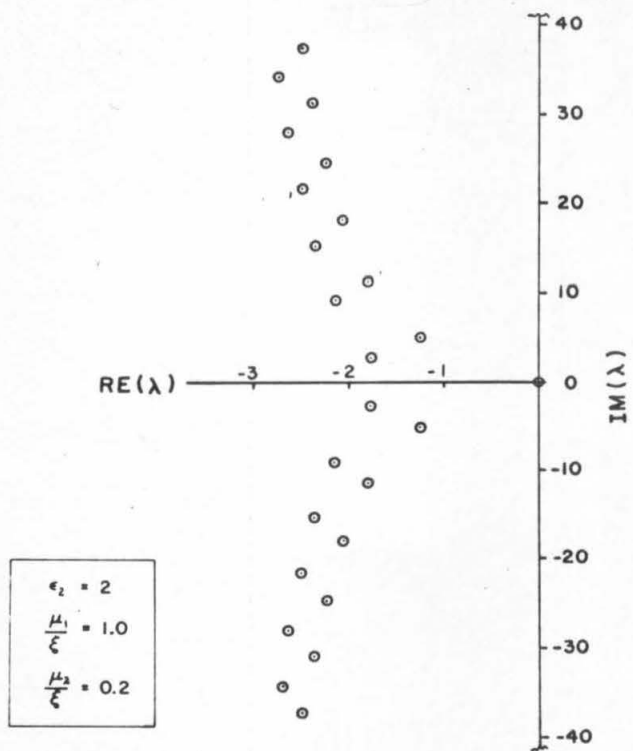


FIGURE 2.7 SAMPLE POLE LOCATIONS

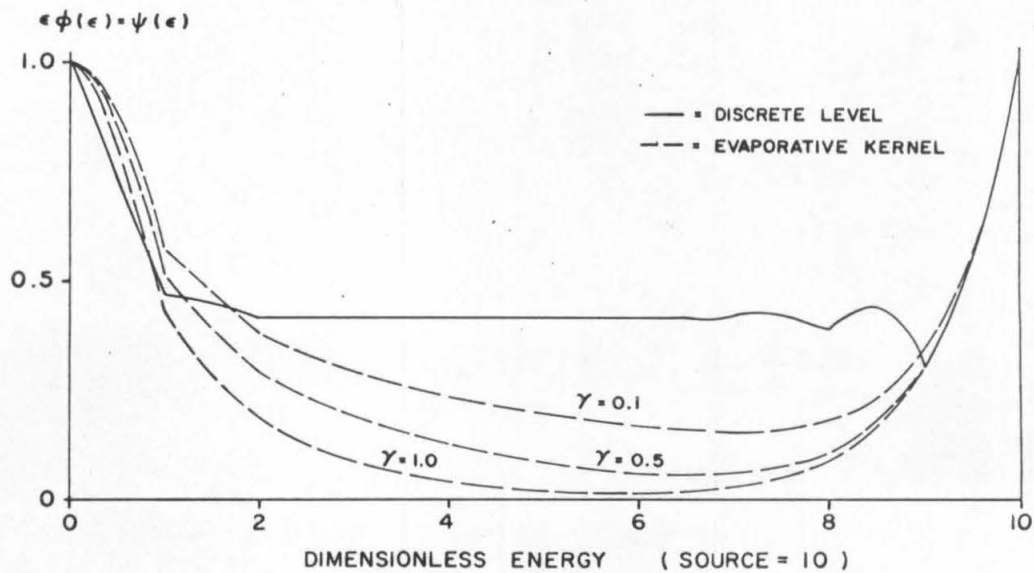


FIGURE 2.8 TWO LEVEL COMPARISON

($\epsilon = 1$). For all regions (except region 0, which we temporarily exclude) a one-sided Green's function can be found via Laplace transformation of a suitable balance equation. We extract the equation for the Green's function from the balance equation 2.30. For the k^{th} region, we have

$$\frac{d\tilde{G}_k(\epsilon)}{d\epsilon} + \sum_{j=1}^N \frac{\mu_j}{\xi} \tilde{G}_k(\epsilon + \epsilon_j) - \left(\sum_{j=1}^k \frac{\mu_j}{\xi} \right) \tilde{G}_k(\epsilon) = 0 \quad k=1, 2, \dots, N \quad (2.44)$$

where

$$\epsilon_k \leq \epsilon < \epsilon_{k+1} \quad k=1, 2, \dots, N$$

$$\tilde{G}_k(\epsilon_{k+1}) = 1$$

$$\tilde{G}_k(\epsilon) = 0 \quad \epsilon > \epsilon_{k+1}$$

Transforming coordinates, we let

$$x = \epsilon_{k+1} - \epsilon$$

$$G_k(x) \equiv \tilde{G}_k(\epsilon).$$

Equation 2.44 then becomes

$$\frac{dG_k(x)}{dx} + \left(\sum_{j=1}^k \frac{\mu_j}{\xi} \right) G_k(x) - \sum_{j=1}^N \frac{\mu_j}{\xi} G_k(x - \epsilon_j) = 0 \quad k=1, 2, \dots, N, \quad (2.45)$$

where

$$0 \leq x \leq \epsilon_{k+1} - \epsilon_k \quad k=1, 2, \dots, N$$

$$G_k(0) = 1$$

$$G_k(x) = 0 \quad x < 0.$$

Note the notation has been slightly changed from that used previously. What was termed $G(z; \frac{\mu_1}{\xi})$ is now $G_1(z)$, and so on. This change will conform to notation used later with arbitrary inelastic cross sections.

Laplace transformation of either Eqns. 2.44 or 2.45 will yield a transcendental characteristic equation, again with an infinite number of simple poles in each energy region. Since the coefficient of the second term in Eqn. 2.45 depends on k , the location of these poles in λ -plane will vary with the energy region considered. Given the pole locations for the k^{th} energy region, the distribution described in Eqn. 2.30 can be recovered from the Green's function:

$$\psi(\epsilon) = \psi(\epsilon_{k+1}) G_k(\epsilon_{k+1} - \epsilon) + \int_{\epsilon}^{\epsilon_{k+1}} G_k(\epsilon' - \epsilon) S_k(\epsilon') d\epsilon' \quad \epsilon_k \leq \epsilon \leq \epsilon_{k+1}, \quad (2.46)$$

where

$$S_k(\epsilon') = \sum_{j=1}^N \frac{\mu_j}{\xi} \psi(\epsilon' + \epsilon_j) \left\{ H(\epsilon' + \epsilon_j - \epsilon_{k+1}) \right\} \quad k=1, 2, \dots, N-1, \quad (2.47)$$

and $H(\dots)$ is the Heaviside function. Equations 2.46 and 2.47 are valid for regions 1 through $N-1$. In the highest energy region we have

$$\psi(\epsilon) = G_N(s - \epsilon) \quad \epsilon_N \leq \epsilon \leq s. \quad (2.48)$$

With the solution for all regions above the first inelastic threshold specified, we can determine the solution in the subthreshold range

(region 0):

$$\psi(\epsilon) = \psi(1) + \sum_{j=1}^N \frac{\mu_j}{\xi} \int_{\epsilon + \epsilon_j}^{\epsilon_j + 1} \psi(\epsilon') d\epsilon \quad 0 \leq \epsilon < 1. \quad (2.49)$$

The difficulty in applying this regional Green's function approach comes from the complexity of the form of the various Green's functions. In the examples (see Figures 2.4 and 2.8), we can see the one and two level Green's functions are quite complicated. As more levels are added in higher regions the difficulties are compounded. A tremendous simplification in these multiple level Green's functions is possible if we make a physically reasonable assumption about the structure of the inelastic levels. This assumption simply is

$$\max_{k=1, \dots, N} (\epsilon_{k+1} - \epsilon_k) \leq 1. \quad (2.50)$$

We thus require the maximum dimensionless width of any region be less than the fundamental width (which is normalized to unity). This is indeed the case with many nuclei. Mathematically this implies Eqn. 2.45 is no longer a differential difference equation, but rather just an ordinary differential equation. This benefit will be detailed and explored in Chapter III, where we will generalize to any inelastic cross section.

D. Constant Inelastic Cross Section – Single Level

In the previous sections we considered steady state slowing down when the inelastic levels were characterized by linear cross sections which were discontinuous at the inelastic thresholds. While such

a model was mathematically convenient, it by no means reflects a universal physical phenomenon. We now turn attention toward a model of somewhat greater physical interest by specifying the inelastic cross section to be constant. Many isotopes have inelastic levels which exhibit nearly constant cross section behavior above threshold. An example is W^{184} , where the inelastic cross sections are roughly constant for the first few levels measured. ⁽⁴¹⁾ We shall retain earlier conditions about constant elastic cross section, zero absorption, and monoenergetic sources. We want to consider inelastic cross sections of the form

$$\frac{\Sigma_{in}(\epsilon)}{\Sigma_s} = \begin{matrix} \mu_0 & \epsilon \geq 1 \\ 0 & \epsilon < 1. \end{matrix}$$

When substituted into Eqn. 2.4, we can write a familiar set of balance equations for the one level problem:

$$\psi(\epsilon) = 0 \quad \epsilon > s, \quad (2.51a)$$

$$\frac{d\psi(\epsilon)}{d\epsilon} + \frac{\mu_0}{\xi} \left[\frac{\psi(\epsilon+1)}{\epsilon+1} - \frac{\psi(\epsilon)}{\epsilon} \right] = 0 ; \quad \psi(s) = 1 \quad 1 \leq \epsilon \leq s, \quad (2.51b)$$

$$\frac{d\psi_b(\epsilon)}{d\epsilon} + \frac{\mu_0}{\xi} \frac{\psi(\epsilon+1)}{\epsilon+1} = 0 ; \quad \psi_b(1^-) = \psi(1^+) \quad 0 < \epsilon \leq 1. \quad (2.51c)$$

As before it is Eqn. 2.51b that is the challenge. Previously we employed the method of formally continuing our balance equation through $\epsilon=0$ in defining a Laplace transform. In the present case, however, $\epsilon=0$ and $\epsilon=-1$ are singular points of the equation, and the continuation

is impeded. It is therefore fruitful, although apparently not mandatory (generalized functions can probably be employed to remove the difficulty⁽⁴²⁾), to consider the equation adjoint⁽⁴⁰⁾ to Eqn. 2.51b. This technique was first used in inelastic scattering problems by Corngold and Yan⁽³⁹⁾.

Multiply Eqn. 2.51b (written with ϵ' as the independent variable) by some function $a(\epsilon', x)$ and integrate from $\epsilon' = \epsilon$ to $\epsilon' = s$. After an integration by parts we have

$$a(\epsilon', x) \psi(\epsilon') \Big|_{\epsilon}^s - \int_{\epsilon}^s \psi(\epsilon') \left\{ \frac{\partial a(\epsilon', x)}{\partial \epsilon'} + \frac{\mu_0}{\xi} \left(\frac{a(\epsilon', x)}{\epsilon'} - \frac{a(\epsilon'-1, x)}{\epsilon'} \right) \right\} d\epsilon' \tag{2.52}$$

$$- \int_{\epsilon}^{\epsilon+1} \frac{\mu_0}{\xi} \frac{a(\epsilon'-1, x)}{\epsilon'} \psi(\epsilon') d\epsilon' = 0.$$

We now demand our adjoint function satisfy the following relations:

$$\frac{\partial a(\epsilon', x)}{\partial \epsilon'} + \frac{\mu_0}{\xi} \frac{1}{\epsilon'} [a(\epsilon', x) - a(\epsilon'-1, x)] = 0 \quad \epsilon' > x, \tag{2.53a}$$

$$a(\epsilon', x) = 0 \quad \epsilon' < x, \tag{2.53b}$$

$$a(\epsilon', x) = 1 \quad \epsilon' = x. \tag{2.53c}$$

By choosing $x = \epsilon$, we see from Eqn. 2.52 that

$$\psi(\epsilon) = a(s, \epsilon), \tag{2.54}$$

and we have an alternate way of obtaining $\psi(\epsilon)$. If the inelastic cross section is left unspecified, the only adjoint equation requiring change is

Eqn. 2.53a, and we have

$$\frac{\partial a(\epsilon', x)}{\partial \epsilon'} + \frac{\sum_{\text{in}}(\epsilon')}{\epsilon' \xi \Sigma_s} [a(\epsilon', x) - a(\epsilon' - 1, x)] = 0 \quad \epsilon' > x. \quad (2.55)$$

Thus to solve Eqn. 2.51b for the distribution $\psi(\epsilon)$, we need to solve Eqns. 2.53 for the adjoint. Since Eqn. 2.51b applies above the inelastic threshold $\epsilon=1$, we are concerned with solving Eqns. 2.53 for $x \geq 1$. The singular point at $\epsilon'=0$ in Eqn. 2.53a is thus not encountered.

We solve for the adjoint in Eqn. 2.53a by defining another Laplace transform (let $x=\epsilon$):

$$\tilde{\alpha}(\lambda, \epsilon) = \int_{\epsilon}^{\infty} e^{-\lambda \epsilon'} a(\epsilon', \epsilon) d\epsilon'. \quad (2.56)$$

Laplace transformation of Eqn. 2.53a yields

$$\lambda \tilde{\alpha}(\lambda, \epsilon) + \frac{\mu_0}{\xi} \int_{\lambda}^{\infty} \tilde{\alpha}(\lambda', \epsilon) [1 - e^{-\lambda'}] d\lambda' = e^{-\lambda \epsilon}. \quad (2.57)$$

The contour is from the point λ to the point at positive infinity. For simplicity assume we do this along a straight line with constant imaginary part. We thus travel to the right parallel to the real axis. Note that as $|\lambda| \rightarrow \infty$, we must have $|\lambda \tilde{\alpha}(\lambda, \epsilon)| \rightarrow 0$. We will use this fact to specify constants of integration. By differentiation, we reduce Eqn. 2.57 to an ordinary differential equation. We have then that $\tilde{\alpha}(\lambda, \epsilon)$ is some solution of

$$\frac{\partial \tilde{\alpha}(\lambda, \epsilon)}{\partial \lambda} + \tilde{\alpha}(\lambda, \epsilon) \left[\frac{1 - \frac{\mu_0}{\xi} + \frac{\mu_0}{\xi} e^{-\lambda}}{\lambda} \right] = -\frac{\epsilon}{\lambda} e^{-\lambda \epsilon}. \quad (2.58)$$

The only singular point of this differential equation for $\tilde{a}(\lambda, \epsilon)$ is at $\lambda=0$. Thus the function $\tilde{a}(\lambda, \epsilon)$ will be analytic in the entire λ -plane (perhaps a cut λ -plane), excluding the origin. Treating ϵ as a parameter, a general solution to Eqn. 2.58 is easily found:

$$\begin{aligned} \tilde{a}(\lambda, \epsilon) = & \epsilon \int_{\lambda}^{\infty} d\lambda' \frac{e^{-\lambda'\epsilon}}{\lambda'} \exp \left\{ \int_{\lambda}^{\lambda'} \frac{\lambda'' (1 - \frac{\mu_0}{\xi}) + \frac{\mu_0}{\xi} e^{-\lambda''}}{\lambda''} d\lambda'' \right\} \\ & + C(\Delta) \exp \left\{ \int_{\lambda}^{\Delta} \frac{\lambda' (1 - \frac{\mu_0}{\xi}) + \frac{\mu_0}{\xi} e^{-\lambda'}}{\lambda'} d\lambda' \right\}, \end{aligned}$$

where Δ is any point in the complex plane, excluding the origin and the point at infinity. The particular $\tilde{a}(\lambda, \epsilon)$ we seek is specified by choosing the constant $C(\Delta)$. Recall we require $|\lambda \tilde{a}(\lambda, \epsilon)| \rightarrow 0$ as $|\lambda| \rightarrow \infty$. If we multiply the above equation by λ , and let $|\lambda| \rightarrow \infty$, we find the second term diverges unless $C(\Delta) = 0$. Thus the solution of Eqn. 2.57 for the transformed adjoint is

$$a(\lambda, \epsilon) = \epsilon \int_{\lambda}^{\infty} d\lambda' \frac{e^{-\lambda'\epsilon}}{\lambda'} \exp \left\{ \int_{\lambda}^{\lambda'} \frac{\lambda'' (1 - \frac{\mu_0}{\xi}) + \frac{\mu_0}{\xi} e^{-\lambda''}}{\lambda''} d\lambda'' \right\}. \quad (2.59)$$

This representation indicates a possible branch point at $\lambda=0$. Further examination reveals that at $\lambda=0$, the function $\tilde{a}(\lambda, \epsilon)$ has a simple pole. To see this, we make the expansion

$$e^{-\lambda''} = \sum_0^{\infty} \frac{(-\lambda'')^n}{n!}, \quad (2.60)$$

and substitute into Eqn. 2.59. We can integrate directly to obtain another form for $\tilde{a}(\lambda, \epsilon)$:

$$\tilde{a}(\lambda, \epsilon) = \frac{\epsilon}{\lambda} e^{\frac{\mu_0}{\epsilon} f(\lambda)} \int_{\lambda}^{\infty} d\lambda' e^{-\lambda' \epsilon} e^{-\frac{\mu_0}{\epsilon} f(\lambda')}. \quad (2.61)$$

The entire function $f(\lambda)$ is defined by

$$f(\lambda) = \lambda - \frac{\lambda^2}{2 \cdot 2!} + \frac{\lambda^3}{3 \cdot 3!} \cdots \quad (2.62)$$

Since $f(\lambda)$ is analytic throughout the λ -plane, Eqn. 2.61 yields $\lambda=0$ is simple pole, and $\tilde{a}(\lambda, \epsilon)$ is analytic everywhere else.

We calculate $\psi(\epsilon)$ from the Laplace inversion of $\tilde{a}(\lambda, \epsilon)$. The inverted adjoint function is

$$a(\epsilon', \epsilon) = \frac{1}{2\pi i} \int_{Br} d\lambda e^{\lambda \epsilon'} \tilde{a}(\lambda, \epsilon). \quad (2.63)$$

To find the distribution $\psi(\epsilon)$, we use Eqn. 2.54:

$$\psi(\epsilon) = a(s, \epsilon) = \frac{1}{2\pi i} \int_{Br} d\lambda e^{\lambda s} \tilde{a}(\lambda, \epsilon). \quad (2.64)$$

Complete inversion of $\tilde{a}(\lambda, \epsilon)$ is not possible. While the nature of the singularities is quite simple, we cannot advantageously close the Bromwich contour, and residue theory cannot be applied. The reason is that

closing the contour in the left half-plane gives us a contribution to $a(\epsilon', \epsilon)$ on the closing segment. In attempts to evaluate the Bromwich contour integral by straightforward integration (for example along the imaginary axis), one encounters a rapidly oscillating, poorly converging integrand.

Fortunately we don't need the full inversion to gain a great deal of insight. In fact $\psi(\epsilon)$ can be approximated by the residue from the simple pole at $\lambda=0$. This approximation gets better for large source energies. As $s \rightarrow \infty$, we call the residue at the origin an approximate form for the adjoint distribution. Taking the residue yields

$$\lim_{s \rightarrow \infty} a(s, \epsilon) \cong \epsilon \int_0^{\infty} dx e^{-\epsilon x} e^{-\frac{\mu_0}{\xi} f(x)}, \quad (2.65)$$

where $f(x)$ is calculated from Eqn. 2.62. By defining

$$\beta(\epsilon, \frac{\mu_0}{\xi}) \equiv \int_0^{\infty} dx e^{-\epsilon x} e^{-\frac{\mu_0}{\xi} f(x)}, \quad (2.66)$$

we have

$$\psi(\epsilon) \cong \epsilon \beta(\epsilon, \frac{\mu_0}{\xi}) \quad (s \gg 1). \quad (2.67)$$

The function $\epsilon \beta(\epsilon, \frac{\mu_0}{\xi})$ is a smooth function which is easy to evaluate numerically. We can go a little further and find a very simple form for $\epsilon \beta(\epsilon, \frac{\mu_0}{\xi})$. Asymptotic evaluation of the approximate solution $\epsilon \beta(\epsilon, \frac{\mu_0}{\xi})$ can be done using Laplace's method, and recognizing that for small x , $f(x) \approx x$. We find

$$\epsilon \beta \left(\epsilon, \frac{H_0}{\xi} \right) \cong \frac{1}{1 + \frac{H_0}{\xi} \cdot \frac{1}{\epsilon}} \quad \left(\epsilon + \frac{H_0}{\xi} \right) \gg 1. \quad (2.68)$$

We should note we can attain the same form as shown in Eqn. 2.68 for an approximate $\psi(\epsilon)$ by expanding the difference term in Eqn. 2.51b in a Taylor series, and keeping only terms including the first derivative. This does not work for general inelastic cross sections however, and expansion in a Taylor series for approximate behavior is a questionable technique.

Thus while we are unable to invert the transformed adjoint function to recover the unknown distribution $\psi(\epsilon)$, we can generate an approximate solution valid for large values of source energy. This solution, given by Eqn. 2.67, can further be approximated by a very simple relation (Eqn. 2.68) when the inelastic strength or the energy is fairly high.

The distribution below the inelastic threshold, posed by Eqn. 2.51c, can be found easily, given the solution above. We find

$$\psi_b(\epsilon) = \psi(1) + \frac{H_0}{\xi} \int_{\epsilon+1}^2 d\epsilon' \frac{\psi(\epsilon')}{\epsilon'} \quad 0 \leq \epsilon \leq 1. \quad (2.69)$$

If we now use the approximate form of $\psi(\epsilon)$ above threshold, we have

$$\psi(\epsilon) \cong \epsilon \beta \left(\epsilon, \frac{H_0}{\xi} \right) \quad (s \gg 1), \quad (2.70)$$

$$\psi_b(\epsilon) \cong \beta \left(1, \frac{H_0}{\xi} \right) + \frac{H_0}{\xi} \int_{\epsilon+1}^2 \beta \left(\epsilon', \frac{H_0}{\xi} \right) d\epsilon' \quad 0 \leq \epsilon \leq 1.$$

By substitution of $\beta(\epsilon', \frac{\mu_0}{\xi})$ from Eqn. 2.66, and interchanging the order of integrations, we have

$$\psi_b(\epsilon) \cong \beta\left(1, \frac{\mu_0}{\xi}\right) + \frac{\mu_0}{\xi} \int_0^{\infty} dx e^{-\frac{\mu_0}{\xi} f(x)} \left\{ \frac{e^{-(\epsilon+1)x} - e^{-2x}}{x} \right\} \quad 0 \leq \epsilon \leq 1. \quad (2.71)$$

We can now compare these approximate forms with the exact numerical solution. This comparison is shown in Figure 2.9 for three values of the inelastic strength parameter.

In these cases, $\epsilon\beta(\epsilon, \frac{\mu_0}{\xi})$ closely approximates the numerical solution when $\epsilon \sim 1$. In fact a very good approximation results everywhere except quite close to the source, where the oscillations are not predicted by the approximate form. Also we note that the simple approximation given by Eqn. 2.68 is a good representation of the solution for essentially the whole energy range. The solution below threshold is also shown in Figure 2.9. Note that the numerical solution and the approximate solution, given by Eqn. 2.71, closely agree. We also see that the recovery phenomenon mentioned before is once again present as $\epsilon \rightarrow 0$. Since we postulate $\epsilon\beta(\epsilon, \frac{\mu_0}{\xi})$ is the solution as $s \rightarrow \infty$, the asymptotic $\psi(\epsilon)$ must also obey the recovery relation.

The decreasing nature of the asymptotic distribution is a rather interesting phenomenon. Recall that in the case previously considered with a linear inelastic cross section, the asymptotic distribution was constant. In another case considered by Corngold and Yan⁽³⁹⁾, with inelastic cross section taken as a linear function vanishing at the threshold, the asymptotic distribution slowly increased as the threshold

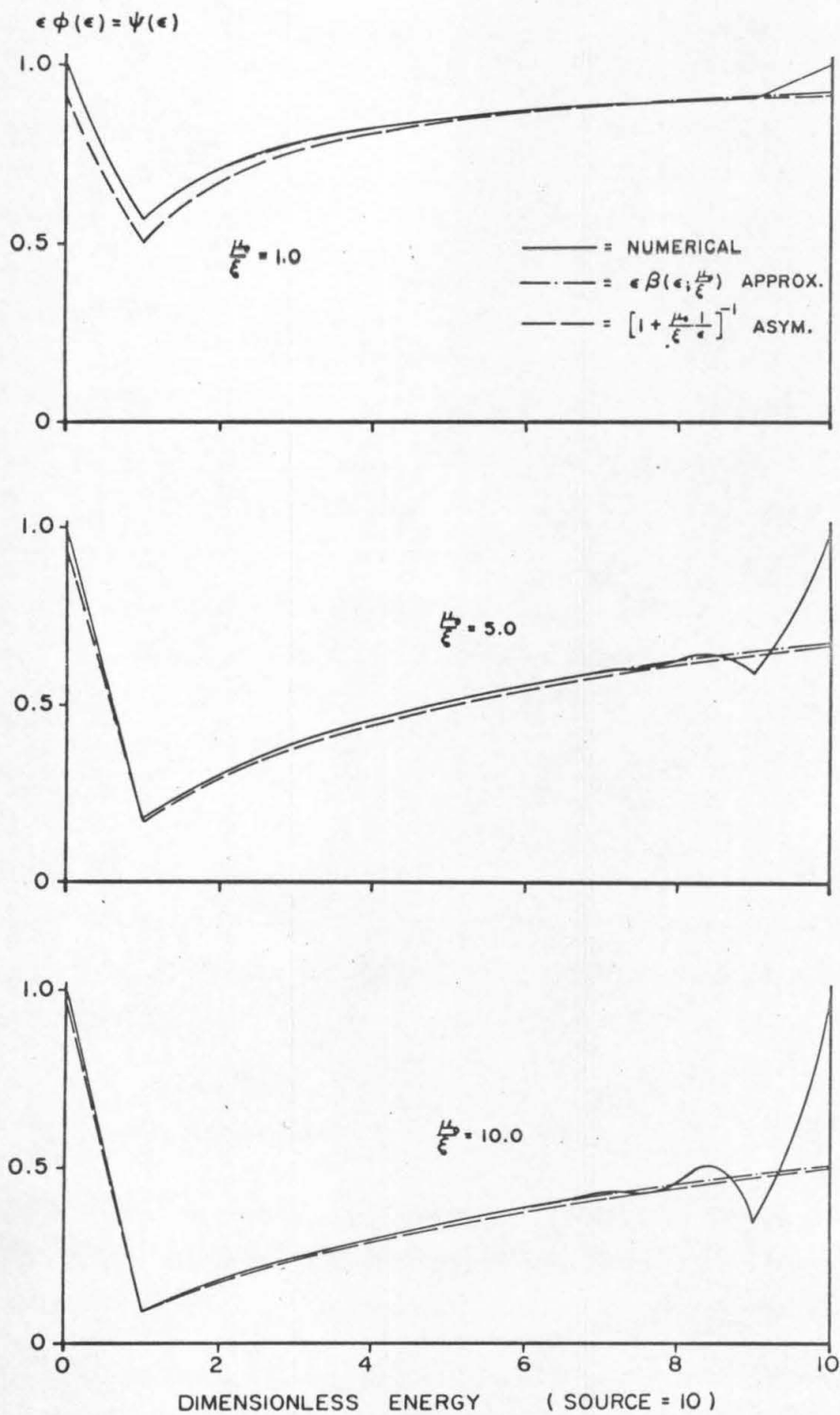


FIGURE 2.9 SINGLE LEVEL SOLUTIONS

was approached from above. Remember we are considering absorptionless slowing down, and therefore neutrons are conserved during the slowing down process. The collision density thus adjusts itself, given a particular inelastic cross section, so that the total slowing down density is always constant.

Again we compare the solution generated with an evaporative inelastic kernel with the discrete level solution (numerically evaluated). Using the same kernel as described in Eqns. 2.18 and 2.19, the comparison is shown in Figure 2.10. We again have a considerably different distribution using the two methods.

The extension of this inelastic model to multiple levels will be deferred until Chapter III, where the bounded region assumption (Eqn. 2.50) will be used. A case of multiple inelastic levels, each with a constant inelastic cross section, is considered there as an example.

E. Arbitrary Inelastic Cross Section - Single Level

In previous sections we considered the neutron spectrum resulting from two simple models of one level inelastic scattering. These models for the inelastic cross section are at least physically plausible, and solutions of the resultant balance equations lead to a fair amount of insight.

It would certainly be a benefit however, to be able to comment on the neutron energy distribution regardless of the form of the inelastic scattering cross section. We shall seek representations for the asymptotic distribution (energies far below the source energy but still

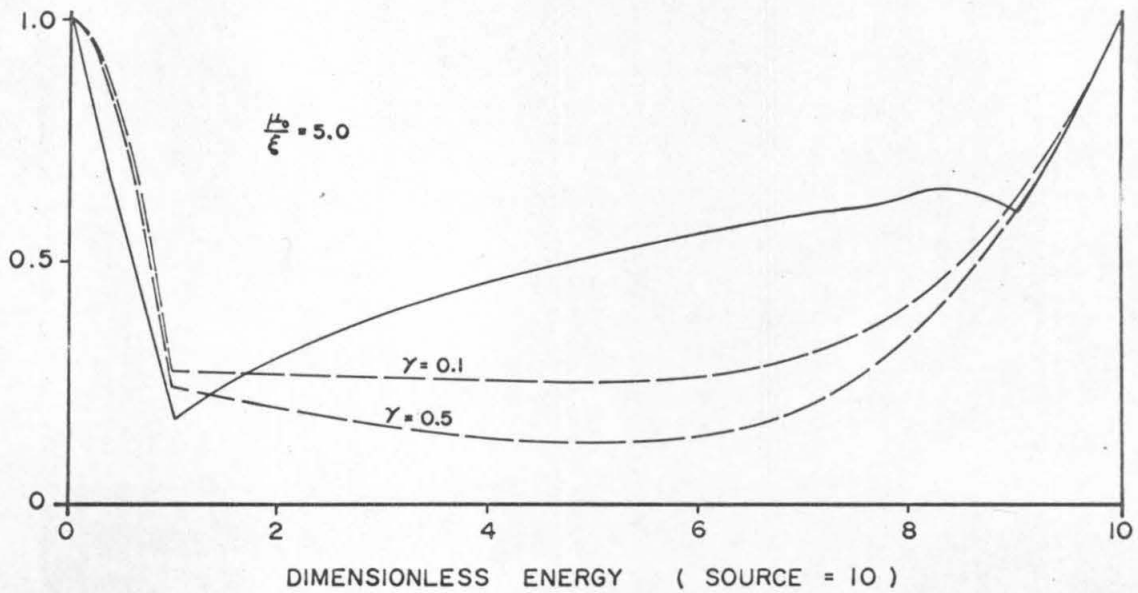
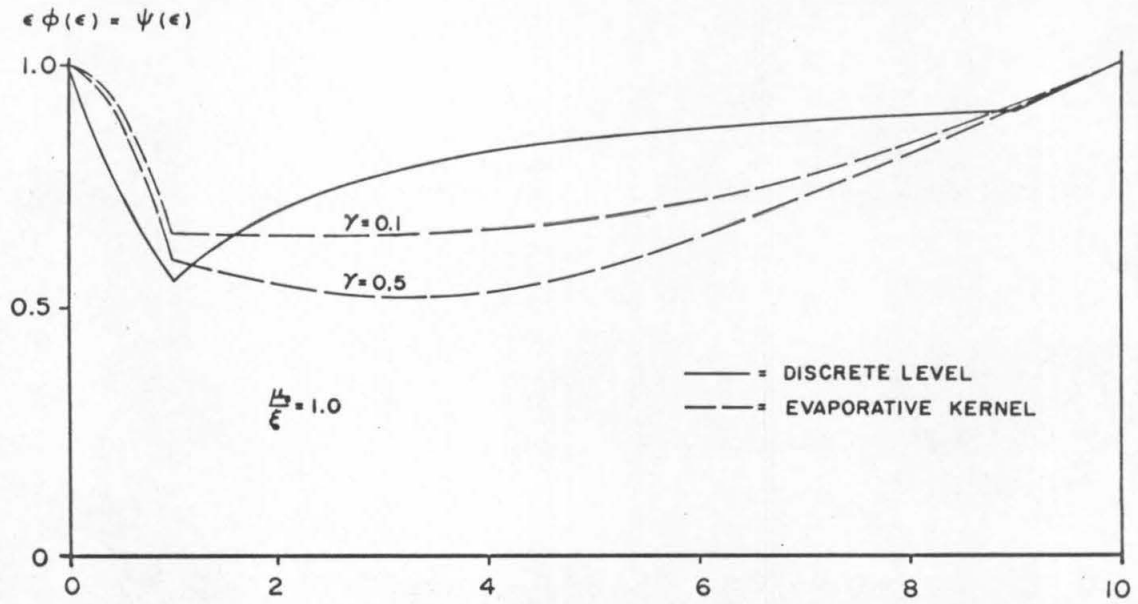


FIGURE 2.10 SINGLE LEVEL COMPARISON

above the inelastic threshold) given an arbitrary single excited inelastic level.

When considering only elastic scattering in an absorptionless medium, we find that the neutron flux is asymptotically inversely proportional to energy. This classical result, nearly axiomatic in slowing down studies, should be our guide. Can such a notion be generalized so that given an inelastic level, we can immediately write down (even approximately) the resultant neutron spectrum?

Again consider an equation derived from Eqn. 2.4 for general inelastic scattering:

$$\frac{d\psi(\epsilon)}{d\epsilon} + \frac{\nu(\epsilon+1)}{\xi} \psi(\epsilon+1) - \frac{\nu(\epsilon)}{\xi} \psi(\epsilon) = 0 \quad ; \quad \psi(s) = 1 \quad 1 \leq \epsilon \leq s, \quad (2.72)$$

where

$$\psi(\epsilon) = 0 \quad \epsilon > s,$$

and

$$\nu(\epsilon) = \frac{\Sigma_{in}(\epsilon)}{\epsilon \Sigma_s}.$$

We have a rather peculiar initial value problem. Initial data are specified at $\epsilon = s$ (instead of the origin), and our inelastic cross section is cut off at $\epsilon = 1$. We find the standard methods of Bellman and Cooke⁽⁴⁰⁾ and Yates⁽⁴³⁾ to develop an asymptotic ($s \rightarrow \infty$) solution are of little use. Even more difficulties occur when the adjoint is considered.

We can make progress by considering, instead of the balance equation (Eqn. 2.72), the slowing down equation. This corresponds

mathematically to an integral of Eqn. 2.72 with due regard for the initial conditions. Integrating Eqn. 2.71 from ϵ to s , we have

$$1 - \psi(\epsilon) = \int_{\epsilon}^s \frac{\nu(x)}{\xi} \psi(x) dx - \int_{\epsilon}^s \frac{\nu(x+1)}{\xi} \psi(x+1) dx.$$

By rearranging and using the fact that $\psi(x) = 0$ if $x > s$, we obtain

$$\psi(\epsilon) = 1 - \frac{1}{\xi} \int_{\epsilon}^{\epsilon+1} dx \nu(x) \psi(x). \quad (2.73)$$

We implicitly build into Eqn. 2.73 the fact that $\psi(s) = 1$ and $\psi(\epsilon) = 0$ for $\epsilon > s$. For generation of the asymptotic spectrum, we let $s \rightarrow \infty$. The implicit conditions are then removed, and Eqn. 2.73 is valid for all $\epsilon \geq 1$.

In integral equations of this type it is natural to seek solutions by successive approximation. We thus iterate a trial function $\psi(\epsilon)$ until, hopefully, it converges. Before consideration of these successive approximation techniques to solve Eqn. 2.73, recall from previous sections the asymptotic solutions for the two inelastic models considered. These results are shown in Table 2.1.

Table 2.1 Asymptotic Solution Summary

	<u>Linear Cross Section</u>	<u>Constant Cross Section</u>
$\nu(\epsilon)$	μ	$\frac{\mu_0}{\epsilon}$
Asymptotic $\psi(\epsilon)$	$\frac{1}{1 + \frac{\mu}{\xi}}$	$\epsilon \beta(\epsilon; \frac{\mu_0}{\xi}) \sim \frac{1}{1 + \frac{\mu_0}{\xi} \cdot \frac{1}{\epsilon}}$

Returning to Eqn. 2.73, consider replacement of the integrand by the first term in a Taylor series about $x = \epsilon$. Thus let

$$\int_{\epsilon}^{\epsilon+1} \frac{v(x)}{\xi} \psi(x) dx = \frac{v(\epsilon)}{\xi} \psi(\epsilon). \quad (2.74)$$

Once this approximation is made, Eqn. 2.73 has the obvious solution

$$\psi(\epsilon) = \frac{1}{1 + \frac{v(\epsilon)}{\xi}}. \quad (2.75)$$

This first guess agrees completely with two known asymptotic results. Perhaps this is a way to start a successive sequence for rapid convergence. It is now necessary to establish the conditions under which convergence is assured.

Given some initial guess $\psi_0(\epsilon)$ (say from Eqn. 2.75, for example), the first iteration yields, from Eqn. 2.73

$$\psi_1(\epsilon) = 1 - \frac{1}{\xi} \int_{\epsilon}^{\epsilon+1} v(x) \psi_0(x) dx. \quad (2.76)$$

Generalizing we have

$$\psi_n(\epsilon) = 1 - \frac{1}{\xi} \int_{\epsilon}^{\epsilon+1} v(x) \psi_{n-1}(x) dx. \quad (2.77)$$

We define difference functions as follows:

$$d_n(\epsilon) = \psi_n(\epsilon) - \psi_{n-1}(\epsilon) \quad n \geq 1. \quad (2.78)$$

By writing the equation for $\psi_{n-1}(\epsilon)$ from Eqn. 2.77, and subtracting from $\psi_n(\epsilon)$, we have

$$d_n(\epsilon) = -\frac{1}{\xi} \int_{\epsilon}^{\epsilon+1} v(x) d_{n-1}(x) dx. \quad (2.79)$$

By summing the difference functions, we form a sequence of partial sums:

$$\psi_n(\epsilon) = \sum_{k=0}^n d_k(\epsilon), \quad (2.80)$$

where $d_0(\epsilon) \equiv \psi_0(\epsilon)$, the initial guess.

Equation 2.79 can be written in terms of magnitudes:

$$|d_n(\epsilon)| \leq \frac{1}{\xi} \int_{\epsilon}^{\epsilon+1} |v(\epsilon')| |d_{n-1}(\epsilon')| d\epsilon' \quad n \geq 2. \quad (2.81)$$

Supposing we agree to start our approximation as suggested in Eqn. 2.75, we now ask what conditions on $v(\epsilon)$ then assure convergence of the sequence of partial sums? To investigate this we consider functions $v(\epsilon)$ obeying

$$0 \leq v(\epsilon) \leq C \quad 1 \leq \epsilon < \infty. \quad (2.82)$$

This corresponds physically (see after Eqn. 2.72) to an inelastic cross section growing no faster than a linear function with dimensionless slope C . We now will find what value of C is allowed for convergence.

The first difference function yields

$$d_1(\epsilon) = \psi_1(\epsilon) - \psi_0(\epsilon) = 1 - \frac{1}{\xi} \int_{\epsilon}^{\epsilon+1} v(x) \psi_0(x) dx - \psi_0(\epsilon).$$

Substitution of our trial function from Eqn. 2.75 yields

$$1 - d_1(\epsilon) = \frac{1}{\xi} \int_{\epsilon}^{\epsilon+1} \frac{v(x) dx}{1 + \frac{v(x)}{\xi}} + \frac{1}{1 + \frac{v(\epsilon)}{\xi}}. \quad (2.83)$$

Using Eqn. 2.82, we replace the right side of Eqn. 2.83 by the greatest and least possible values:

$$1 - d_1(\epsilon) \geq \frac{1}{1 + \frac{C}{\xi}}, \quad (2.84)$$

$$1 - d_1(\epsilon) \leq \frac{C}{\xi} \cdot \frac{1}{1 + \frac{C}{\xi}} + 1. \quad (2.85)$$

These two equations can be combined into the single equation

$$|d_1(\epsilon)| \leq \frac{\frac{C}{\xi}}{1 + \frac{C}{\xi}}. \quad (2.86)$$

When this is substituted into Eqn. 2.81, we obtain

$$|d_2(\epsilon)| \leq \frac{\left(\frac{C}{\xi}\right)^2}{1 + \frac{C}{\xi}}. \quad (2.87)$$

Repeated application generates the obvious relation

$$|d_n(\epsilon)| \leq \frac{\left(\frac{C}{\xi}\right)^n}{1 + \frac{C}{\xi}}. \quad (2.88)$$

Using Eqn. 2.80 we conclude the sequence of partial sums $\psi_n(\epsilon)$ converges to $\psi(\epsilon)$ for $\left(\frac{C}{\xi}\right) < 1$. Thus when the inelastic cross section is constrained by

$$0 \leq \Sigma_{in}(\epsilon) < \xi \Sigma_s \epsilon \quad \epsilon > 1, \quad (2.89)$$

we have a guaranteed convergent procedure for developing the neutron energy distribution. The region for guaranteed convergence is shown in Figure 2.11.

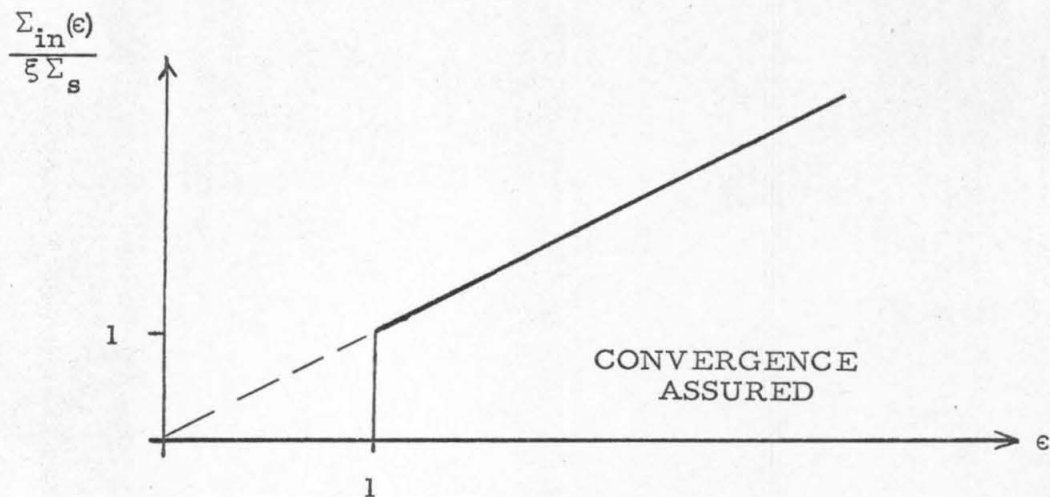


Figure 2.11 Successive Approximation Convergence

The above results certainly do not depend on the use of Eqn. 2.75 to begin the iterations. Using the classical method of Picard⁽⁴⁴⁾, we let the initial function be the homogeneous term, in this case unity. Bounding $v(\epsilon)$ again as in Eqn. 2.82, the equation for $d_1(\epsilon)$ becomes

$$|d_1(\epsilon)| \leq \frac{C}{\xi}.$$

Application of Eqn. 2.81 implies

$$|d_n(\epsilon)| \leq \left(\frac{C}{\xi}\right)^n.$$

Thus $\psi_n(\epsilon)$ again converges uniformly to $\psi(\epsilon)$ if $\left(\frac{C}{\xi}\right) < 1$. Use of the Picard method in these problems apparently leads to generally slower convergence, as will be demonstrated in the examples to follow.

Example 1: Linear inelastic cross section. Take the over-worked case $\nu(\epsilon) = \mu$. Using the initial guess as in Eqn. 2.75, we let

$$\psi_0(\epsilon) = \frac{1}{1 + \frac{\mu}{\xi}}.$$

Calculation yields $\psi_1(\epsilon) = \psi_0(\epsilon)(d_1(\epsilon) = 0)$. Thus $d_n(\epsilon) = 0$ for all n , and $\psi(\epsilon) = \psi_0(\epsilon)$. This solution is valid for all $\frac{\mu}{\xi}$, even outside the limit specified by Eqn. 2.82. Note this solution agrees with the asymptotic form found earlier.

Application of the Picard method leads to a different representation. Using this technique we find

$$\begin{array}{lll} \psi_0(\epsilon) = 1 & \psi_1(\epsilon) = 1 - \frac{\mu}{\xi} & d_1(\epsilon) = -\frac{\mu}{\xi} \\ & \psi_2(\epsilon) = 1 - \frac{\mu}{\xi} + \left(\frac{\mu}{\xi}\right)^2 & d_2(\epsilon) = \left(\frac{\mu}{\xi}\right)^2 \\ & \vdots & \vdots \\ & \psi_n(\epsilon) = 1 - \frac{\mu}{\xi} + \dots + \left(-\frac{\mu}{\xi}\right)^n & d_n(\epsilon) = \left(-\frac{\mu}{\xi}\right)^n. \end{array}$$

Clearly $\psi(\epsilon) = \left(1 + \frac{\mu}{\xi}\right)^{-1}$ provided $\frac{\mu}{\xi} < 1$. The Picard method thus gives a convergent solution only in the established domain, and convergence is much slower.

Example 2: Constant inelastic cross section. Taking $\nu(\epsilon) = \mu_0$, and following Eqn. 2.75 for our initial guess, we have

$$\psi_0(\epsilon) = \frac{1}{1 + \frac{\mu_0}{\xi} \cdot \frac{1}{\epsilon}}.$$

Recall from the preceding section that this form is asymptotic to the approximate solution $\epsilon\beta\left(\epsilon; \frac{\mu_0}{\xi}\right)$. We saw in Figure 2.9 that $\psi_0(\epsilon)$ provided a good estimate of the far-from-source solution for all values of $\frac{\mu_0}{\xi}$ considered. In particular, while Eqn. 2.82 would limit $\frac{\mu_0}{\xi}$ to values less than unity, Figure 2.9 reflects the fact that $\psi_0(\epsilon)$ is in fact a better approximation as $\frac{\mu_0}{\xi}$ gets very large.

This apparent contradiction can be explained by computation of the higher order terms. What we observe is that the series

$$\psi(\epsilon) = \sum_{k=0}^{\infty} d_k(\epsilon)$$

changes from a convergent series to an asymptotic one as $\frac{\mu_0}{\xi}$ passes through unity. Thus while the initial guess happens to give closer agreement for $\frac{\mu_0}{\xi} > 1$, calculation of higher order terms (more d_k 's) leads to divergence. To see this consider the first iteration:

$$\psi_1(\epsilon) = 1 - \frac{\mu_0}{\xi} \log\left(1 + \frac{1}{\epsilon + \frac{\mu_0}{\xi}}\right).$$

We then find that

$$d_1(\epsilon) = 1 - \frac{\mu_0}{\xi} \log \left(1 + \frac{1}{\epsilon + \frac{\mu_0}{\xi}} \right) - \frac{1}{1 + \frac{\mu_0}{\xi} \cdot \frac{1}{\epsilon}}.$$

Making an expansion of the logarithm, this can be written as

$$d_1(\epsilon) = \frac{\mu_0}{\xi} \left[\frac{1}{2 \left(\epsilon + \frac{\mu_0}{\xi} \right)} - \frac{1}{3 \left(\epsilon + \frac{\mu_0}{\xi} \right)} + \dots \right]$$

As $\frac{\mu_0}{\xi}$ gets very large, $d_1(\epsilon) \sim \left[\frac{2\mu_0}{\xi} \right]^{-1}$. As $\frac{\mu_0}{\xi} \rightarrow \infty$, $d_1(\epsilon)$ does indeed vanish, implying that $\psi_1(\epsilon) \rightarrow \psi_0(\epsilon)$. But calculation of the next difference function $d_2(\epsilon)$, from Eqn. 2.79 yields

$$d_2(\epsilon) = - \frac{\mu_0}{\xi} \int_{\epsilon}^{\epsilon+1} \frac{d\epsilon'}{\epsilon'} d_1(\epsilon').$$

As $\frac{\mu_0}{\xi}$ becomes very large, we have

$$d_2(\epsilon) \sim - \frac{1}{2} \log \left(\frac{\epsilon+1}{\epsilon} \right).$$

In calculations of succeeding $d_n(\epsilon)$, we find each grows by a factor of $\left(\frac{\mu_0}{\xi} \right)$ times a function of ϵ . For fixed ϵ , inclusion of more and more terms leads to a divergent sequence.

The results of this section are fairly easy to summarize: If the inelastic scattering cross section is bounded by Eqn. 2.89, we are guaranteed successive approximations will generate a solution to Eqn. 2.73. If Eqn. 2.89 does not hold, the series generated may be

convergent, asymptotic, or meaningless. Many physically interesting isotopes in fact obey Eqn. 2.89. But the main point is that the simple relation given by our first guess (Eqn. 2.75)

$$\psi_0(\epsilon) = \frac{1}{1 + \frac{\nu(\epsilon)}{\xi}}$$

apparently gives a good representation of the solution $\psi(\epsilon)$ regardless of the magnitude of the inelastic cross section, provided the source energy is high enough. While we are not able to derive a direct analog of the $1/E$ behavior of the neutron flux in classical slowing down theory, we are thus able to suggest an approximate representation when a single level of inelastic scattering is included.

III. STEADY STATE MULTIPLE LEVEL ANALYSIS

We have taken care to compare each discrete level solution found thus far with the solution to the slowing down equation when inelastic scattering is modeled with an evaporative kernel. Since we've considered only one or two excited levels, such a comparison must be judged as somewhat unfair. We consider now the treatment of multiple inelastic levels, and in examples to follow the number of levels allowed will be chosen sufficiently large to provide a real test of (at least) the evaporative kernel adopted in this research.

We saw in Section C of the preceding chapter that a general analytical treatment of neutron slowing down with multiple discrete inelastic levels was not a very promising venture. The one-sided Green's functions were difficult to generate and complicated in form. We mentioned that if certain physically reasonable conditions were imposed on the structure of the inelastic levels, then simplifications were possible. In order to detail this analysis, consider again the multiple level balance equation with absorption included (an extension of Eqn. 2.5):

$$\frac{d\psi(\epsilon)}{d\epsilon} - \frac{(\Sigma_{in}(\epsilon) + \Sigma_a(\epsilon))}{\epsilon \xi \Sigma_s} \psi(\epsilon) + \sum_{j=1}^N \frac{\Sigma_{in}^j(\epsilon + \epsilon_j)}{(\epsilon + \epsilon_j) \xi \Sigma_s} \psi(\epsilon + \epsilon_j) = -\delta(\epsilon - s) \quad (3.1)$$

where

$$\Sigma_{in}(\epsilon) = \sum_{j=1}^N \Sigma_{in}^j(\epsilon).$$

Remembering that each inelastic level has a threshold cross section, $\Sigma_{in}^k(\epsilon) = 0$ for $\epsilon < \epsilon_k$, we again define regions bounded by the inelastic thresholds:

$$k^{th} \text{ region} \equiv \epsilon \in [\epsilon_k, \epsilon_{k+1}).$$

If N inelastic levels are excited, the highest energy region is the N^{th} , with boundaries ϵ_N and $\epsilon_{N+1} = s$ (the source energy). The lowest energy region (region 0) is bounded by zero and the first inelastic threshold at $\epsilon = 1$. For all regions except the lowest (we temporarily exclude it), an equation for the one-sided Green's function can be extracted from Eqn. 3.1. For the k^{th} region, we have

$$\frac{dG_k(\epsilon, \epsilon_{k+1})}{d\epsilon} + \sum_{j=1}^N \frac{\Sigma_{in}(\epsilon + \epsilon_j)}{(\epsilon + \epsilon_j) \xi \Sigma_s} G_k(\epsilon + \epsilon_j, \epsilon_{k+1}) - \frac{(\Sigma_a(\epsilon) + \sum_{j=1}^k \Sigma_{in}^j(\epsilon))}{\epsilon \xi \Sigma_s} G_k(\epsilon, \epsilon_{k+1}) = 0 \quad (3.2)$$

where

$$\epsilon_k \leq \epsilon < \epsilon_{k+1} \quad k = 1, 2, \dots, N$$

$$G_k(\epsilon_{k+1}, \epsilon_{k+1}) = 1$$

$$G_k(\epsilon, \epsilon_{k+1}) = 0 \quad \epsilon > \epsilon_{k+1}$$

Now we bound the maximum width of any energy region by demanding that Eqn. 2.50 hold:

$$\max_{k=1, \dots, N} (\epsilon_{k+1} - \epsilon_k) \leq 1. \quad (2.50)$$

If this is the case, then the second term of Eqn. 3.2 is identically zero, and the resultant balance equation for the one-sided Green's function in the k^{th} region is an ordinary differential equation. Physically we've built in the condition that if a neutron suffers an inelastic collision in region k , it must then jump to a new region. By choosing level structures according to Eqn. 2.50, intraregional jumps are not allowed, and the simplification results.

With the regions thus bounded, Eqn. 3.2 can be easily solved for $G_k(\epsilon, \epsilon_{k+1})$:

$$G_k(\epsilon, \epsilon_{k+1}) = \exp\left\{-\frac{1}{\xi} \int_{\epsilon}^{\epsilon_{k+1}} \frac{\Sigma_a(\epsilon')}{\epsilon' \Sigma_s} d\epsilon'\right\} \exp\left\{-\frac{1}{\xi} \int_{\epsilon}^{\epsilon_{k+1}} \sum_{j=1}^k \frac{\Sigma_{in}^j(\epsilon')}{\epsilon' \Sigma_s} d\epsilon'\right\} \quad k=1, 2, \dots, N \quad (3.3)$$

With the Green's function known, we can solve for the distribution $\psi(\epsilon)$ in the k^{th} region:

$$\psi(\epsilon) = \psi(\epsilon_{k+1}) G_k(\epsilon, \epsilon_{k+1}) + \int_{\epsilon}^{\epsilon_{k+1}} G_k(\epsilon, \epsilon') S_k(\epsilon') d\epsilon' \quad \epsilon_k \leq \epsilon \leq \epsilon_{k+1} \quad (3.4)$$

where

$$S_k(\epsilon') = \frac{1}{\xi} \sum_{j=1}^N \frac{\psi(\epsilon' + \epsilon_j) \Sigma_{in}^j(\epsilon' + \epsilon_j)}{(\epsilon' + \epsilon_j) \Sigma_s} \quad k=1, 2, \dots, N-1. \quad (3.5)$$

In Eqn. 3.5, we interpret the term $\psi(\epsilon' + \epsilon_j)$ in the summation as being zero if $(\epsilon' + \epsilon_j) > s$. We thus compute the source at each energy point as a superposition of terms from higher regions where the solutions are

known. Eqns. 3.4 and 3.5 are valid in regions 1 through N-1. In the highest energy region, where the process of generating a solution begins, we have

$$\psi(\epsilon) = G_N(\epsilon, s) \quad \epsilon_N \leq \epsilon \leq s. \quad (3.6)$$

With the solution in all above-threshold regions specified, we can calculate the solution in the subthreshold range (region 0):

$$\begin{aligned} \psi(\epsilon) = & \left[\psi(1) + \frac{1}{\xi} \sum_{j=1}^N \int_{\epsilon_j}^{\epsilon_j+1} \frac{\psi(\epsilon') \Sigma_{in}^j(\epsilon')}{\epsilon' \Sigma_s} \exp \left\{ \frac{1}{\xi} \int_{\epsilon' - \epsilon_j}^1 \frac{\Sigma_a(\epsilon'')}{\epsilon'' \Sigma_s} d\epsilon'' \right\} d\epsilon' \right] \\ & \cdot \exp \left[-\frac{1}{\xi} \int_{\epsilon}^1 \frac{\Sigma_a(\epsilon')}{\epsilon' \Sigma_s} d\epsilon' \right]. \end{aligned} \quad (3.7)$$

Generation of a solution thus proceeds by first finding the Green's functions for the desired regions via Eqn. 3.3. We then use Eqn. 3.6 to find the distribution $\psi(\epsilon)$ in the highest energy region (region N). We use this information in Eqns. 3.4 and 3.5 to find $\psi(\epsilon)$ in region N-1, and so on. Finally we use Eqn. 3.7 to find the distribution below the first threshold. We shall illustrate with two examples.

Example 1: Consider the familiar case of multiple levels, each with linear cross sections:

$$\frac{\Sigma_{in}^j(\epsilon)}{\epsilon \Sigma_s} = \begin{cases} \mu_j & \epsilon \geq \epsilon_j \\ 0 & \epsilon < \epsilon_j \end{cases}$$

When this is the case, and absorption is taken as zero, we can easily find the Green's functions from Eqn. 3.3:

$$G_k(\epsilon, \epsilon_{k+1}) = \exp\left\{-\left(\epsilon_{k+1} - \epsilon\right) \sum_{j=1}^k \frac{\mu_j}{\xi}\right\} \quad k=1, 2, \dots, N.$$

We see that for this case $G_k(\epsilon, \epsilon_{k+1}) = G_k(\epsilon_{k+1} - \epsilon)$, as we found in Chapter II.

Choosing the inelastic levels to lie on the integers of the dimensionless energy scale

$$\epsilon_j = j \quad \text{for } j \geq 1,$$

and choosing the set $\{\mu_j\}$ to be constant

$$\frac{\mu_j}{\xi} = 0.1 \quad j \geq 1,$$

we take the source at $s=10$ and compute the solution using Eqns. 3.4 - 3.7. We find

$$\begin{aligned} \psi(\epsilon) = & \psi(\epsilon_{k+1}) \exp\left\{-\left(\epsilon_{k+1} - \epsilon\right) \sum_{j=1}^k \frac{\mu_j}{\xi}\right\} \\ & + \int_{\epsilon}^{\epsilon_{k+1}} \exp\left\{-\left(\epsilon' - \epsilon\right) \sum_{j=1}^k \frac{\mu_j}{\xi}\right\} S_k(\epsilon') d\epsilon' \quad \epsilon_k \leq \epsilon \leq \epsilon_{k+1} \end{aligned}$$

where

$$S_k(\epsilon') = \sum_{j=1}^N \psi(\epsilon' + \epsilon_j) \cdot \frac{\mu_j}{\xi} \quad k = 1, 2, \dots, N-1.$$

This solution is then calculated and compared with the numerical results using the familiar evaporative kernel. The comparison is shown in Figure 3.1 for various values of the evaporation parameter.

Example 2: Constant inelastic cross sections. Using the same level structure, source, and zero absorption conditions as in Example 1, consider now the case of multiple levels with constant cross sections.

Taking

$$\frac{\Sigma_{in}^j(\epsilon)}{\epsilon \Sigma_s} = \begin{cases} \frac{\mu_j}{\epsilon} & \epsilon \geq \epsilon_j \\ 0 & \epsilon < \epsilon_j \end{cases}$$

we find from Eqn. 3.3 that

$$G_k(\epsilon, \epsilon_{k+1}) = \left(\frac{\epsilon}{\epsilon_{k+1}} \right)^{\sum_{j=1}^k \frac{\mu_j}{\xi}}$$

The distribution is then

$$\psi(\epsilon) = \psi(\epsilon_{k+1}) \left(\frac{\epsilon}{\epsilon_{k+1}} \right)^{\sum_{j=1}^k \frac{\mu_j}{\xi}} + \int_{\epsilon}^{\epsilon_{k+1}} \left(\frac{\epsilon}{\epsilon'} \right)^{\sum_{j=1}^k \frac{\mu_j}{\xi}} S_k(\epsilon') d\epsilon'$$

where

$$S_k(\epsilon') = \sum_{j=1}^N \frac{\mu_j}{\xi} \frac{\psi(\epsilon' + \epsilon_j)}{\epsilon + \epsilon_j}$$

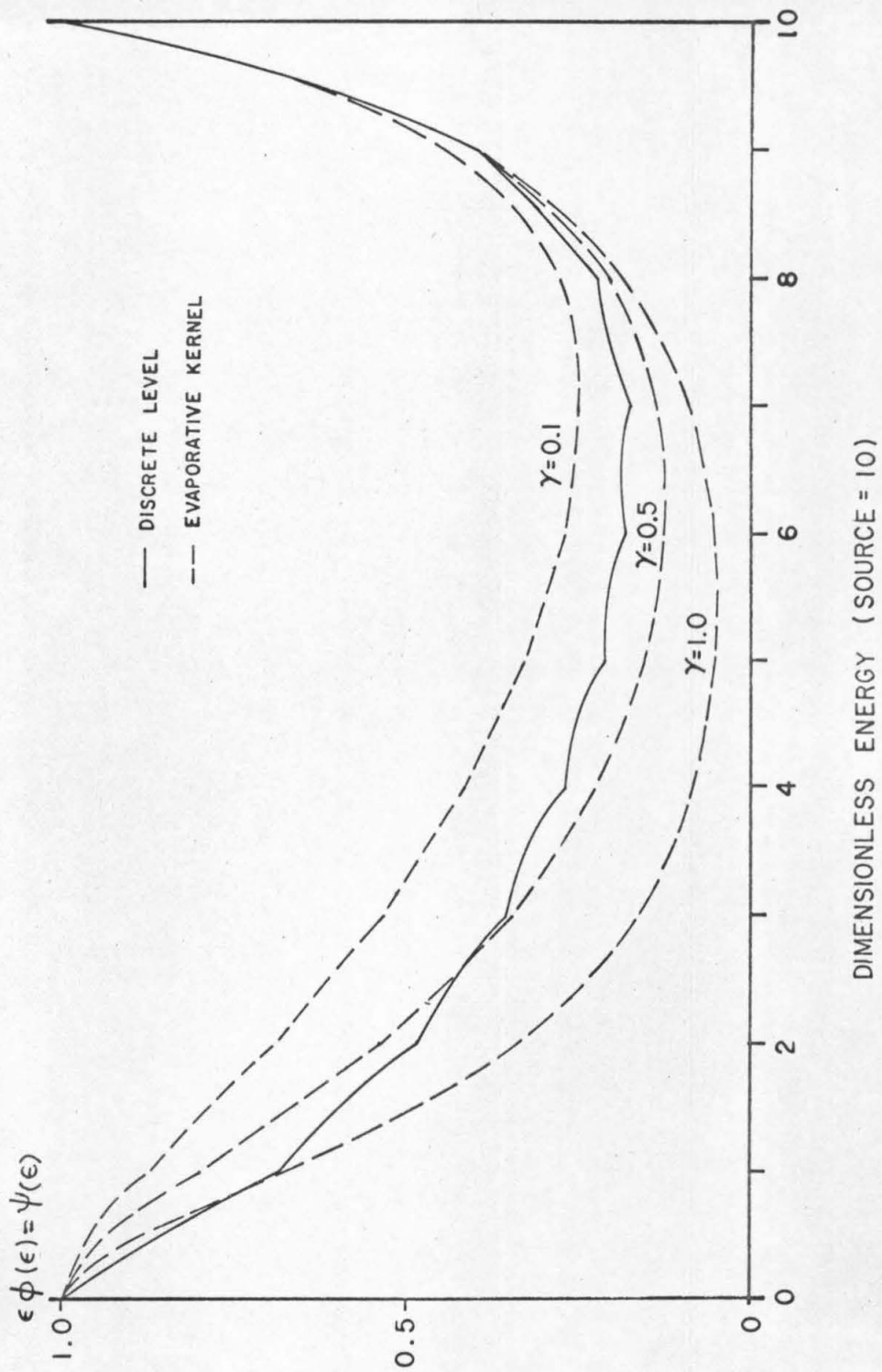


FIGURE 3.1 MULTIPLE LEVEL COMPARISON

We again take all the coefficients $\{\mu_j\}$ to be the same

$$\frac{\mu_j}{\xi} = 0.1 \quad j \geq 1,$$

and calculate the solution. That solution and the numerical solution for the evaporative kernel are shown in Figure 3.2.

We see the comparison is indeed somewhat better than in the single or double level cases considered previously. There remains however, a decided discrepancy in the two approaches, especially in Example 1 where the inelastic strengths are taken somewhat higher (the linear cross sections imply high inelastic cross sections at high energies). The real question is how should we select the nuclear temperature for best agreement? In the discussion in Chapter II we roughly estimated γ should be chosen in the range $(\frac{1}{8}, \infty)$. In these examples, we take γ between 0.1 and 1. The resultant differences in the comparison leaves considerable room for argument. Perhaps a more sophisticated choice for the evaporative kernel would lead to better agreement and less parameter ambiguity.

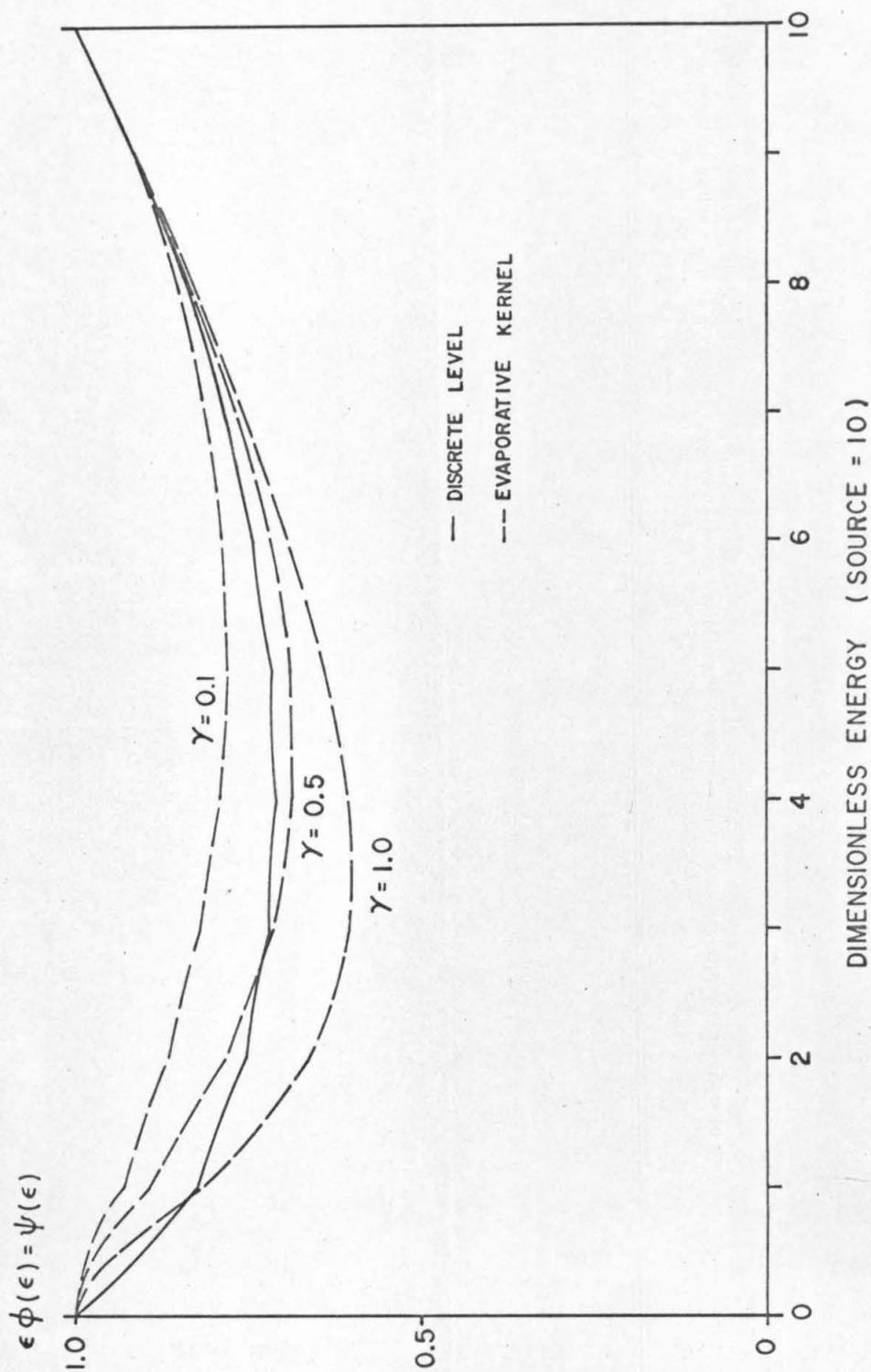


FIGURE 3.2 MULTIPLE LEVEL COMPARISON

IV. TIME DEPENDENT SLOWING DOWN

The addition of time dependence to the theory of neutron slowing down with inelastic scattering introduces many complications. In particular, it appears that straightforward analytical treatment of a general balance equation is a hopeless case. We are thus compelled to seek approximations and simple cross section forms in order to generate solutions. In this chapter we develop solutions to the time dependent problem. We first examine slowing down in the absence of elastic scattering. After qualitatively discussing the effects of this exclusion, we include age elastic scattering by assuming simple forms for the cross sections considered.

A. Elastic Scattering Excluded Above Threshold

We assume a situation exists in which the inelastic scattering completely dominates the slowing down process. Elastic scattering above the inelastic threshold is then excluded. Of course, we insert age elastic scattering below threshold, since it then becomes the only energy transfer process. Consider a balance equation for the time and energy dependent flux with a single level of inelastic scattering. We assume the distribution is driven by a monoenergetic pulse of neutrons:

$$\frac{1}{\sqrt{\epsilon}} \frac{\partial \varphi(\epsilon, \tau)}{\partial \tau} = \Sigma_{\text{in}}(\epsilon+1) \varphi(\epsilon+1, \tau) - (\Sigma_{\text{in}}(\epsilon) + \Sigma_a(\epsilon)) \varphi(\epsilon, \tau) + S_0 \delta(\epsilon-s) \delta(\tau) \quad 1 \leq \epsilon \leq s, \quad (4.1)$$

$$\frac{1}{\sqrt{\epsilon}} \frac{\partial \varphi_b(\epsilon, \tau)}{\partial \tau} = \xi \frac{\partial}{\partial \epsilon} (\epsilon \Sigma_s(\epsilon) \varphi_b(\epsilon, \tau)) - \Sigma_a(\epsilon) \varphi_b(\epsilon, \tau) + \Sigma_{\text{in}}(\epsilon+1) \varphi(\epsilon+1, \tau) \quad 0 < \epsilon \leq 1, \quad (4.2)$$

with

$$\varphi_b(l, \tau) = \varphi(l, \tau).$$

Here we have introduced some additional notation

$$\begin{aligned} \varphi(\epsilon, \tau) &= \text{neutron flux above threshold} \\ \varphi_b(\epsilon, \tau) &= \text{neutron flux below threshold} \\ \tau &= \text{scaled time, } \sqrt{2E_1/m} t \text{ (units of cm.)} \\ E_1 &= \text{energy of the inelastic threshold.} \end{aligned}$$

The technique is to first solve Eqn. 4.1 for the flux above threshold, and then use the solution generated to solve Eqn. 4.2. Note that Eqn. 4.2 is easily solved once $\varphi(\epsilon+1, \tau)$ is known.

To solve Eqn. 4.1, we Laplace transform the time variable, and rearrange (take $S_0=1$):

$$\varphi^*(\epsilon+1, p) - \frac{(\Sigma_{in}(\epsilon) + \Sigma_a(\epsilon) + \frac{p}{\sqrt{\epsilon}})}{\Sigma_{in}(\epsilon+1)} \varphi^*(\epsilon, p) = -\frac{\delta(\epsilon-s)}{\Sigma_{in}(\epsilon+1)}. \quad (4.3)$$

Define a new dependent variable, the transformed neutron density,

$n^*(\epsilon, p) = \varphi^*(\epsilon, p) / \sqrt{\epsilon}$. Also, we let

$$r(\epsilon, p) = \frac{\sqrt{\epsilon} \Sigma_{in}(\epsilon) + \sqrt{\epsilon} \Sigma_a(\epsilon) + p}{\sqrt{\epsilon+1} \Sigma_{in}(\epsilon+1)}. \quad (4.4)$$

Then Eqn. 4.3 becomes

$$n^*(\epsilon+1, p) - r(\epsilon, p)n^*(\epsilon, p) = \frac{-\delta(\epsilon-s)}{\sqrt{\epsilon+1} \Sigma_{in}(\epsilon+1)} \quad 1 \leq \epsilon \leq s. \quad (4.5)$$

Excluding the point $\epsilon = s$, which we treat later, Eqn. 4.5 is a homogeneous algebraic difference equation. A closed form solution can be obtained if we take $r(\epsilon, p)$ to be a rational function of ϵ ⁽⁴⁵⁾:

$$r(\epsilon, p) = c \frac{(\epsilon - \alpha_1)(\epsilon - \alpha_2) \dots (\epsilon - \alpha_k)}{(\epsilon - \beta_1)(\epsilon - \beta_2) \dots (\epsilon - \beta_l)}, \quad (4.6)$$

where in general

$$\begin{aligned} \alpha_j &= \alpha_j(p) \\ c &= c(p) \\ \beta_j &= \text{constant.} \end{aligned}$$

The solution is then

$$n^*(\epsilon, p) = c \epsilon^{\frac{\Gamma(\epsilon - \alpha_1)\Gamma(\epsilon - \alpha_2) \dots \Gamma(\epsilon - \alpha_k)}{\Gamma(\epsilon - \beta_1) \dots \Gamma(\epsilon - \beta_l)}} \bar{w}(\epsilon, p). \quad (4.7)$$

The function $\bar{w}(\epsilon, p)$ is an arbitrary periodic function with unit period, and must be selected so that Eqn. 4.7 agrees with the initial data specified. In our case, initial data are given on the interval $\epsilon \in [s, \infty)$:

$$n_0^*(\epsilon, p) = \frac{\delta(\epsilon - s)}{\sqrt{s} \Sigma_{in}(s) + \sqrt{s} \Sigma_a(s) + p} \quad s \leq \epsilon < \infty. \quad (4.8)$$

We thus have $\bar{w}(\epsilon, p)$ as the periodic repetition of

$$\bar{w}(\epsilon, p) = \frac{1}{c} \frac{\Gamma(s - \beta_1) \dots \Gamma(s - \beta_l)}{\Gamma(s - \alpha_1) \dots \Gamma(s - \alpha_k)} \frac{\delta(\epsilon - s)}{(\sqrt{s} \Sigma_{in}(s) + \sqrt{s} \Sigma_a(s) + p)} \quad s - 1 < \epsilon \leq s. \quad (4.9)$$

We let the periodic nature of $\bar{w}(\epsilon, p)$ be reflected in a delta function sequence. The solution for the transformed density is thus

$$n^*(\epsilon, p) = \sum_{j=0}^N c^{\epsilon-s} \frac{\Gamma(\epsilon - \alpha_1) \cdots \Gamma(\epsilon - \alpha_k)}{\Gamma(\epsilon - \beta_1) \cdots \Gamma(\epsilon - \beta_\ell)} \frac{\delta(s - \epsilon - j)}{[\sqrt{s}(\Sigma_{in}(s) + \Sigma_a(s)) + p]}, \quad (4.10)$$

where the limits on the summation build in the fact that the energy is restricted to $1 \leq \epsilon \leq s$. This implies $N_s = IP(s^- - 1)$, where IP denotes integer part notation ($IP(4.8) = 4$, for example). Because c and the components of $\{\alpha\}$ can depend on p , inversion of Eqn. 4.10 must be deferred until specific examples are considered. In general, however, Eqn. 4.10 tells us what to expect. We will see delta function pulses, with amplitudes (areas) dependent on time and cross sections, appearing at $\epsilon = s, s-1, s-2, \dots$. This reflects the fact that the only available way for the original pulse to lose energy is via a discrete inelastic interaction.

Generation of the solution below the inelastic threshold must also be deferred because the reaction rate of inelastic collisions in the interval $1 \leq \epsilon < 2$ cannot be extracted from the equation for $r(\epsilon, p)$. Rather, we must know the inelastic cross section explicitly.

We now consider a simple example which will illustrate all the salient features of this problem. We choose cross sections so that solutions are easy to obtain.

Example:

Above threshold we take $\Sigma_{in}(\epsilon) = \rho/\sqrt{\epsilon}$, $\Sigma_a(\epsilon) = 0$. We find by rearrangement that

$$r(\epsilon, p) = c(p) = \frac{p + \rho}{\rho}.$$

Eqn. 4.10 thus yields

$$n^*(\epsilon, p) = \sum_{j=0}^{N_s} \frac{\rho^{s-\epsilon}}{(\rho+p)^{s-\epsilon+1}} \delta(s-\epsilon-j) \quad 1 \leq \epsilon \leq s.$$

Inversion of this expression, and rearrangement, yields

$$n(\epsilon, \tau) = e^{-\rho\tau} \sum_{j=0}^{N_s} \frac{(\rho\tau)^j}{j!} \delta(s-\epsilon-j). \quad (4.11)$$

Eqn. 4.11 provides the solution for the neutron density above the inelastic threshold. The solution consists of the sequence of pulses mentioned before. The amplitudes (or areas) of the pulses, corresponding to an energy integral of Eqn. 4.11, are shown below.

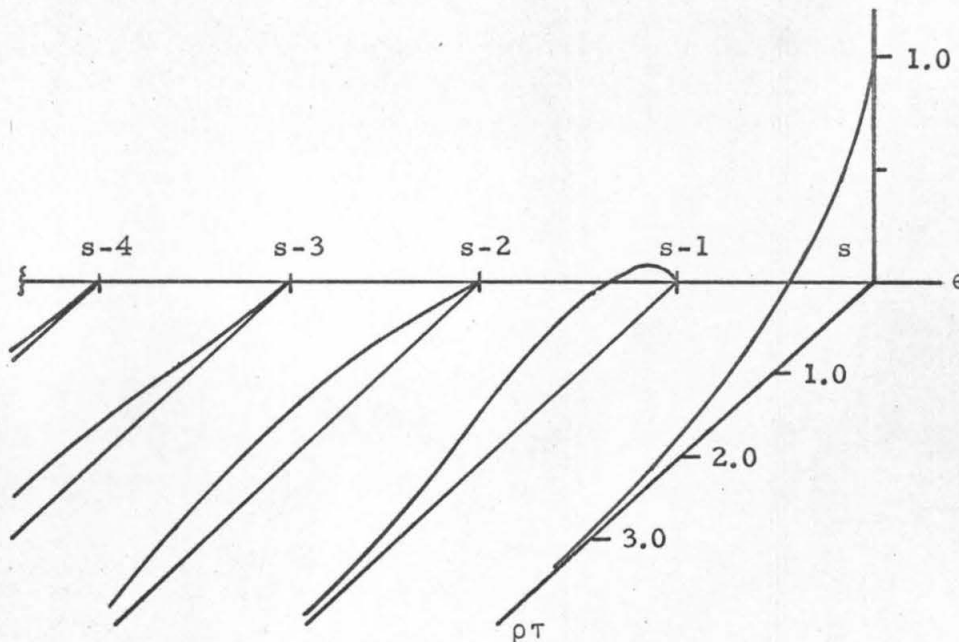


Figure 4.1 Pulse Amplitudes

Since the neutron density in the above threshold region is known, we can solve Eqn. 4.2 for the subthreshold neutron flux. As a convenience, we take the elastic scattering cross section to be constant, and consider no absorption. Computation of the inelastic reaction rate in the interval $1 \leq \epsilon < 2$, followed by substitution into Eqn. 4.2, yields

$$\frac{1}{\sqrt{\epsilon}} \frac{\partial \varphi_b(\epsilon, \tau)}{\partial \tau} = \xi \sum_s \frac{\partial}{\partial \epsilon} (\epsilon \varphi(\epsilon, \tau)) + S(\tau) \delta(\epsilon - \epsilon_b) \quad \epsilon \leq \epsilon_b, \quad (4.12)$$

$$\varphi_b(\epsilon, \tau) = 0 \quad \epsilon_b < \epsilon \leq 1.$$

Here $S(\tau)$, the inelastic source term, is computed from Eqn. 4.11:

$$S(\tau) = \frac{\rho(\rho\tau)^{N_s}}{N_s!} e^{-\rho\tau}. \quad (4.13)$$

The dimensionless energy ϵ_b is given by subtracting integers away from the source energy until the result is in the range $(0, 1]$. Thus

$$\epsilon_b = \begin{cases} s - IP(s) & s \neq \text{integer} \\ 1 & s = \text{integer.} \end{cases}$$

We can solve Eqn. 4.12 by Laplace transformation of the time variable:

$$\frac{p}{\sqrt{\epsilon}} \varphi_b^*(\epsilon, p) = \xi \sum_s \frac{\partial}{\partial \epsilon} (\epsilon \varphi_b^*(\epsilon, p)) + S^*(p) \delta(\epsilon - \epsilon_b), \quad (4.14)$$

where

$$S^*(p) = \left(\frac{\rho}{p + \rho} \right)^{N_s + 1}.$$

Replace the source in the above equation by an initial condition

$$\xi \sum_s \epsilon_b [\varphi_b^*(\epsilon_b^+, p) - \varphi_b^*(\epsilon_b^-, p)] = -S^*(p).$$

But $\varphi_b^*(\epsilon_b^+, p) = 0$. Therefore our initial condition is

$$\varphi_b^*(\epsilon_b^-, p) = \frac{S^*(p)}{\xi \sum_s \epsilon_b}.$$

The solution to Eqn. 4.14 is then

$$\varphi_b^*(\epsilon, p) = \frac{S^*(p)}{\epsilon \xi \sum_s} \exp[-p\tau(\epsilon, \epsilon_b)],$$

where *

$$\tau(\epsilon, \epsilon_b) = \frac{2}{\xi \sum_s} \left(\frac{1}{\sqrt{\epsilon}} - \frac{1}{\sqrt{\epsilon_b}} \right). \quad (4.15)$$

Inverting by the convolution theorem, we have

$$\epsilon \varphi_b(\epsilon, \tau) = \frac{1}{\xi \sum_s} \int_0^\tau S(\tau-x) \delta(x-\tau(\epsilon, \epsilon_b)) dx.$$

Thus

$$\epsilon \varphi_b(\epsilon, \tau) = \begin{cases} 0 & \tau < \tau(\epsilon, \epsilon_b) \\ \frac{\rho}{\xi \sum_s} \frac{1}{N_s!} \left\{ \rho[\tau - \tau(\epsilon, \epsilon_b)] \right\}^{N_s} \exp\left\{ -\rho[\tau - \tau(\epsilon, \epsilon_b)] \right\} & \tau \geq \tau(\epsilon, \epsilon_b). \end{cases}$$

The solution below threshold is sketched below for two representative energies, one at neutron arrival below threshold ($\epsilon = \epsilon_b$), and then at some lower energy.

* $\tau(\epsilon, \epsilon_b)$ is the time (cm.) for a neutron at energy ϵ_b to elastically slow down to energy ϵ . This quantity will be used extensively.

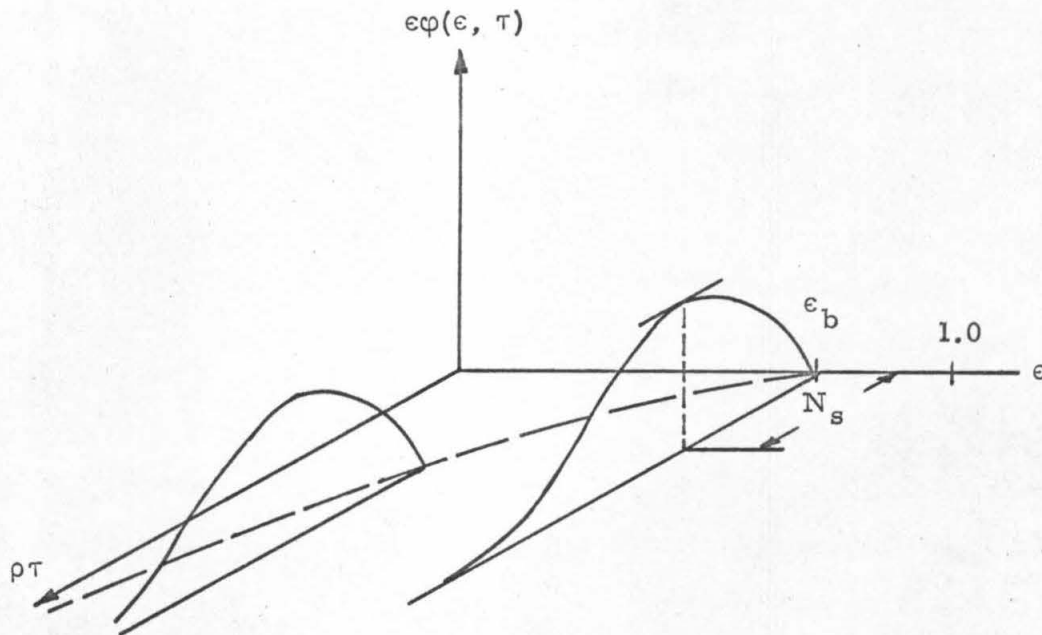


Figure 4.2 Below-Threshold Solution

We see the subthreshold flux can be viewed as a disturbance which travels without dispersion along the characteristic trajectory

$$\tau = \tau(\epsilon, \epsilon_b) + z \quad z \geq 0.$$

We can generalize the simple cross section used in this example quite easily. The essential features of the neutron flux are similar. Once Eqn. 4.10 is used to predict the pulse amplitudes, the subthreshold flux can be found.

B. Elastic Scattering Included in a Simple Form

In the analysis thus far, elastic scattering above threshold has been neglected. What effect does elastic scattering have on the time-energy distribution? Clearly, if an elastic transfer mechanism is

allowed, neutrons will arrive at a given energy sooner than when only inelastic transfer was considered. In order for the analysis of the previous section to be a good approximation, we need $\Sigma_{in}(\epsilon)/\xi \Sigma_s(\epsilon) \gg 1$. Whether or not this condition holds largely depends on the energy considered. In lead, for example, the ratio $\Sigma_{in}(\epsilon)/\xi \Sigma_s(\epsilon)$ varies from zero at the inelastic threshold (803 keV for Pb^{206}), to about ten at 1.6 MeV. Whenever the inelastic strength does not dominate, elastic transfer will play a significant role.

We can see this by including an age elastic scattering term above threshold. The balance equation we want to consider is

$$\frac{1}{\sqrt{\epsilon}} \frac{\partial \varphi(\epsilon, \tau)}{\partial \tau} = \xi \frac{\partial}{\partial \epsilon} (\Sigma_s(\epsilon) \epsilon \varphi(\epsilon, \tau)) + \Sigma_{in}(\epsilon+1) \varphi(\epsilon+1, \tau) - \Sigma_{in}(\epsilon) \varphi(\epsilon, \tau) + \delta(\epsilon-s) \delta(\tau). \quad (4.16)$$

We assume only a single inelastic level is excited, and that there is no absorption. Eqn. 4.16 is valid for $1 \leq \epsilon \leq s$. The subthreshold distribution is described by Eqn. 4.2. For reasons soon to become clear, we demand the elastic cross section satisfy

$$\Sigma_s(\epsilon) = \begin{cases} \frac{\Sigma_s}{\epsilon^{3/2}} & \epsilon \geq 1 \\ \Sigma_s(\epsilon) & \epsilon < 1. \end{cases} \quad (4.17)$$

We thus consider continuous elastic cross sections which decrease above the inelastic threshold, and have any functional dependence below. Using Eqn. 4.17, and again transforming to neutron density, Eqn. 4.16 becomes

$$\frac{\partial n(\epsilon, \tau)}{\partial \tau} = \beta \frac{\partial n(\epsilon, \tau)}{\partial \epsilon} + \sqrt{\epsilon+1} \Sigma_{in}(\epsilon+1)n(\epsilon+1, \tau) - \sqrt{\epsilon} \Sigma_{in}(\epsilon)n(\epsilon, \tau) + \delta(\epsilon-s) \delta(\tau), \quad (4.18)$$

where $\beta = \xi \Sigma_s$ (constant).

Before solving the balance equations for the neutron time-energy distribution, some general comments might be helpful. We expect the solution to be composed of two rather different types of functions. First, there will be delta function components, and this part of the distribution is zero except at a definite locus of points in the (ϵ, τ) plane. These delta functions arise from the particular delta function source we have chosen. The second type of function to be encountered will be distributions which occupy a finite portion of the (ϵ, τ) plane. In fact, these distributions will occupy only certain portions of the (ϵ, τ) plane, and will be zero elsewhere.

In the interest of concise presentation, we shall refer to the delta function terms as pulses, and shall associate the words "pulse amplitude" with the area under the delta function. To denote the other components, the distributed terms, we shall use the term "surface".

Returning to Eqn. 4.18, the solution can be obtained by considering the characteristics of the equation. Define the characteristic transformation

$$\begin{aligned} (\epsilon, \tau) &\leftrightarrow (\lambda, \eta) \\ \tau &= \lambda \quad (0 \leq \lambda < \infty) \\ \epsilon &= \eta - \beta \lambda \quad (1 \leq \eta \leq s) \end{aligned} \quad (4.19)$$

$$N(\lambda, \eta) \equiv n(\epsilon, \tau)$$

(4.19)
cont.

$$\Delta(\lambda, \eta) = \sqrt{\epsilon} \Sigma_{in}(\epsilon) = \sqrt{\eta - \beta\lambda} \Sigma_{in}(\eta - \beta\lambda).$$

Equation 4.18 can then be written in characteristic coordinates:

$$\frac{\partial N(\lambda, \eta)}{\partial \lambda} - \Delta(\lambda, \eta + 1)N(\lambda, \eta + 1) + \Delta(\lambda, \eta)N(\lambda, \eta) = 0, \quad (4.20)$$

with the initial data $N(0, \eta) = N_0(\eta) = \delta(s - \eta)$.

Conversion to characteristic coordinates thus leaves us with another partial differential difference equation, but the difference term now appears more simply in the equation. We see from Eqn. 4.19 that when $\epsilon \rightarrow \epsilon + 1$ (for fixed τ), $\eta \rightarrow \eta + 1$ (λ remains the same). This simple reflection is a consequence of modeling elastic scattering by Eqn. 4.17. If other elastic cross sections were considered, changing ϵ to $\epsilon + 1$ would imply a functional change in λ, η :

$$\lambda \rightarrow \lambda + g(\lambda, \eta)$$

$$\eta \rightarrow \eta + h(\lambda, \eta).$$

I. A Specific Example — A Simple Inelastic Cross Section

Before considering the solution to Eqn. 4.20 for general inelastic cross sections, we can point out the essential elements by considering the simple inelastic cross section

$$\Sigma_{in}(\epsilon) = \begin{cases} \frac{\Sigma_{in}}{\sqrt{\epsilon}} & \epsilon \geq 1 \\ 0 & \epsilon < 1. \end{cases}$$

Given this prescription, the functions Δ appearing in Eqn. 4.20 are constant, equal to the constant Σ_{in} . We have

$$\frac{\partial N(\lambda, \eta)}{\partial \lambda} - \Sigma_{in} N(\lambda, \eta+1) + \Sigma_{in} N(\lambda, \eta) = 0, \quad (4.21)$$

with the initial condition $N(0, \eta) = \delta(s-\eta)$.

Define a Laplace transform with respect to the variable λ

$$N^*(p, \eta) = \int_0^{\infty} e^{-p\lambda} N(\lambda, \eta) d\lambda.$$

Substitution yields

$$\begin{aligned} \Sigma_{in} N^*(p, \eta+1) - (\Sigma_{in} + p) N^*(p, \eta) &= 0 & \eta < s \\ N^*(p, \eta) &= 0 & \eta > s \end{aligned} \quad (4.22)$$

$$N^*(p, s) = -\frac{\delta(s-\eta)}{(\Sigma_{in} + p)}.$$

The first equation has the following general solution⁽⁴⁵⁾:

$$N^*(p, \eta) = \left(\frac{p + \Sigma_{in}}{\Sigma_{in}} \right)^{\eta} \omega_1(\eta),$$

where $\omega_1(\eta)$ is an arbitrary periodic function of η , with period unity.

Choosing this function to satisfy the second and third of Eqns. 4.22, we have

$$N^*(p, \eta) = \frac{\Sigma_{in}^{s-\eta}}{(p + \Sigma_{in})^{s-\eta+1}} \sum_{l=0}^{N_s} \delta(s-\eta-l). \quad (4.23)$$

Inversion of the transformed solution yields

$$N(\lambda, \eta) = \frac{\sum_{\text{in}}^{s-\eta}}{\Gamma(s-\eta+1)} \lambda^{s-\eta} e^{-\lambda \sum_{\text{in}}^{N_s}} \sum_{l=0}^{N_s} \delta(s-\eta-l). \quad (4.24)$$

By transforming back to energy-time coordinates we find

$$n(\epsilon, \tau) = e^{-\sum_{\text{in}} \tau} \sum_{l=0}^{N_s} \frac{(\sum_{\text{in}} \tau)^l}{l!} \delta(s-\epsilon-\beta\tau-l). \quad (4.25)$$

The solution above threshold is thus specified as a sequence of pulses, with time and energy dependent amplitudes, which follow straight line trajectories in the energy-time plane. The pulse trajectories are shown below.

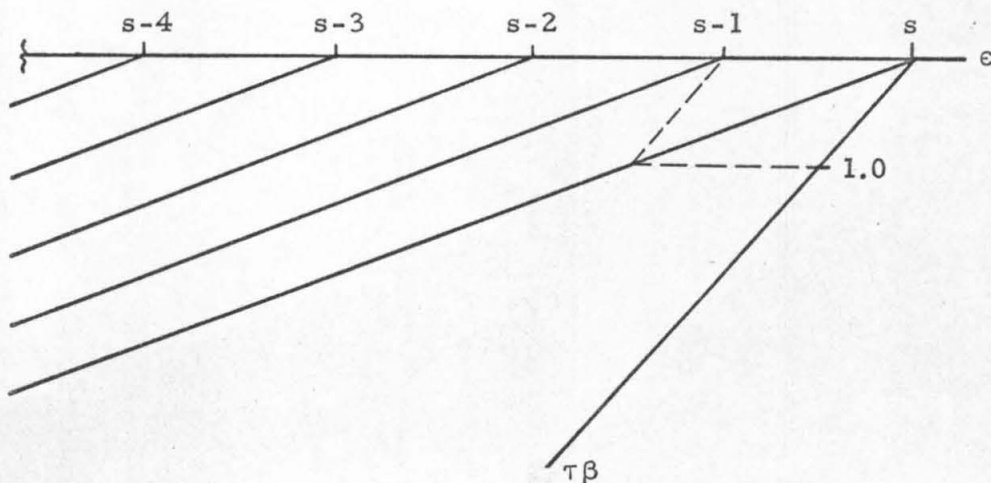


Figure 4.3 Energy-Time Pulse Trajectories

We see that in the first unit energy interval below the source there is a single pulse. In the second interval there are two pulses, and so on. Along each trajectory, we can view the amplitudes A_l of the pulses described above in a simple way:

$$A_l = \frac{(\Sigma_{in} \tau)^l}{l!} e^{-\Sigma_{in} \tau}$$

The amplitude for the l^{th} pulse is thus shown below for the lowest values of l . Note that at early times $A_l \sim \tau^l$.

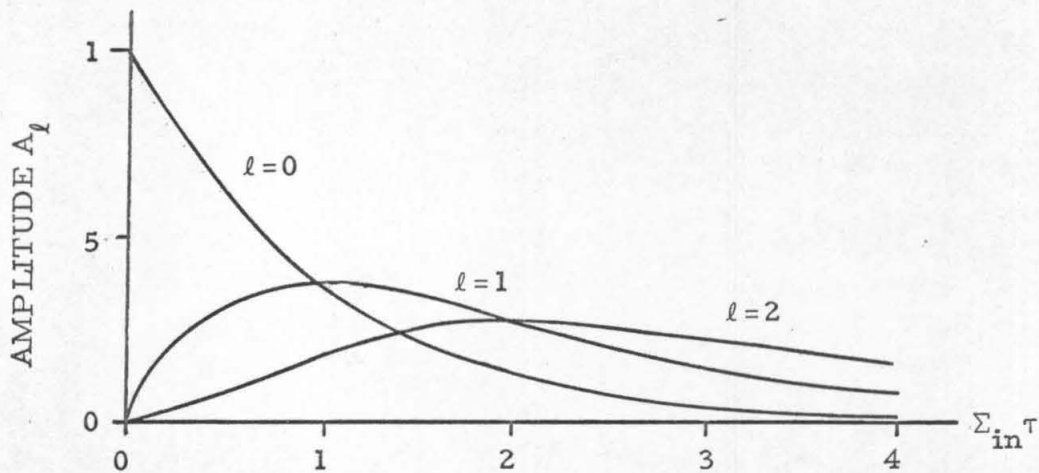


Figure 4.4 Pulse Amplitudes

We can now visualize the importance of modeling elastic cross sections as in Eqn. 4.17. In Figure 4.3 we see that with a monoenergetic source at energy $\epsilon = s$ and time $\tau = 0$, information is carried along straight line characteristics. If a neutron suffers no inelastic collisions,

it slows down by elastic transfer on this characteristic path (l is conserved). If, however, a neutron is scattered inelastically, it is transferred to a new characteristic, with the index l increasing by one unit. All scattering events thus interfere constructively, and pulses of varying amplitudes result. If a different elastic cross section were used, a spreading neutron distribution would give rise to solution surfaces (in addition to pulses) in the energy intervals below the source.

To illustrate the phenomenon, we will use the above-threshold solution already obtained as a source of neutrons for the subthreshold region. Consider the balance equation for the neutron flux below the inelastic threshold. For convenience, we choose the elastic cross section to be constant ($\beta = \xi \Sigma_s$) in this energy range. Eqn. 4.2 becomes

$$\frac{1}{\sqrt{\epsilon}} \frac{\partial \varphi_b(\epsilon, \tau)}{\partial \tau} = \beta \frac{\partial}{\partial \epsilon} (\epsilon \varphi_b(\epsilon, \tau)) + \Sigma_{in}(\epsilon+1) \sqrt{\epsilon+1} n(\epsilon+1, \tau) \quad 0 \leq \epsilon \leq 1 \quad (4.26)$$

$$\varphi_b(1^-, \tau) = n(1^+, \tau).$$

The last term in the balance equation is the source of neutrons below threshold due to inelastic events in the region above. The term $n(\epsilon+1, \tau)$ comes from Eqn. 4.25 with ϵ restricted to $1 \leq \epsilon \leq 2$ (so that one inelastic collision carries the neutron below threshold).

After defining

$$\psi(\epsilon, \tau) = \epsilon \varphi_b(\epsilon, \tau) \quad (4.27)$$

$$S_{in}(\epsilon, \tau) = \Sigma_{in}(\epsilon+1) \sqrt{\epsilon+1} n(\epsilon+1, \tau),$$

we Laplace transform the time variable in the usual way. Eqn. 4.26 becomes

$$\frac{d\psi^*(\epsilon, p)}{d\epsilon} - \frac{p}{\beta} \frac{\psi^*(\epsilon, p)}{\epsilon^{3/2}} = -\frac{1}{\beta} S_{in}^*(\epsilon, p) \quad , \quad \psi^*(l^-, p) = n^*(l^+, p). \quad (4.28)$$

The transform plane solution is

$$\psi^*(\epsilon, p) = e^{-\frac{2p}{\beta\sqrt{\epsilon}}} \int_{\epsilon}^1 \frac{S_{in}^*(\epsilon', p)}{\beta} e^{\frac{2p}{\beta\sqrt{\epsilon'}}} d\epsilon' + n^*(l, p) e^{-\frac{2p}{\beta}(\frac{1}{\sqrt{\epsilon}} - 1)}. \quad (4.29)$$

This expression may be inverted using the convolution theorem:

$$\begin{aligned} \epsilon \varphi_b(\epsilon, \tau) = & \frac{1}{\beta} \int_{\epsilon}^1 d\epsilon' \left[\int_0^{\tau} S_{in}(\epsilon', \tau-x) \delta(x-\tau(\epsilon, \epsilon')) dx \right] \\ & + \int_0^{\tau} n(l, \tau-x) \delta(x-\tau(\epsilon, l)) dx. \end{aligned} \quad (4.30)$$

The first term in Eqn. 4.30 will give rise to a discontinuous distribution, while the second term will correspond to pulses propagating into the region $\epsilon < l$ from above on their characteristic trajectories (which change shape due to the change in elastic cross section below threshold). The discontinuous distribution results from the functional change in the elastic cross section at the inelastic threshold. We can perform the integrations over the dummy variable x , and change the dependent variable to neutron density, to obtain

$$n(\epsilon, \tau) = \frac{\varphi_b(\epsilon, \tau)}{\sqrt{\epsilon}} = \frac{1}{\beta\epsilon^{3/2}} \int_{\epsilon}^1 d\epsilon' \left\{ \begin{array}{l} S_{in}(\epsilon', \tau - \tau(\epsilon, \epsilon')) \\ 0 \end{array} \right\} \begin{array}{l} \tau - \tau(\epsilon, \epsilon') \geq 0 \\ \text{otherwise} \end{array} \quad (4.31)$$

$$+ \frac{1}{\epsilon^{3/2}} \left\{ \begin{array}{l} n(1, \tau - \tau(\epsilon, 1)) \\ 0 \end{array} \right\} \begin{array}{l} \tau - \tau(\epsilon, 1) \geq 0 \\ \text{otherwise.} \end{array}$$

On a more physical basis, the first term corresponds to neutrons entering the subthreshold region via inelastic collisions, while the second comes from neutrons crossing the threshold by elastic scattering. We may speculate that the delta function behavior of the term $S_{in}(\epsilon', \dots)$ (Equations 4.25 and 4.27) will, when integrated as in Eqn. 4.31, give rise to a surface in the (ϵ, τ) plane. Similarly the second term is just a pulse of neutrons with a different (ϵ, τ) trajectory in the below threshold region. In fact, breaking up $n(\epsilon, \tau)$ in Eqn. 4.31 into separate components for the surface and pulse part, we have, using Eqns. 4.25 and 4.27:

$$n(\epsilon, \tau) = [n(\epsilon, \tau)]_s + [n(\epsilon, \tau)]_p \quad (4.32)$$

$$[n(\epsilon, \tau)]_s = \frac{\Sigma_{in}}{\beta\epsilon^{3/2}} \int_{\epsilon}^1 \left[\frac{\left\{ \Sigma_{in} [\tau - \tau(\epsilon, \epsilon')] \right\}^{s - \epsilon' - 1 - \beta\tau + \beta\tau(\epsilon, \epsilon')}}{\Gamma(s - \epsilon' - \beta\tau + \beta\tau(\epsilon, \epsilon'))} \right. \quad (4.33)$$

$$\left. \cdot \exp \left\{ -\Sigma_{in} [\tau - \tau(\epsilon, \epsilon')] \right\} \sum_{l=0}^{N_s} \delta(s - \epsilon' - 1 - \beta\tau + \beta\tau(\epsilon, \epsilon') - l) \right] d\epsilon'$$

$$[n(\epsilon, \tau)]_p = \frac{1}{\epsilon^{3/2}} \frac{(\sum_{in} \tau)^{s-3-\beta\tau+2/\sqrt{\epsilon}}}{\Gamma(s-2-\beta\tau+\frac{2}{\sqrt{\epsilon}})} \exp\left\{-\sum_{in} [\tau-\tau(\epsilon, 1)]\right\} \sum_{l=0}^{N_s} \delta(s-3-\beta\tau+\frac{2}{\sqrt{\epsilon}}-l). \quad (4.34)$$

We implicitly assume that in each of the above two equations (ϵ, τ) are chosen so that the non-zero condition in Eqn. 4.31 is valid. Actually the index N_s in the delta function summation performs precisely this task, so that the zero option in Eqn. 4.31 is not possible.

Dealing now with Eqn. 4.33, we find

$$[n(\epsilon, \tau)]_s = \frac{\sum_{in}}{\beta \epsilon^{3/2}} \sum_{l=0}^{N_s} \frac{\left\{ \frac{\sum_{in}}{\beta} (s-\epsilon_*-1-l) \right\}^l}{l!} \exp \left\{ -\frac{\sum_{in}}{\beta} (s-\epsilon_*-1-l) \right\}, \quad (4.35)$$

$$\frac{1}{(1/\epsilon_*)^{3/2-1}}$$

where $\epsilon_*(\epsilon, \tau)$ is defined as the solution to

$$s-1-\beta\tau+\frac{2}{\sqrt{\epsilon}}-l = \epsilon_* + \frac{2}{\sqrt{\epsilon_*}} \quad \epsilon \leq \epsilon_* \leq 1. \quad (4.36)$$

We see from Eqn. 4.35 that the surface term is thus composed of a series of surface components. The boundary of each surface component is given by solutions ϵ_* (from Eqn. 4.36) which lie in the range $\epsilon \leq \epsilon_* \leq 1$. If, for a given (ϵ, τ) pair, one cannot find an ϵ_* satisfying Eqn. 4.36, then that surface component is zero at (ϵ, τ) . Because of the monotonic nature of the function $\epsilon_* + 2/\sqrt{\epsilon_*}$ in the region $\epsilon_* \in [\epsilon, 1]$ ($\epsilon \leq 1$), we can easily find the limits for a non-zero solution in the subthreshold region. This is done by replacing ϵ_* in Eqn. 4.36 by its greatest and least values;

ϵ and unity. We thus find non-zero solutions for the l^{th} component of $[n(\epsilon, \tau)]_s$ between

$$s - 2 - \beta\tau + 2 \left(\frac{1}{\sqrt{\epsilon}} - 1 \right) = l \quad (4.37)$$

$$s - \epsilon - 1 - \beta\tau = l.$$

If $\epsilon_* = 1$ in Eqn. 4.35, $[n(\epsilon, \tau)]_s$ is then singular. Since $\epsilon_* = 1$ is admitted by Eqn. 4.36, we encounter a locus of singular points in our surface term prescription. In order for neutrons to be conserved, the singularity must be integrable in energy. Consider integrating Eqn. 4.35, with some weight function, over all subthreshold energies:

$$c_s(\tau) = \int_0^1 [n(\epsilon, \tau)]_s f(\epsilon) d\epsilon = \sum_{l=0}^{N_s} \int_{\epsilon_l^l}^{\epsilon_c^l} \frac{f_l(\epsilon, \tau)}{\left(\frac{1}{\epsilon_*}\right)^{3/2} - 1} d\epsilon. \quad (4.38)$$

The limits of integration explicitly build in the fact that only certain (ϵ, τ) coordinates offer a non-zero contribution. The lower limit corresponds to that value of ϵ satisfying the second of Eqns. 4.37 (if the solution ϵ_l^l is negative, we take it to be zero). The upper limit, ϵ_c^l , is defined to be that value of ϵ which yields $\epsilon_* = 1$. The first of Eqns. 4.37, with $\epsilon_* = 1$, thus becomes

$$\frac{2}{\sqrt{\epsilon_c^l}} = 4 - s + \beta\tau + l. \quad (4.38a)$$

Take ϵ slightly less than this end-point value by defining some new small parameter x such that

$$\epsilon = \epsilon_c^l(\tau) - x \quad (4.38b)$$

$$\frac{2}{\sqrt{\epsilon}} = \frac{2}{\sqrt{\epsilon_c^l(\tau) - x}} .$$

Returning now to Eqn. 4.36, we have

$$\epsilon_* + \frac{2}{\sqrt{\epsilon_*}} = 3 - \frac{2}{\sqrt{\epsilon_c^l(\tau)}} + \frac{2}{\sqrt{\epsilon_c^l(\tau) - x}} .$$

Now we let $\epsilon_* = 1 - y$, and seek to relate the small parameter x to the small parameter y . We have

$$1 - y + \frac{2}{\sqrt{1 - y}} = 3 - \frac{2}{\sqrt{\epsilon_c^l(\tau)}} + \frac{2}{\sqrt{\epsilon_c^l(\tau) - x}} .$$

Expansion of the square roots yields

$$\frac{3}{4} y^2 + \frac{15}{24} y^3 + \dots = \frac{x}{(\epsilon_c^l)^{3/2}} + \frac{3}{4} \frac{x^2}{(\epsilon_c^l)^{3/2}} + \dots$$

If x is very small, we have

$$y = \frac{2}{\sqrt{3}} \frac{1}{(\epsilon_c^l)^{3/4}} \sqrt{x} + \dots \quad (4.38c)$$

Therefore near $\epsilon_* = 1$

$$\left[\left(\frac{1}{\epsilon_*} \right)^{3/2} - 1 \right]^{-1} = \left[\left(\frac{1}{1 - y} \right)^{3/2} - 1 \right]^{-1} = \frac{\sqrt{3}}{2} (\epsilon_c^l)^{3/4} \frac{1}{\sqrt{x}} + \dots \quad (4.38d)$$

Returning to Eqn. 4.38, we find that $c_s(\tau)$, which corresponds to counting neutrons, is given by

$$c_s(\tau) = \sum_l^{N_s} \frac{\sqrt{3}}{2} (\epsilon_c^l)^{3/4} \int_{\epsilon_c^l}^{\epsilon_c^l} \frac{f_l(\epsilon, \tau)}{\sqrt{\epsilon_c^l(\tau) - \epsilon}} d\epsilon. \quad (4.38e)$$

The number of neutrons is thus conserved because the integral is finite. Moreover, as the singular point $\epsilon = \epsilon_c^l(\tau)$ is approached, Eqn.4.35 predicts that the surface term approaches

$$\lim_{\epsilon \rightarrow \epsilon_c^l(\tau)} [n(\epsilon, \tau)]_s = \frac{\sum_{in}}{\beta} \sum_{l=0}^{N_s} \lim_{\epsilon \rightarrow \epsilon_c^l(\tau)} \frac{1}{\epsilon_c^l(\tau)^{3/2}} \frac{\left\{ \frac{\sum_{in}}{\beta} (s-2-l) \right\}^l}{l!} \exp \left\{ -\frac{\sum_{in}}{\beta} (s-2-l) \right\} \frac{1}{\sqrt{\epsilon - \epsilon_c^l(\tau)}},$$

or

$$\lim_{\epsilon \rightarrow \epsilon_c^l(\tau)} [n(\epsilon, \tau)]_s = \frac{\sum_{in}}{\beta} \frac{1}{\epsilon_c^l(\tau)^{3/2}} \frac{\left\{ \frac{\sum_{in}}{\beta} (s-2-l) \right\}^l}{l!} \exp \left\{ -\frac{\sum_{in}}{\beta} (s-2-l) \right\} \frac{1}{\sqrt{\epsilon - \epsilon_c^l(\tau)}}.$$

Thus as ϵ approaches that value which yields $\epsilon_* = 1$, the function $[n(\epsilon, \tau)]_s$ has a square-root singularity. This conclusion is verified by numerical calculation.

The other component of the solution $n(\epsilon, \tau)$, given by Eqn. 4.34, corresponds to neutrons entering the subthreshold region via elastic scattering. This contribution is a sum of delta function pulses, and is simply a projection of the above threshold pulses below threshold. We see that the division of the neutron population shifts between the surface terms and the pulse terms as time evolves. Once the $l=0$ characteristic intersects $\epsilon=1$ (so that no more neutrons are above threshold) the population division is fixed.

Consider now a sample calculation. Taking $s=5$, and $(\Sigma_{in}/\beta)=1.0$, we can plot in Figures 4.5a and 4.5b the solution $n(\epsilon, \tau)$ for various values of the scaled time $\beta\tau$. To better understand the details shown, a fronting page serves as a guide to the figures. To see the time scale more vividly, we consider a specific system to remove the non-dimensionality of energy, and return to real time. Within the framework of the above example, take $\xi = 0.01$ (implying a mass number of about 200), $\Sigma_s = 0.5 \text{ cm}^{-1}$ (therefore $\Sigma_{in} = 0.005 \text{ cm}^{-1}$ because $\Sigma_{in}/\beta = 1$ in the example), and threshold energy $E_{th} = 500 \text{ kev}$ (then the source is five times larger, at 2.5 mev). With these choices the real time t is related to $\tau\beta$ via

$$t = 0.212 \times 10^{-6} (\tau\beta) \text{ (seconds)},$$

while the real energy E is related to ϵ via

$$E = E_{th} \epsilon = 5.0 \times 10^5 (\epsilon) \text{ (electron volts)}.$$

Thus all neutrons fall below 500kev 850 nanoseconds after the burst ($\tau\beta=4$), and the last figure ($\tau\beta=1000$) shows the neutrons focused rather well at about 2.0ev some 212 microseconds following the source burst.

II. Generalization to any Inelastic Cross Section

We return now to Eqn. 4.20 to construct a solution when the inelastic scattering cross section is any arbitrary function of energy. The functions $\Delta(\lambda, \eta+1)$, $\Delta(\lambda, \eta)$ appearing in Eqn. 4.20 contain the inelastic cross sections. We see, however, that these functions play no role in determining the characteristics. Rather, the characteristic

Time Dependent Neutron Density Graphs

On the following pages we show the time dependent neutron density for the example considered. Remember that the density in this case is composed of two types of functions. Above threshold the density consists of delta functions, or pulses, with varying amplitudes. Below threshold neutrons also appear in pulses, corresponding to those neutrons entering the subthreshold region by elastic collisions. Also, the subthreshold density is augmented by a distributed term (or surface), which comes from neutrons crossing the threshold by inelastic collision.

The amplitudes of the delta functions are shown as number of neutrons per unit source neutron. For each time, the population division is specified as the percentage of neutrons distributed in the surface term. Recall that the source strength was chosen to be one neutron per second, and that no absorption was considered. We have then that the sum of the pulse amplitudes, plus the area under the distributed term, must always equal one.

We see that after the burst the pulse is rapidly dispersed by inelastic scattering. For $\tau\beta \geq 1.0$, part of the surface term contains the square-root singularities discussed before. In a relatively short time ($\tau\beta=4$) all neutrons have dropped below threshold energy, and the pulse-surface population division is then fixed for all later times. The slowing down is then simply governed by the elastic scattering with a peculiar initial distribution. As time increases, we thus see the expected result of the distribution focusing toward a sharper energy value.

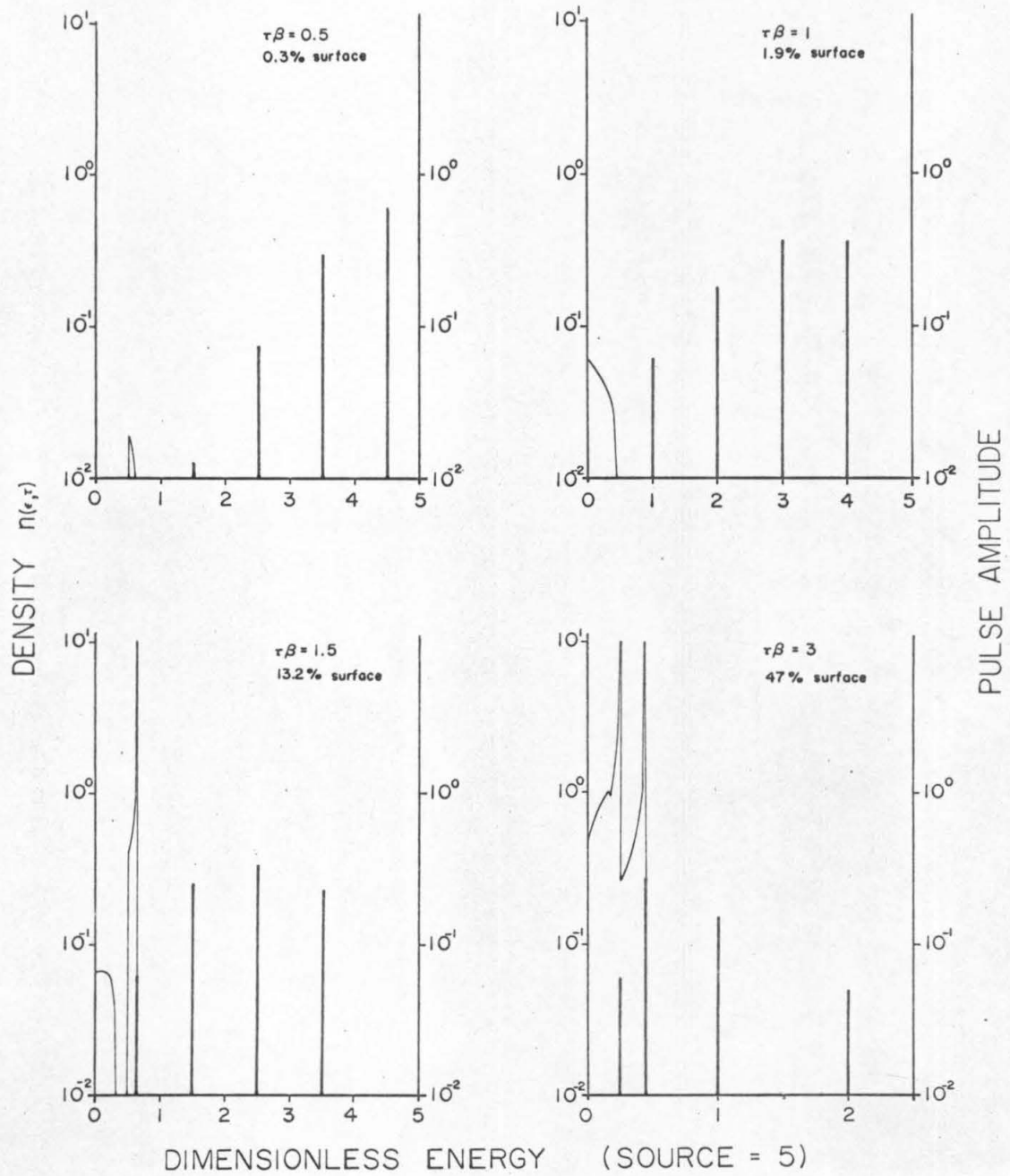


FIGURE 4.5a TIME DEPENDENT NEUTRON DENSITY

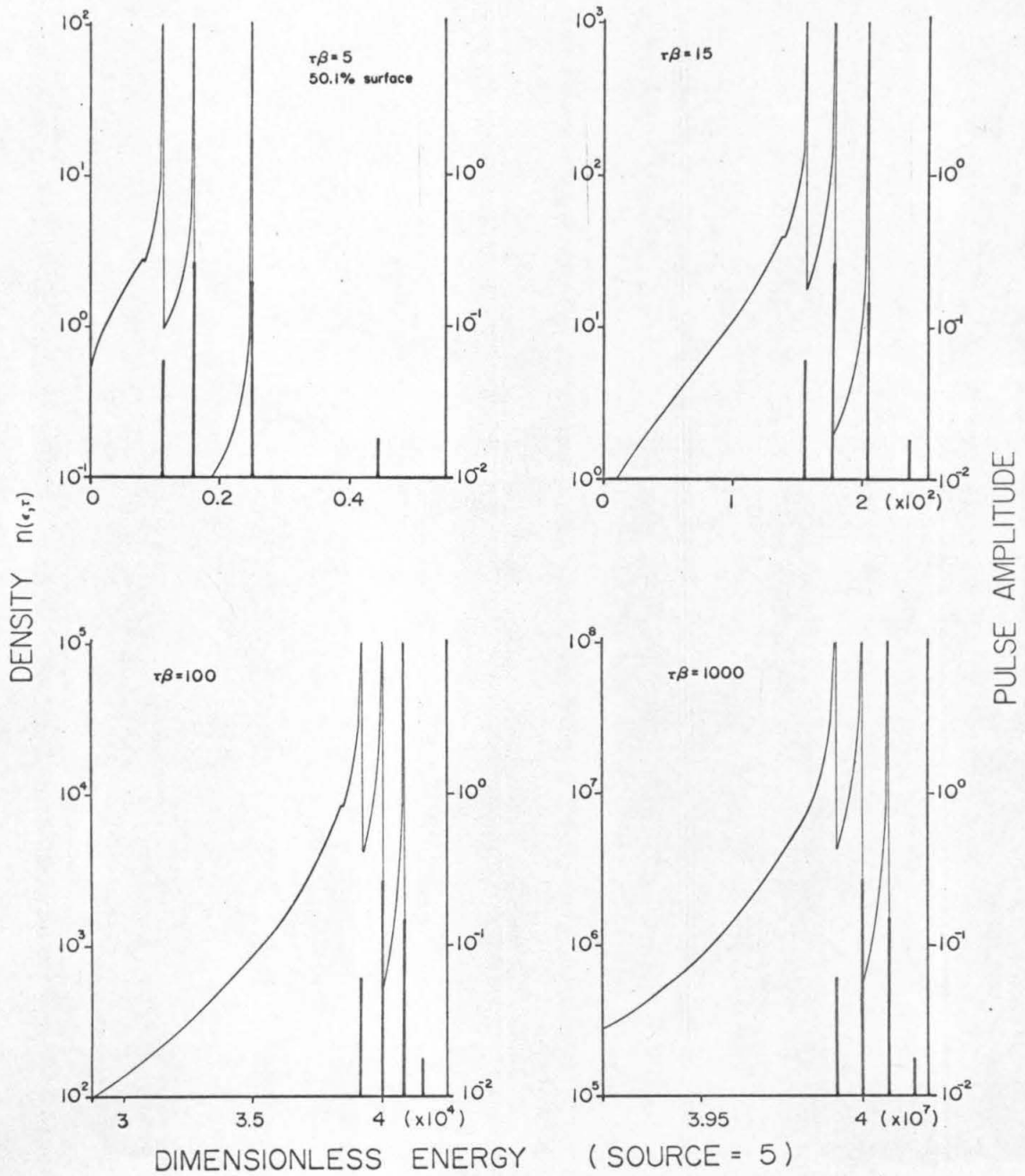


FIGURE 4.5b TIME DEPENDENT NEUTRON DENSITY

trajectories are determined only by the elastic scattering cross section, which is assumed to obey Eqn. 4.17. Thus the characteristics above threshold for general inelastic scattering are the same as they were for the specific case considered on the preceding pages, and we may thus seek a solution to Eqn. 4.20 (above threshold) in a form suggested by Eqn. 4.24:

$$N(\lambda, \eta) = \sum_{\ell=0}^{N_s} a_{\ell}(\lambda) \delta(s - \eta - \ell). \quad (4.39)$$

Formal substitution of the series into Eqn. 4.20, followed by recognition of the linear independence of the delta functions, allows us to write the following coupled equations for the vector \vec{a} :

$$\begin{aligned} \frac{da_0(\lambda)}{d\lambda} + \Delta(\lambda, s) a_0(\lambda) &= 0 \quad a_0(0) = 1 \\ \frac{da_{\ell}(\lambda)}{d\lambda} + \Delta(\lambda, s - \ell) a_{\ell}(\lambda) &= \Delta(\lambda, s - \ell + 1) a_{\ell-1}(\lambda) \quad a_{\ell}(0) = 0 \quad \ell = 1, \dots, N_s. \end{aligned} \quad (4.40)$$

The solution to Eqns. 4.40 is

$$\begin{aligned} a_0(\lambda) &= \exp \left\{ - \int_0^{\lambda} \Delta(\lambda', s) d\lambda' \right\} \\ a_{\ell}(\lambda) &= \int_0^{\lambda} \Delta(\lambda', s - \ell + 1) a_{\ell-1}(\lambda') \exp \left\{ \int_{\lambda}^{\lambda'} \Delta(\lambda'', s - \ell) d\lambda'' \right\} d\lambda' \quad \ell = 1, \dots, N_s. \end{aligned} \quad (4.41)$$

We can transform back to (ϵ, τ) coordinates by recalling Eqns. 4.19. We have

$$n(\epsilon, \tau) = \sum_{\ell=0}^{N_s} a_{\ell}(\tau) \delta(s-\epsilon-\beta\tau-\ell), \quad (4.42)$$

where

$$a_0(\tau) = \exp \left\{ - \int_0^{\tau} \sqrt{s-\beta\tau'} \Sigma_{\text{in}}(s-\beta\tau') d\tau' \right\} \quad (4.43)$$

$$a_{\ell}(\tau) = \exp \left\{ - \int_0^{\tau} \sqrt{s-l-\beta\tau'} \Sigma_{\text{in}}(s-l-\beta\tau') d\tau' \right\}$$

$$\int_0^{\tau} \sqrt{s-l+1-\beta\tau'} \Sigma_{\text{in}}(s-l+1-\beta\tau') a_{\ell-1}(\tau') \exp \left\{ \int_0^{\tau'} \sqrt{s-l-\beta\tau''} \Sigma_{\text{in}}(s-l-\beta\tau'') d\tau'' \right\}$$

$$\ell=1, \dots, N_s.$$

The solution above threshold is thus the same sequence of pulses as appeared in the previous example, but with different amplitudes (given by Eqns. 4.43). Construction of the solution below threshold proceeds exactly as before. If we again assume that the elastic cross section is constant below threshold (this is not necessary, but convenient), we have Eqn. 4.31 as a valid solution below threshold, where Eqns. 4.27 are used to interpret the inelastic source and Eqn. 4.42 is used for calculation. Finally, we note solutions to Eqns. 4.43, which ultimately yield the density, are easy to handle numerically. The simple coupling and straightforward integrals allow rapid integration.

To illustrate the effect of more physical inelastic cross sections, we consider another calculation. Rather than evaluating Eqns. 4.43 numerically, we will choose parameters so that analytical integration is possible. Consider the following inelastic cross section:

$$\Sigma_{\text{in}}(\epsilon) = \Sigma_{\text{in}} \left(\sqrt{\epsilon} - \frac{1}{\sqrt{\epsilon}} \right) \quad \epsilon \geq 1. \quad (4.44)$$

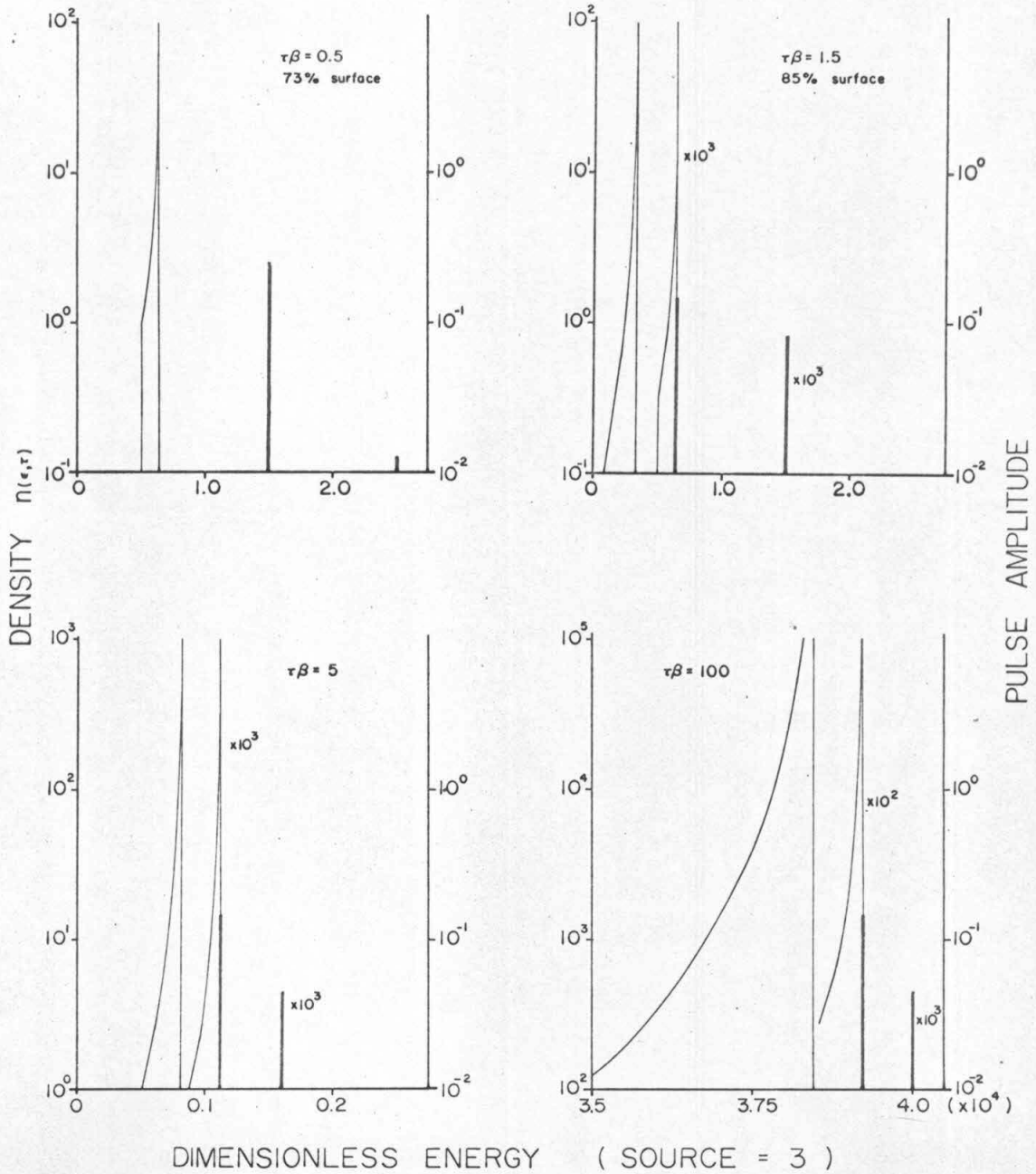
If we choose the source at $s=3$, we need only evaluate $a_0(\tau)$ and $a_1(\tau)$ in Eqns. 4.43. Further, we let $\Sigma_{\text{in}}/\beta=5.0$, corresponding to a rather strong inelastic scattering transfer. Very roughly, this is characteristic of the inelastic strength for materials with $A \sim 60-100$ ⁽⁴¹⁾. Evaluation of Eqns. 4.43 yields

$$a_0(\tau) = \exp \left\{ \frac{\Sigma_{\text{in}}}{\beta} \left[\frac{(\tau\beta)^2}{2} - 2\tau\beta \right] \right\} \quad 0 \leq \tau \leq 2$$

$$a_1(\tau) = \frac{1}{(\Sigma_{\text{in}}/\beta)} \exp \left\{ \frac{\Sigma_{\text{in}}}{\beta} \left[\frac{(\tau\beta)^2}{2} - \tau\beta \right] \right\}$$

$$\cdot \left\{ \left(2 \frac{\Sigma_{\text{in}}}{\beta} - 1 \right) + \exp \left[- \frac{\Sigma_{\text{in}}}{\beta} (\tau\beta) \right] \left(1 - \frac{\Sigma_{\text{in}}}{\beta} [2 - \tau\beta] \right) \right\} \quad 0 \leq \tau \leq 1.$$

The solutions above and below threshold are shown in Figure 4.6 for various times after the source burst. The interpretation is the same as for the previous example. We note some similarities with the case before, but there are some striking differences. At very short times we see a majority of neutrons (73% at 0.5 dimensionless time units) have fallen below threshold by inelastic scattering. These



DIMENSIONLESS ENERGY (SOURCE = 3)
FIGURE 4.6 TIME DEPENDENT NEUTRON DENSITY

are all neutrons which have suffered two inelastic collisions ($\ell=1$). The pulse terms, corresponding to neutrons entering the subthreshold region via elastic scattering, are much smaller than in the previous case. In fact, the pulse term for neutrons suffering just one inelastic event is three orders of magnitude larger than the term for neutrons which suffer no inelastic collisions. Thus for every neutron injected at $\tau\beta=0$, 0.147 cross the threshold elastically after one inelastic collision, 0.000045 cross the threshold elastically with no inelastic collisions, and the rest enter the subthreshold region by inelastic collision. Further, of this resultant 85.3%, practically all are neutrons which have undergone two inelastic events. The distribution in Figure 4.6 demonstrates that for late times, the surface resulting from neutrons twice scattered inelastically overwhelms the surface for those scattered once.

All of these observations can be attributed to a single fact: In this example, we considered a strong inelastic transfer with a cross section which increases with energy. Neutrons thus cascade below the inelastic threshold at very short times.

C. Prospects of Extension to More General Elastic Cross Sections.

The extension of the analysis of the previous section to include more general forms for the elastic scattering cross section is an obvious next step. This generalization is impeded by the mathematical complexity of the resultant equations.

Consider the attempt to transform the balance equation to characteristic coordinates, similar to Eqns. 4.19. We can certainly

specify the characteristic trajectories irrespective of the form of the elastic cross section. In fact, the characteristics for the neutron density are

$$(\epsilon, \tau) \Leftrightarrow (\lambda, \eta) \quad 1 \leq \eta \leq s \quad 0 \leq \lambda \leq \infty$$

$$\epsilon = \eta - \xi \lambda$$

(4.45)

$$\tau = \frac{1}{\xi} \int_{\eta}^{\xi \lambda + \eta} \frac{dx}{\Sigma_s(x) x^{3/2}}$$

While the characteristics are thus known by an easy calculation, computation of the difference term resulting from the inelastic scattering is another matter. In Eqn. 4.20 we saw that when $\Sigma_s(\epsilon) \sim 1/\epsilon^{3/2}$, we had the difference term $n(\epsilon+1, \tau)$ reflected in a simple way in the transformed coordinates $N(\lambda, \eta+1)$. As we pointed out before, if general elastic cross sections are used, this simple reflection is destroyed. Instead of a relatively simple differential difference equation, we then have a very complex functional differential difference equation. While it does not seem beneficial to pursue solutions in characteristic coordinates further, it is still likely that the notions of characteristic trajectories will be of great benefit in seeking solutions by alternate means.

One can make progress in another direction by using double Laplace transforms⁽⁴⁶⁾. This method is slightly complicated by the fact that, as shown in Chapter II, the point $\epsilon=0$ is usually singular, and therefore one must use the adjoint function to avoid some difficulties.

Inversion of the resultant transformed adjoint is a difficult matter. Use of characteristic coordinates to specify limits of the solution surfaces may be a useful tool in ultimately recovering the neutron density. This problem forms the basis for continued research in time dependent slowing down with discrete inelastic scattering.

REFERENCES

1. A. Weinberg and E. Wigner, The Physical Theory of Neutron Chain Reactors, University of Chicago Press, Chicago (1958).
2. R. Meghreblian and D. Holmes, Reactor Analysis, McGraw-Hill, New York (1960).
3. J. Lamarsh, Introduction to Nuclear Reactor Theory, Addison-Wesley, Reading, Massachusetts (1966).
4. T. D. Beynon, "A Kernel for the Scattering of Neutrons From an Excited Nuclear State", Journal of Nuclear Energy, 24, p. 565 (1970).
5. R. Marshak, "Theory of the Slowing Down of Neutrons by Elastic Collision with Atomic Nuclei", Rev. Mod. Phys. 19, p. 185 (1947).
6. G. Placzek, "On the Theory of Slowing Down of Neutrons in Heavy Substances", Physical Review, 69, p. 423 (1946).
7. F. T. Adler, "On the Slowing Down of Neutrons by Elastic Collisions", Physical Review, 60, p. 279 (1941).
8. G. Goertzel and E. Greuling, "An Approximate Method for Treating Neutron Slowing Down", Nuc. Sci. Eng., 7, p. 69 (1960).
9. H. Volkin, "The Effect of Inelastic Collisions on the Slowing Down Length of Neutrons in a Hydrogenous Mixture", Journal of Applied Physics, 25, p. 83 (1954).
10. J. M. Blatt and V. Weisskopf, Theoretical Nucl. Phys., Wiley, New York (1952).
11. D. Okrent, R. Avery and H. Hummel, "A Survey of Theoretical and Experimental Aspects of Fast Reactor Physics", Inter. Conf. Peaceful Uses At. Energy, 5, p. 347 (1955).
12. K. Inoue, "Scattering Process Approach to Neutron Spectrum in Fast Reactors", Journal of Nuclear Science and Technology, 5, p. 333 (1968).
13. B. Nicolaenko, "Energy-Dependent Boltzmann Equation in the Fast Domain", Journal of Mathematical Physics, 11, p. 174 (1970).
14. J. T. Mihalczo, "Sensitivity of Neutron-Spectrum-Dependent Quantities in Uranium Metal Assemblies to Inelastic Scattering Models for U-235", Trans. Am. Nuc. Soc., 9, p. 489 (1966).

15. T. Murley and I. Kaplan, "A Modal Representation of Fast Reactor Spectra", Trans. Am. Nuc. Soc., 8, p. 238 (1965).
16. M. Driscoll and I. Kaplan, "A Simple Shape Function for Correlating Fast Reactor Spectra", Trans. Am. Nuc. Soc., 9, p. 137 (1966).
17. M. Cadhilac and M. Pujol, "Continuous Model for the Inelastic Slowing Down of Fast Neutrons", Fast Reactor Physics, I. A. E. A., Vienna, p. 189 (1968).
18. M. Cadhilac and M. Pujol, "A Simple Model for the Inelastic Scattering of Fast Neutrons", Journal Nuc. Energy, 21, p. 58 (1967).
19. R. Malakoff and B. Malaviya, "Simple Analytical Models for Studying Fast Neutron Spectra", Trans. Am. Nuc. Soc., 11, p. 608 (1968).
20. F. Dunn and M. Becker, "Analytic Representations of Fast Reactor Flux and Importance Spectra", Trans. Am. Nuc. Soc., 11, p. 213 (1968).
21. F. Dunn and M. Becker, "Application of Analytic Methods to Fast Reactor Spectra", Trans. Am. Nuc. Soc., 12, p. 640 (1969).
22. W. M. Stacey, "A New Definition of Composite Moderating Parameters for the Goertzel-Greuling Slowing Down Theory", Trans. Am. Nuc. Soc., 13, p. 199 (1970).
23. P. Walti and L. Grossman, "A Synthetic Scattering Kernel for Fast Reactor Theory", Trans. Am. Nuc. Soc., 12, p. 155 (1969).
24. E. Burns and M. Becker, "The Formulation of Continuous Slowing Down Theory for General Processes in Terms of Separable Kernels", Nuc. Sci. Eng., 42, p. 100 (1970).
25. E. Burns and M. Becker, "Fast Neutron Spectrum Models and Their Application to Specific Materials", Trans. Am. Nuc. Soc., 13, p. 687 (1970).
26. C. Syros, "Energy Distribution of Inelastically and Elastically Slowed Down Fast Neutrons", Nukleonik, 8, p. 396 (1966).
27. M. Segev, "An Approximate Solution to the Asymptotic Slowing Down Equations of Fast Neutrons", Nuc. Sci. Eng., 40, p. 424 (1970).

28. A. A. Bergmann, A. I. Isacoff, I. D. Murin, F. L. Shapiro, I. V. Shtranikah and M. V. Cazarnovsky, "A Neutron Spectrometer Based on the Slowing Down Time of Neutrons in Lead", Proc. First Intl. Conf. Peaceful Uses At. Energy, Geneva, 4, p. 135 (1955).
29. L. E. Beghian, N. C. Rasmussen, R. Thews and J. Weber, "The Investigation of Neutron Kinetics and Cross Sections in Fast Nonmoderating Assemblies by the Nanosecond Pulsed Neutron Source Technique", Nuc. Sci. Eng., 15, p. 375 (1963).
30. L. E. Beghian, A. E. Profio, J. Weber and S. Wilensky, "The Investigation of Nonelastic Cross Sections for Iron by the Nanosecond Pulsed Neutron Source Technique", Nuc. Sci. Eng., 17, p. 82 (1963).
31. T. Gozani, "Experimental Kinetic Studies in a U^{238} Sphere", Gulf General Atomic Report No. GA-8465 (1968).
32. T. Hiraoka, T. Iijima, N. Hirakawa, T. Nakamura and M. Nozawa, "Pulsed Neutron Experiments in Fast Natural Uranium Systems", Journal of Nuc. Sci. and Technology, 1, p. 108 (1964).
33. N. Corngold, "Some Transient Phenomena in Thermalization", Nuc. Sci. Eng., 19, p. 80 (1964).
34. J. Dorning and B. Nicolaenko, "Time Dependence of Finite, Subcritical Fast Multiplying Assemblies", Trans. Am. Nuc. Soc., 11, p. 577 (1968).
35. J. Dorning, B. Nicolaenko and J. K. Thurber, "Some Comments on Pseudo-Mode Solutions of the Initial Value Problem Obtained by Analytic Continuation: Thermal and Fast Systems", Proceedings of Conference on Neutron Transport Theory, A. E. C. Report ORO-3858-1, p. 36 (1969).
36. U. Adalioglu, "Time Decay of Neutron Pulses in Fast Subcritical Assemblies", Ph.D. Thesis, University of Michigan (1971).
37. T. J. Williamson and R. W. Albrecht, "Calculations of Neutron Time-Energy Distributions in Heavy Moderators", Nuc. Sci. Eng., 42, p. 97 (1970).
38. T. D. Beynon, M. Coleman and M. A. W. Mondal, "On the Behavior of a Neutron Pulse in the Vicinity of an Inelastic Threshold", Journal Nuc. Energy, 24, p. 367 (1970).

39. N. Corngold and C. Yan, "Slowing Down With Inelastic Scattering", Proceedings of Second Conference on Transport Theory, U.S.A. E. C., CONF-710107, p. 83 (1971).
40. R. Bellman and K. Cooke, Differential Difference Equations, Academic Press, New York (1963).
41. Neutron Cross Sections, BNL-325, Supplement No. 2, Vol. IIC (1966).
42. M. Lighthill, Generalised Functions, Cambridge University Press, Cambridge, England (1958).
43. B. G. Yates, "The Linear Difference Differential Equation with Linear Coefficients", Trans. Amer. Math. Soc., 80, p. 281 (1955).
44. F. G. Tricomi, Integral Equations, Interscience Publishers, New York (1967).
45. L. M. Milne Thomson, The Calculus of Finite Differences, Chapter XI, MacMillian and Co., Ltd., London (1933).
46. N. R. Corngold, private communication.

APPENDIX I

THE MECHANICS OF INELASTIC SCATTERING

In this study we have repeatedly used the notion that we could view the energy loss of an inelastically scattered neutron as a discrete lump in the laboratory system. This, of course, is an approximation, and we must study the two body problem to determine the actual distribution of final energies. Much of what follows is described in work by Beynon⁽⁴⁾ and Lamarsh⁽³⁾.

If a neutron of laboratory speed v_l approaches a stationary target nucleus (mass number A), let the laboratory recoil speed of the neutron be v'_l , and that of the target V'_l . As viewed in the center of mass system, the neutron and target approach each other with speeds v_c and V_c , and after interaction leave with speeds v'_c and V'_c . We have

$$\vec{v}_c = \frac{A}{A+1} \vec{v}_l$$

$$\vec{V}_c = -\frac{1}{A+1} \vec{v}_l \quad (\text{I.1})$$

$$\vec{v}_0 = \frac{1}{A+1} \vec{v}_l,$$

where \vec{v}_0 is the center of mass velocity. These vectors can be related as shown in Figure I.1.

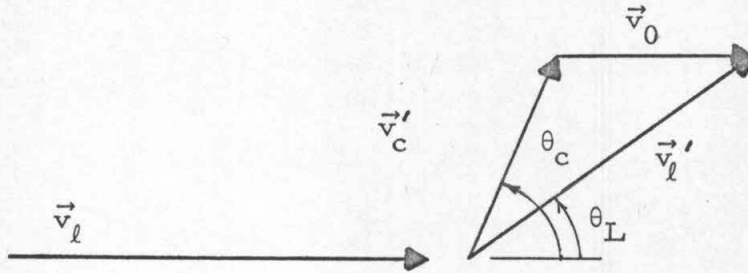


Figure I.1 Velocity Vectors

The angle of scattering in the center of mass system is θ_c , and in the laboratory system θ_L . Using the law of cosines, we have

$$(\vec{v}'_l)^2 = (\vec{v}'_c)^2 + (v_0)^2 + 2 v_0 v'_c \mu_c, \quad (\text{I.2})$$

where $\mu_c = \cos \theta_c$.

If we assume the energy of excitation of the nucleus is Q , measured in the center of mass system, conservation of energy in the center of mass system yields

$$\frac{1}{2} m v_c^2 + \frac{1}{2} A m V_c^2 = \frac{1}{2} m (\vec{v}'_c)^2 + \frac{1}{2} A m (V'_c)^2 + Q. \quad (\text{I.3})$$

Momentum conservation in the center of mass system implies

$$\begin{aligned} m \vec{v}_c &= A m \vec{V}_c \\ m \vec{v}'_c &= A m \vec{V}'_c. \end{aligned} \quad (\text{I.4})$$

Substitution of Eqns. I.1 and I.4 into Eqn. I.3 yields

$$|v'_c| = \sqrt{\frac{A^2}{(A+1)^2} v_l^2 - \frac{2Q}{m} \frac{A}{A+1}}. \quad (\text{I.5})$$

Multiplication of Eqn. I.2 by $\frac{m}{2}$, followed by recognition of Eqn. I.5, yields

$$E'_l = \frac{A^2}{(A+1)^2} E_l - \frac{AQ}{A+1} + \frac{E_l}{(A+1)^2} + \frac{\mu_c}{A+1} \sqrt{\frac{4A^2}{(A+1)^2} E_l^2 - \frac{4E_l QA'}{A+1}},$$

where E_l , E'_l are the initial and final laboratory kinetic energies. This can be further simplified to

$$E'_l = E_l \left\{ \frac{1}{2}(1+\alpha) + \frac{1}{2}(1-\alpha) \mu_c \sqrt{1 - \frac{Q}{\beta E_l} - \frac{\beta Q}{E_l}} \right\}, \quad (\text{I.6})$$

where

$$\beta = \frac{A}{A+1}$$

$$\alpha = \left[\frac{A-1}{A+1} \right]^2.$$

We can determine the maximum and minimum recoil kinetic energies from Eqn. I.6 by putting in the maximum and minimum values for $\mu_c (\pm 1)$:

$$E_{\max} = E_l \left\{ \frac{1}{2}(1+\alpha) + \frac{1}{2}(1-\alpha) \sqrt{1 - \frac{E_{th}}{E_l}} \right\} - \beta^2 E_{th} \quad (\text{I.7})$$

$$E_{\min} = E_l \left\{ \frac{1}{2}(1+\alpha) - \frac{1}{2}(1-\alpha) \sqrt{1 - \frac{E_{th}}{E_l}} \right\} - \beta^2 E_{th},$$

where $E_{th} = Q/\beta$, the threshold energy in the laboratory system.

The relative width of the distribution of final laboratory energies can be obtained by subtraction:

$$\frac{E_{max} - E_{min}}{E_l} = (1 - \alpha) \sqrt{1 - \frac{E_{th}}{E_l}}.$$

Since

$$\sqrt{1 - \frac{E_{th}}{E_l}} \leq 1 \quad (E_l > E_{th}),$$

$$\frac{E_{max} - E_{min}}{E_l} \leq 1 - \alpha = \frac{4A}{(A+1)^2}.$$

Thus for $A \gg 1$

$$\frac{E_{max} - E_{min}}{E} \leq \frac{4}{A}. \tag{I.8}$$

We see the relative width of the final energy distribution is about 0.02 ($A \sim 200$). This clearly provides adequate justification for the discrete energy loss assumption for heavy moderators.

One can continue with inelastic scattering mechanics to describe the scattering kernel. This is done in a very detailed paper by Beynon⁽⁴⁾.

APPENDIX II

RECOVERY RELATIONS

It is well known that if we consider neutron slowing down in an infinite medium of zero absorption, and treat elastic scattering with Fermi age theory, the elastic collision density is inversely proportional to energy for energies below the source cut-off:

$$\Sigma_s(E)E\phi(E) = \frac{1}{\xi} \quad \text{for } E < E_s, \quad (\text{II.1})$$

where

$$S(E < E_s) = 0,$$

and

$$\int_{E_s}^{\infty} S(E')dE' = 1.$$

Considering the particular case $S(E) = \delta(E - E_s)$, we have

$$\Sigma_s(E)E\phi(E) = \begin{cases} \frac{1}{\xi} & 0 \leq E \leq E_s \\ 0 & E > E_s. \end{cases} \quad (\text{II.2})$$

Inclusion of inelastic scattering will obviously alter these results. We wish to investigate the end points of the slowing down problem posed with a monoenergetic source; we will study the flux (or collision density) at $E = E_s$ and $E \rightarrow 0$. This will be done with two models of inelastic scattering; discrete level and evaporative kernel.

A. Discrete Level Inelastic Scattering

Using the same notation as in the text, we can write an equation for the neutron slowing down density:

$$q(E) = \xi \Sigma_s(E) E \varphi(E) + \sum_{j=1}^N \int_E^{E+E_j} dE' \Sigma_{in}^j(E') \varphi(E'). \quad (II.3)$$

Differentiation of this equation yields

$$\frac{dq(E)}{dE} = \xi \frac{d}{dE} (\Sigma_s(E) E \varphi(E)) + \sum_{j=1}^N \Sigma_{in}^j(E+E_j) \varphi(E+E_j) - \Sigma_{in}(E) \varphi(E), \quad (II.4)$$

where

$$\Sigma_{in}(E) = \sum_{j=1}^N \Sigma_{in}^j(E).$$

Noting the balance equation for the neutron flux

$$\xi \frac{d}{dE} (\Sigma_s(E) E \varphi(E)) + \sum_{j=1}^N \Sigma_{in}^j(E+E_j) \varphi(E+E_j) - \Sigma_{in}(E) \varphi(E) = -S(E), \quad (II.5)$$

we substitute into Eqn. II.4 to obtain the familiar result

$$\frac{dq(E)}{dE} = -S(E). \quad (II.6)$$

If $S(E < E_s) = 0$ and $\int_{E_s}^{\infty} S(E) dE = 1$, then

$$q(E) = c \quad E < E_s. \quad (II.7)$$

In particular, if $S(E) = \delta(E - E_s)$, then

$$q(E) = \begin{cases} 1 & 0 \leq E \leq E_s \\ 0 & E > E_s \end{cases} \quad (\text{II.8})$$

With the source chosen so that Eqn. II.8 holds, we obviously have $\varphi(E) = 0$ for $E > E_s$. Returning to Eqn. II.3, we let $E \rightarrow E_s^-$:

$$q(E_s) = 1 = \xi \Sigma_s(E) E \varphi(E) \Big|_{E=E_s}$$

or

$$\Sigma_s(E) E \varphi(E) \Big|_{E=E_s} = \frac{1}{\xi}. \quad (\text{II.9})$$

Now let $E \rightarrow 0$ in Eqn. II.3. The range of the inelastic integral then becomes very small, and we can perform a Taylor series expansion of the integrand about the lower limit of integration. We find

$$1 = \lim_{E \rightarrow 0} \left[\xi \Sigma_s(E) E \varphi(E) + \sum_{j=1}^N \left\{ \varphi(E_j) \Sigma_{in}^j(E_j) E + O(E^2) \right\} \right].$$

Thus

$$\frac{1}{\xi} = \lim_{E \rightarrow 0} \Sigma_s(E) E \varphi(E). \quad (\text{II.10})$$

Thus $\Sigma_s(E) E \varphi(E)$ recovers at $E=0$ to the same value it has at $E=E_s$, and this result is independent of the number of inelastic levels. We indicate schematically in Figure II.1 the behavior.

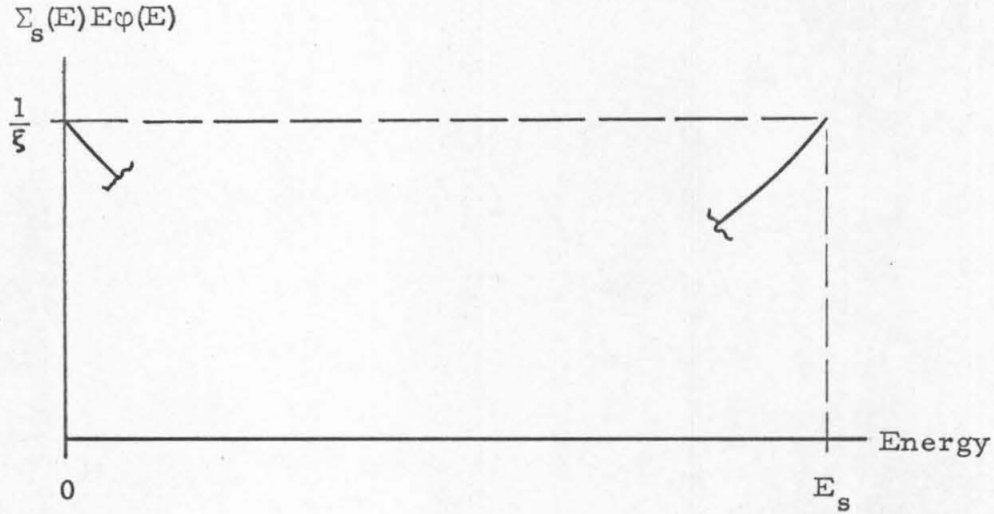


Figure II.1 End Point Behavior

B. Evaporative Kernel Inelastic Scattering

When the inelastic scattering is modeled with a separable inelastic kernel, the equation for the slowing down density becomes

$$q(E) = \xi \Sigma_s(E) E \phi(E) + \int_0^E dE' \int_E^\infty K_{in}(E'' \rightarrow E') \Sigma_{in}(E'') \phi(E'') dE'', \quad (II.11)$$

where we choose kernels of the type

$$K_{in}(E'' \rightarrow E') = g(E') h(E'').$$

Thus

$$q(E) = \xi \Sigma_s(E) E \phi(E) + \int_0^E dE' g(E') \int_E^\infty h(E'') \Sigma_{in}(E'') \phi(E'') dE''. \quad (II.12)$$

Again we differentiate with respect to energy to obtain

$$\frac{dq(E)}{dE} = \xi \frac{d}{dE} \left(\Sigma_s(E) E \varphi(E) \right) + g(E) \int_E^{\infty} h(E'') \Sigma_{in}(E'') \varphi(E'') dE''$$

(II.13)

$$- \left\{ \int_0^E dE' g(E') \right\} h(E) \Sigma_{in}(E) \varphi(E).$$

The balance equation for the neutron flux is

$$\xi \frac{d}{dE} \left(\Sigma_s(E) E \varphi(E) \right) + g(E) \int_E^{\infty} h(E') \Sigma_{in}(E') \varphi(E') dE' - \Sigma_{in}(E) \varphi(E) = -S(E).$$

(II.14)

Therefore

$$\frac{dq(E)}{dE} = -S(E),$$

(II.15)

provided that

$$h(E) \left\{ \int_0^E dE' g(E') \right\} = 1.$$

(II.16)

Equation II.16 is the condition that a neutron scattered inelastically appear at some energy lower than the incident energy. Any evaporative kernel we propose to use must certainly obey this relation.

If we let $S(E) = \delta(E - E_s)$, we have again

$$q(E) = \begin{cases} 1 & 0 \leq E \leq E_s \\ 0 & E > E_s. \end{cases}$$

(II.17)

Noting that $\varphi(E > E_s) = 0$, we let $E \rightarrow E_s$ in Eqn. II.11. The integral term is identically zero for $E = E_s$, and we have

$$\left. \Sigma_s(E) E \varphi(E) \right|_{E=E_s} = 1. \quad (\text{II.18})$$

Again we require $\Sigma_{\text{in}}(E) = 0$ for $E < E_1$. This reflects the threshold nature of the inelastic cross sections ($E_1 = \min_{j=1, \dots, \infty} \{E_j\}$, the level energies). Letting $E \rightarrow 0$ in Eqn. II.11, we have

$$\lim_{E \rightarrow 0} \left\{ \xi \Sigma_s(E) E \varphi(E) + O(E) = q(E) \right\} \quad (\text{II.19})$$

or

$$\lim_{E \rightarrow 0} \Sigma_s(E) E \varphi(E) = \frac{1}{\xi}. \quad (\text{II.20})$$

Recovery is once again demonstrated. Using Fermi age theory to model elastic scattering we see the occurrence of recovery apparently depends on the threshold nature of the inelastic scattering cross section, not on the way in which the inelastic processes are modeled.

C. General Scattering Kernels

Having thus considered the case $A \rightarrow \infty$ (so that Fermi age elastic scattering and discrete level inelastic scattering could be used), we might ask about recovery for all moderators. We can generalize the notions thus far developed, needing only to assume isotropic scattering in the laboratory system (for convenience). We allow any inelastic transfer kernel, including one with upscatter. Discrete levels

are then a special case (see reference (4)). We will see that a recovery relation holds here also, but it is slightly different in form from that gained earlier. The difference will arise from the more general treatment of elastic scattering, which gives rise to the Placzek oscillations⁽⁶⁾ discussed earlier.

The net slowing down density is given by

$$\begin{aligned}
 q(E) = & \int_E^{E/\alpha} dE' \frac{\Sigma_s(E')\varphi(E')}{E'(1-\alpha)} (E-\alpha E') + \int_0^E dE' \int_E^\infty K_{in}(E'' \rightarrow E') \Sigma_{in}(E'') \varphi(E'') dE'' \\
 & - \int_E^\infty dE' \int_0^E K_{in}(E'' \rightarrow E') \Sigma_{in}(E'') \varphi(E'') dE''.
 \end{aligned}
 \tag{II.21}$$

The first term is due to elastic collisions, the second is due to inelastic events resulting in downscatter, and the third is due to inelastic events resulting in upscatter. The difference of the last two terms yields the net slowing down density due to inelastic events. (Note if no upscatter is allowed $K_{in}(t \rightarrow x) = 0$ if $t < x$, and the last term is identically zero).

Since the integrands in the last two terms exist (we assume $\Sigma_{in}(E) = 0$ for $E < E_1$ as before, so that behavior of $\varphi(E)$ as $E \rightarrow 0$ is of no concern), we can interchange order of integration, defining

$$p(E'', E) = \int_0^E K_{in}(E'' \rightarrow E') dE'
 \tag{II.22}$$

$$v(E'', E) = \int_E^{\infty} K_{in}(E'' \rightarrow E') dE'. \quad (II.23)$$

Substitution yields

$$q(E) = \int_E^{E/\alpha} \frac{dE' \Sigma_s(E') \varphi(E') (E - \alpha E')}{E'(1 - \alpha)} + \int_E^{\infty} \Sigma_{in}(E'') \varphi(E'') p(E'', E) dE'' \quad (II.24)$$

$$- \int_0^E \Sigma_{in}(E'') \varphi(E'') v(E'', E) dE''.$$

Again we differentiate with respect to energy to obtain

$$\frac{dq(E)}{dE} = -\Sigma_s(E) \varphi(E) + \int_E^{E/\alpha} \frac{dE' \Sigma_s(E') \varphi(E')}{E'(1 - \alpha)} + \int_E^{\infty} \Sigma_{in}(E'') \varphi(E'') \frac{\partial p(E'', E)}{\partial E} dE'' \quad (II.25)$$

$$- \Sigma_{in}(E) \varphi(E) \{p(E, E) + v(E, E)\} - \int_0^E \Sigma_{in}(E'') \varphi(E'') \frac{\partial v(E'', E)}{\partial E} dE''.$$

From Eqns. II.22 and II.23, we note

$$\frac{\partial p(E'', E)}{\partial E} = K_{in}(E'' \rightarrow E)$$

$$\frac{\partial v(E'', E)}{\partial E} = -K_{in}(E'' \rightarrow E).$$

Also we note that

$$p(E'', E) + v(E'', E) = \int_0^{\infty} K_{in}(E'' \rightarrow E') dE',$$

which is just the probability that a neutron scattered inelastically at energy E'' appear at some energy E' . We clearly demand, for neutron conservation, that this be unity. Therefore

$$\frac{dq(E)}{dE} = \int_E^{E/\alpha} \frac{dE' \Sigma_s(E') \varphi(E')}{E'(1-\alpha)} + \int_0^\infty K_{in}(E'' \rightarrow E) \Sigma_{in}(E'') \varphi(E'') dE'' \quad (II.26)$$

$$- (\Sigma_{in}(E) + \Sigma_s(E)) \varphi(E).$$

For the case presently considered the balance equation for the flux is

$$\int_E^{E/\alpha} \frac{dE' \Sigma_s(E') \varphi(E')}{E'(1-\alpha)} + \int_0^\infty K_{in}(E'' \rightarrow E) \Sigma_{in}(E'') \varphi(E'') dE'' \quad (II.27)$$

$$- (\Sigma_{in}(E) + \Sigma_s(E)) \varphi(E) = -S(E).$$

Taken together the last two equations yield the familiar result

$$\frac{dq(E)}{dE} = -S(E), \quad (II.28)$$

and as before, if $S(E) = \delta(E - E_s)$ ($\varphi(E > E_s) = 0$), we have

$$q(E) = \begin{cases} 1 & 0 \leq E \leq E_s \\ 0 & E > E_s. \end{cases} \quad (II.29)$$

With $q(E) = 1$ as $E \rightarrow 0$ we return to Eqn. II.24. Noting that $p(E'', E) \rightarrow 0$ as $E \rightarrow 0$, and $\Sigma_{in}(E) = 0$ for $E < E_1$, we have

$$\lim_{E \rightarrow 0} \int_E^{E/\alpha} \frac{dE' \Sigma_s(E') \varphi(E')(E - \alpha E')}{E'(1 - \alpha)} = 1. \quad (\text{II.30})$$

If we now let $\Sigma_s(E') E' \varphi(E') = C$ in Eqn. II.30, we find

$$1 = C \left(1 + \frac{\alpha}{1 - \alpha} \ln \alpha \right),$$

or

$$C = \frac{1}{\xi}.$$

Thus

$$\lim_{E \rightarrow 0} \Sigma_s(E) E \varphi(E) = \frac{1}{\xi}. \quad (\text{II.31})$$

Just as before we have recovery to $\frac{1}{\xi}$ as $E \rightarrow 0$. Making the expansion as $E \rightarrow E_s$ is not fruitful here due to the way in which elastic scattering is treated. With such a treatment Placzek oscillations affect the solution near $E = E_s$, and the quantity $\Sigma_s(E) E \varphi(E)$ at $E \rightarrow E_s$ is dependent on cross sections and mass number (see, for example, Lamarsh⁽³⁾).

We conclude that recovery is a phenomenon we can observe with about any absorptionless slowing down model, provided the inelastic cross section satisfies a physical requirement by vanishing below threshold.